# A Repeated Injury Model of Intervertebral Disc Degeneration and the In-Vivo Effects of Thermal Therapy

by

**Jill Alison Ulrich**

DISSERTATION

Submitted in partial satisfaction of the requirements for the degree of

DOCTOR OF PHILOSOPHY

in

Bioengineering

in the

GRADUATE DIVISIONS

of the

UNIVERSITY OF CALIFORNIA SAN FRANCISCO

and

UNIVERSITY OF CALIFORNIA BERKELEY

**Acknowledgements**

I would like to express my appreciation to those whose support and encouragement have made this work possible. First, I would like to thank my research advisor, Jeff Lotz, for his advice and guidance in completing this project. I would also like to thank Chris Diederich for providing his expertise and assistance for this work. In addition, I would like to thank my committee members Sharmila Majumdar and Serena Hu for their continued support.

I would like to thank the members of the Orthopaedic Bioengineering Lab and Thermal Therapy Research Group, both past and present, who have provided me with technical support, advice, and friendship. In addition, I appreciate the constant support of my friends, both near and far, who have made this process fun.

Finally, I would like to thank my parents, Marsha and James D. Ulrich, my sister and brother, Susan Holmes and James T. Ulrich, and my boyfriend, Mark McCoy. I could not have completed this without your love, patience, and encouragement along the way.

Abstract

A Repeated Injury Model of Intervertebral Disc Degeneration and the In-Vivo Effects of Thermal Therapy

By

Jill Alison Ulrich

Doctor of Philosophy in Bioengineering

University of California, San Francisco and Berkeley

Professor Jeffrey C. Lotz, Chair

Low back pain caused by disc degeneration is a significant health and economic issue. The objective of this research was to advance the understanding of disc degeneration and back pain therapy by developing an animal model of disc degeneration and investigating the effects of thermal therapy on degenerated intervertebral discs. In order to do this, two models of disc degeneration were characterized using rat tail intervertebral discs, and several potential therapeutic mechanisms of thermal therapy were examined using both *in vitro* and *in vivo* methods.

A single-stab incision was successful in creating histologic changes consistent with human degenerative discs. Cytokines, primarily located in the wound tract, were transiently elevated following the single-stab injury. A triple-stab injury induced inflammation that continued over the 56-day recovery period and was present throughout the annulus. Features associated with human disc degeneration were also observed

following triple-stab injury, including a complete disappearance of normal nuclear matrix.

Both *in vitro* and *in vivo* experiments were completed to investigate the effects of thermal therapy on degenerative discs. The *in vitro* study demonstrated that sublethal heat can induce an HSP70 response and affect cytokine production in disc cells. The cytokine response to thermal therapy was dependent upon thermal dose.

To investigate the *in vivo* effects of thermal therapy on degenerated discs, a miniature RF heating probe was designed and used to examine the morphological and inflammatory effects of three different thermal exposures on degenerated discs. TNF-α levels in the disc were reduced twenty-eight days following treatment with all three thermal exposures. Besides increased proteoglycan production in the tissue surrounding the treatment region, no evidence of disc remodeling was observed in the discs.

This research has implications for the prevention and treatment of disc degeneration. The triple-stab degeneration model induced clinically relevant outcomes including morphological disruption and inflammation and provides a convenient platform to evaluate the impact of anti-inflammatory treatments. The results of the thermal therapy studies suggest that high temperature treatments do not induce a remodeling response and can be harmful to the disc, so future research should focus on the potential therapeutic effects of low thermal exposures.

**Table of Contents**

**List of Figures**

# Chapter 1 Introduction

## 1.1 Motivation

Low back pain is a significant health and economic problem affecting an estimated 60-80% of the population in industrialized countries [1]. At any given time, between 5.6% and 28.7% of the population is suffering from back pain [2-7]. For a substantial number of these patients (up to 40%), the pain has been related to disorders of the intervertebral disc [8]. Estimated direct and indirect costs for low back pain in the United States range from $100 billion to $200 billion annually, with up to two-thirds of these costs attributed to lost wages and productivity [9]. The magnitude of the health and economic burden caused by disc pain underscores the importance of continuing research into both the pathogenesis and treatment of disc disease.

## 1.2 Disc Structure and Function

Intervertebral discs, which lie between each pair of adjacent vertebrae in the spine, provide support, transmit and absorb force, and allow for movement. The intervertebral disc consists of three structures: the nucleus pulposus, the annulus fibrosis, and the vertebral endplates. The annulus fibrosis is an outer ring of concentric collagen layers that surrounds the gelatinous nucleus pulposus. The disc is bordered superiorly and inferiorly by cartilaginous vertebral endplates.

The annulus fibrosis is composed primarily of type I collagen rings. Each disc contains up to 25 concentric rings with adjacent layer collagen fibers alternating orientations of approximately 60º to the spine's axis [10]. This arrangement allows the annulus to resist tensile forces experienced during bending and twisting activities [10].

The collagen rings also serve to contain the nucleus pulposus and anchor the disc to the vertebral body [11]. The outer annulus is mostly composed of type I collagen; however, the concentration of type II collagen in the annular rings increases towards the center of the disc [12].

The nucleus pulposus is primarily composed of proteoglycan and water held together by a network of type II collagen and elastin fibers [13]. The most abundant proteoglycan in the nucleus is aggrecan, which is composed of negatively charged glycosaminoglycans that cause the nucleus to imbibe water [14]. Swelling of the nucleus is bounded by the annulus rings laterally and by the vertebral endplates superiorly and inferiorly, which allows the nucleus to maintain hydrostatic pressure. In health, the majority of a compressive load applied to the spine is transferred from one vertebrae to the next through the nucleus pulposus [10].

Vertebral endplates are typically less than one millimeter thick and cover the vertebral body both above and below the annulus and nucleus [15]. Endplates are composed of proteoglycan molecules reinforced by collagen fibrils [16] in an arrangement similar to other hyaline cartilage structures [17]. In health, the endplates are innervated and can contain small blood vessels [18, 19]. Because the disc is mostly avascular, disc cells rely on diffusion through the vertebral endplates for a supply of oxygen and nutrients and the removal of waste products [12]. The endplates act as selectively permeable barriers to solutes passing into and out of the discs [17].

Disc cells in the annulus fibrosis are described as fibroblast-like and cells in the nucleus pulposus as chondrocyte-like. These descriptions are based on cell morphology and extracellular matrix production: primarily type I collagen by fibroblast-like cells and

type II collagen and proteoglycan by chondrocyte-like cells [20]. Notochordal cells are present in the nucleus during childhood; however, these cells usually disappear by adolescence [21]. Like other hyaline cartilaginous structures, the vertebral endplates contain chondrocytes [22]. The cell density of the disc is low, approximately 4 x $10^6$ cells/$cm^3$ in the nucleus pulposus and 9 x $10^6$ cells/$cm^3$ in the annulus [19], making it difficult for the disc cells to maintain the extensive disc extracellular matrix [10].

The disc is mostly avascular with capillaries present only in the outer few layers of the annulus fibrosis [13]. Nutrients primarily reach disc cells, which are up to 8 mm from blood vessels [11], by diffusion from the vertebral vasculature through the cartilaginous endplate [10]. The lack of blood vessels creates a low oxygen environment requiring the disc cells to undergo anaerobic metabolism, which results in an acidic disc environment since the disc is unable to readily rid itself of lactic acid waste [10].

In healthy discs, numerous studies have identified nerve fibers in the outer portion of the annulus while failing to find evidence of nerve in the inner annulus or nucleus [23-25]. Nerves have also been identified in the endplates. The innervation density of the outer annulus and vertebral endplates is similar, with a possible increase of nerve fiber concentration in the central portion of the endplate adjacent to the nucleus pulposus [18].

### 1.3 Disc Degeneration

Because the disc supports high loads, has low cellularity, and contains few blood vessels and nerves, it is prone to degeneration. With aging, all discs undergo structural, chemical, and mechanical changes. It is unclear why some discs become degenerative and painful, while others age asymptomatically. While there is no consensus on a

definition of disc degeneration [13, 26], Adams and Roughley recently suggested that disc degeneration can be defined as "an aberrant, cell-mediated response to progressive structural failure. A degenerate disc is one with structural failure combined with accelerated or advanced signs of aging." [13] This definition attempts to distinguish degeneration from aging; however, many of the natural changes that occur during the aging process are identical to those observed in disc degeneration. These changes include impaired metabolite transport, altered enzyme activity, cell senescence, changes in matrix macromolecules and water content, structural failure, neurovascular ingrowth, and cell death [27]. Pain has been associated with disc degeneration, and painful discs have shown a loss of mechanical stability, increased levels of pro-inflammatory factors, and nerve ingrowth; however, the precise relationship between disc degeneration and pain is unknown [21].

*Morphological Changes*

Several studies suggest that the degenerative process begins with a decline in the nutrient supply to disc cells, which is caused by a reduction in the number of endplate blood vessels and endplate calcification [17, 21]. With aging, endplate cartilage is resorbed and replaced by calcified cartilage and bone, endplate cell density is reduced [20], and endplate fissures occur [22]. These factors, coupled with a decrease in disc water content, limit the diffusion of nutrients and waste products to and from disc cells [27]. An inadequate nutrient supply and the increasingly acidic environment due to the accumulation of lactic acid waste prevent disc cells from producing and maintaining the proper matrix components [21]. Not only does the lack of nutrition affect cell function,

but it also decreases cell viability with up to 80% of nucleus cells being necrotic in the elderly [27]. As a result, annular layers become disorganized, collagen crosslinks are broken [28], and both concentric and radial tears form [29]. Collagen fibers can fragment and degenerate, weakening the anchoring of the annulus to the vertebra [30]. The anatomic distinction between the nucleus and annulus is lost as the nucleus becomes more fibrotic, the annulus becomes more disorganized, and annular layers bulge into the nucleus [21, 29]. Granulation tissue appears in the disc and neovascularization and innervation occur from the outside of the annulus inwards [20]. Nerves and blood vessels have been identified growing into the inner annulus and even the nucleus in degenerating discs [31]. Osteophytes and Schmorl's nodes, protrusions of the nuclear material into the vertebrae, are frequently observed on the vertebrae adjacent to degenerative discs [16].

*Biomechanical Changes*

The morphological changes of the disc are associated with changes in disc biomechanics [32]. Loss of proteoglycan and decreased water content affect the ability of the nucleus pulposus to transmit loads from one vertebra to the next, causing increased loading of the collagen network. This abnormal annular loading leads to failure of the matrix, loss of disc shape, and changes in mechanical function [27]. Disc connective tissues lose elasticity and strength resulting from modifications to the components of collagen, proteoglycan, and elastin [27]. Degenerative discs have more laxity and less range of motion than healthy discs, which could be related to a loss in disc height [33]. In addition, discs lose symmetry and regularity of elastic modulus as they degenerate [34]. Stiffness decreases during early degeneration and then increases with more

advanced degeneration [34, 35]. Changes in disc biomechanics and fluid pressure alter the mechanical environment of disc cells [35]. Because cell metabolism is influenced by mechanical forces, abnormal loading can lead to improper matrix and enzyme synthesis encouraging further degeneration [11].

*Biochemical Changes*

Abnormal stresses trigger changes to the biochemical environment of the disc. By stimulating disc cells, mechanical stress can increase the presence of matrix metalloproteinases (MMPs), which break down tissue and weaken the disc [36]. High concentrations of nerve growth factor (NGF) encourages nerve ingrowth into the inner layers of the annulus and nucleus [37]. In addition to the increased presence of certain MMPs and growth factors, the disc environment is altered by the presence of inflammatory factors such as cytokines. Cytokines are proteins that affect the functions of other cells and can modulate connective tissue anabolism and catabolism [38, 39]. Higher concentrations of pro-inflammatory cytokines are present in painful degenerative discs than in healthy discs [40].

Cytokines identified in degenerative disc tissue either from cadavers or excised during surgery include: interleukin 1 (IL-1) [41-43], tumor necrosis factor alpha (TNF-$\alpha$) [38, 41, 42, 44, 45], interleukin 6 (IL-6) [41, 42, 46], and interleukin 8 (IL-8) [45]. In these tissues, it is unclear whether the cytokines are released by disc cells themselves or by surrounding tissue. Disc cells cultured *in vitro* have been shown to produce IL-1 [42, 43], IL-6 [42, 47], IL-8 [47], prostaglandin $E_2$ ($PGE_2$) [42, 47], and TNF-$\alpha$ [48, 49]. These pro-inflammatory cytokines are involved both in the process of disc matrix

degeneration and in the genesis of pain through nerve contact [41]. The precise action of each cytokine is unclear due to the high degree of redundancy and cross-talk among the induction pathways [50].

IL-1 has two forms, IL-1α and IL-1β, which have similar functional effects on cells since they target the same cellular receptors [39]. IL-1 has been shown to increase production of MMPs [43, 51] , $PGE_2$ [42, 51, 52], nitric oxide (NO) [51, 53], IL-1 [43], and IL-6 [22]. In addition, IL-1 can transition chondrocytes from anabolism to catabolism [41, 54, 55], increase proteoglycan release [52, 56], decrease proteoglycan and collagen production [43, 57], and may play a role in vessel and nerve ingrowth [58]. IL-1 can also inhibit the regulator of the chondrocytic phenotype resulting in chondrocyte metaplasia to a fibroblastic phenotype [43]. IL-1β has been shown to increase the mechanosensitivity of lumbar dorsal roots [59] and induce disc cell apoptosis [53]. Cells from older animals have a higher sensitivity to IL-1 than younger cells, indicating that as cells age and degenerate, they become even more susceptible to the deleterious effects of IL-1 [56]. Because the actions of IL-1 not only promote tissue degradation, but also inhibit tissue repair [39], IL-1 may play an important role in disc degeneration.

TNF-α increases the production of MMPs [44], $PGE_2$ [44, 60, 61], NO [53, 61], IL-8 [44], IL-1 [44], and IL-6 [41]. TNF-α also promotes degradation of proteoglycan and decreases the rate of collagen and proteoglycan synthesis [44]. TNF-α can induce chondrocyte apoptosis [53]. Because TNF-α has been shown to cause inflammatory hyperalgesia [44], endoneuraonal edema, and nerve fiber demyelination it has been linked to increased nerve sensitivity [41]. In the disc, TNF-α has been shown to increase

the mechanosensitivity of lumbar dorsal roots [59] and has been associated with pain related behavior in rat disc herniation models [62].

IL-6 has been shown to increase MMP production, stimulate $PGE_2$ production, and play a role in the breakdown of collagen [57, 63]. IL-6 can also increase aggrecanase modulated proteoglycan breakdown and inhibit proteoglycan synthesis [57, 64]. A study involving genetically altered IL-6 knockout mice confirms the involvement of IL-6 in the development of degenerative musculoskeletal diseases. The knockout mice in the study were unable to develop rheumatoid arthritis whereas wild-type mice subjected to the same conditions developed the disease [65].

IL-8 is associated with acute inflammation, the development of radicular pain, increased nerve sensitivity, and blood vessel growth [66]. Because IL-8 is an important regulator of angiogenesis, it is thought to be associated with the pathogenesis of chronic inflammatory disorders [67]. IL-8 can increase the production of IL-6 and can interact with chondrocytes to affect metabolism and catabolism of the extracellular matrix [68]. Because IL-8 can increase the sensitivity of the dorsal root ganglion, it has been linked to the development of back pain [45].

$PGE_2$ is an eicosanoid derived from arachidonic acid and is commonly discussed in relation to disc pain and degeneration. $PGE_2$ can regulate chondrocyte anabolism and catabolism [50] and is involved in the IL-1 related inhibition of proteoglycan synthesis [69] and collagen synthesis [50]. In addition, $PGE_2$ can increase the production of MMPs [70], induce the production of other inflammatory mediators [55], and increase nerve sensitivity [71].

NO is involved in inhibition of proteoglycan [72-74] and collagen synthesis [75], enhancement of MMP activity and chondrocyte apoptosis [76, 77], and reduction of IL-1 receptor antagonist [78]. NO inhibits chondrocyte proliferation [76]. In addition, NO is a vasodialater and increases vessel permeability [40].

### 1.4 Discogenic Pain

The precise relationship between disc pain and disc degeneration is unclear. Some degenerative discs are asymptomatic while morphologically similar discs are painful. When discs degenerate, nerve and blood vessel growth into the previously aneural inner annulus and nucleus has been associated with pain [31, 79]. Abnormal loading of the outer annulus and endplate can compress nerve fibers in these structures [11]. Radial fissures originating in the nucleus can reach nerve endings in the outer annulus exposing nerve fibers to inflammatory chemicals as well as to enzymes present in the nucleus [80]. Abnormal loading of facet joints and ligaments adjacent to the discs could also be sources of pain as both of these structures contain nerve fibers [11]. Inflammatory cytokines can sensitize nerve fibers [41, 45, 59], and significantly more IL-6, IL-8, and $PGE_2$ has been found in disc tissue excised from painful discs compared to asymptomatic discs [44, 71]. In addition, studies on a large population of low back pain sufferers found an association between the presence of IL-1 in disc tissue and low back pain [81].

### 1.5 Treatment Options

Conservative treatment options for back pain include non-steroidal anti-inflammatory drugs (NSAIDs), muscle relaxants, antidepressants, exercise, back schools, bed rest, behavioral therapy, physical therapy, lumbar supports, spinal manipulation, traction, transcutaneous electrical nerve stimulation (TENS), acupuncture, and massage [82]. Several of these treatments have been shown to be effective for pain relief and improvement of function in acute back pain cases. Some of these treatment options are also effective for short-term pain relief of chronic back pain; however, there is no evidence that these interventions provide long-term pain reduction or improvement of function in chronic pain cases [82]. Although most patients respond well to conservative treatment and do not develop chronic pain, there remains a subset of patients who continue to suffer symptoms which negatively affect their lifestyle [83].

Traditionally, patients who fail conservative therapy have few treatment options outside of discectomy or fusion, or more recently, disc replacement. Spinal fusion, with or without discectomy, can result in significant morbidity and variable outcomes [84]. In addition, because of its affect on spine motion, fusion can lead to degenerative changes in adjacent discs and facets [85, 86]. The long term benefits of disc replacement are uncertain and research has yet to demonstrate whether total disc replacement will be superior to spinal fusion in terms of clinical outcomes [87, 88].

To fill the gap between conservative treatment and invasive surgery, less invasive techniques are being investigated including ultrasound, intradiscal steroid injection, ramus communicans block, thermal therapy, cell therapy, enzyme therapy, and gene therapy [89, 90]. Some of these therapies are currently available and there are a limited

number of studies that show these treatments are effective and safe. Conclusive evidence for the long-term efficacy of these minimally invasive therapies is unavailable. In addition, the anatomical and pathophysiological changes associated with these treatments are not well understood [89]. The promise of less invasive and more cost effective back pain treatment underlines the importance of further basic science research to investigate the biologic effects of these therapies as well as their efficacy for long term pain relief [89].

One of these minimally invasive therapies, intradiscal electrothermal annuloplasty (IDET) has been performed over 60,000 times worldwide, yet the evidence for the efficacy of IDET remains weak and the mechanisms of action are still unclear [91]. Some studies have reported a statistically significant reduction in patient pain levels, improvements in function, and a higher quality of life following IDET [92-94]. Other studies have shown no such benefit [95-98]. Possible therapeutic mechanisms from IDET include collagen denaturation, cell and nerve ablation, the induction of a remodeling response, and pro-inflammatory cytokine level reduction [99-101]; however, the precise mechanism or combination of mechanisms is not known. Optimization of thermal therapies for disc treatment requires an understanding of the mechanisms of thermal therapy, namely, the biologic response in the disc over time.

### 1.6 Objectives

The objective of this thesis was to advance the understanding of disc degeneration and back pain therapy by developing an animal model of disc degeneration and

investigating the *in-vivo* effects of thermal therapy on degenerated intervertebral discs. In order to accomplish this, several specific aims were completed:

1. Development of an appropriate animal model of disc degeneration to use to study the *in-vivo* effects of thermal therapy.
    a. Chapter 2 describes the morphological, biochemical, and biomechanical effects of a single annular stab to a rat intervertebral disc. This work has been published in Spine (Rousseau MA*, Ulrich JA**, Bass EC, Rodriguez AG, Liu JJ, and Lotz JC. Stab Incision for Inducing Intervertebral Disc Degeneration in the Rat. (*co-first authors) *Spine*, 2007. 32(1): p. 17-24).
    b. Chapter 3 describes the effects of a triple-stab to a rat intervertebral disc using morphological, immunohistochemical, and biochemical outcomes and compares this model of degeneration to the single-stab. This work has been awarded the ISSLS Prize and will be published in the December 1st, 2007 issue of Spine (Ulrich JA, Liebenberg EC, Thuillier DU, and Lotz JC. Repeated Injury Causes Persistent Inflammation. *Spine*: in press for Dec 2007).
2. Design and characterization of a miniaturized heating probe. In order to heat a limited region of a rat intervertebral disc, a miniature radiofrequency (RF) heating probe was fabricated and characterized at a number of different temperature and time combinations. Chapter 4 describes the design of the heating probe and the *in vivo* effects of various thermal exposures to a rat intervertebral disc. This work has been published in the SPIE Proceedings (Ulrich JA, Bass EC, Lotz JC, and Diederich CJ. Effects of Thermal Therapy

on Intervertebral Discs: Investigations using a Miniaturized RF Heating Probe in a Small Animal Model. *Proceedings of SPIE.* 2005; Vol 5698: 48-55).

3. Examine the effects of heat on disc cells. Rat nucleus and annulus cells were harvested, cultured, and exposed to several different sublethal thermal doses. Chapter 5 discusses the effects of sublethal heat on disc heat shock protein production and pro-inflammatory factor production.
4. Investigate the *in-vivo* effects of thermal therapy on degenerated intervertebral discs. Using the heating probe design described in Chapter 4 and the animal model described in Chapter 3, thermal therapy was performed on degenerated rat-tail discs. Chapter 6 presents the results from the evaluation of the effects of thermal therapy at three different thermal exposures on degenerated intervertebral discs using biochemical and histological outcomes.

# Chapter 2 Analysis of a Single Annular Stab to Induce Intervertebral Disc Degeneration

## 2.1 Introduction

Because the pathogenesis of disc degeneration, the cause of disc pain, and the optimal treatment for back pain remain unclear, researchers continue to investigate these topics. Animal models for disc degeneration are essential for the development and evaluation of ideas as they pass from the laboratory to the clinic [102]. Animal models of disc degeneration should mimic the human degenerated disc. An ideal animal model would replicate the morphological, biochemical, and biomechanical aspects of human disc degeneration and provide a reproducible platform for analysis. Other factors such as ethics, cost, and time also affect the appropriateness of an animal model [102-104].

Rodents are desirable models for disc repair studies due to their low cost, ease of care, and fast healing times [105]. Tail discs are advantageous because they have an easy surgical approach and multiple discs can be analyzed in each animal [106]. Rodent disc mechanical properties, when normalized to geometry, are comparable to those of human lumbar discs [106]. Although adult rat discs contain notochordal cells, rodent disc morphology and cellularity are comparable to young human discs, and rats are among the few species that retain disc cell populations similar to those found in adult humans [107]. In addition, rat discs have been found to have similar innervation patterns to human discs [108].

Although successful in larger animals [109-119], no rodent model for degenerative disc disease has been investigated using stab-induced degeneration. Annular stab has been investigated as a means for inducing degenerative disc disease in

several animals: rabbit [109-113, 120], dog [114], sheep [115, 116], goat [117], and pig [118, 119]. The morphological evidence of stab-related disc degeneration reported in these studies is similar to many human age-related degenerative disc disease features including [21]: radial and concentric annular tears, trabecular bone formation in the endplate, and nucleus pulposus cell changes associated with increased production of proteoglycan, collagen II, and metalloproteinases. In addition to morphological signs of degeneration, several of these studies found other similarities to human disc degeneration such as high levels of pro-inflammatory cytokines [121], changes in disc mechanical properties [122], and loss of signal intensity on MRI images [120, 123].

Currently, disc degeneration in rodents is observed after several different mechanical, chemical, or nutritional alterations, and it can occur spontaneously in some species. Multiple abnormal disc loading regimens have been shown to induce rodent disc degeneration: static loading [124, 125], cyclic loading [126], and bending [127]. Tail suspension [128], forced bipedalism [129], segmental instability [130, 131] and tiptoe walking [132] are also rodent models in which atypical loading leads to disc degeneration. Rat tail disc degeneration can also be initiated chemically through the injection of chontriotinase ABC into the disc [133]. By affecting disc nutrition, smoking models can lead to rodent disc degeneration [134]. Spontaneous disc degeneration can be observed in certain rodent species such as sand rats [135] or be induced through genetic modifications [136]. While there is currently no consensus regarding the 'best' degeneration model, a cost-efficient system with a consistent starting point and reproducible outcomes is attractive for disc regeneration research. The purpose of this study was to investigate a stab injury model in the rat tail. To assess the effects of the

stab injury, morphological, cytochemical, biomechanical, and immunohistochemical changes were analyzed at time points ranging from 4 to 112 days.

## 2.2 Methods

*Animals*

Three month-old Sprague Dawley rats were used. All procedures were approved by the Institutional Animal Care and Use Committee of the University of California at San Francisco. Because rats reach skeletal maturity before 3 months of age, animal growth did not interfere with disc remodeling [137].

*Surgical Approach*

Each rat was anesthetized using ketamine (90 mg/kg IP) and xylazine (10 mg/kg IP). Buprenorphine (0.01 mg/kg SQ) was administered once before recovery and then as needed to control postoperative pain. Atipamezole HCL (0.2 mg/kg IP) was used for anesthesia reversal. Food, drink, and activity were unrestricted post-operatively. A 2.5 cm longitudinal incision was made along the tail to expose the lateral portion of tail discs Co5/Co6, Co6/Co7, and Co7/Co8. Lateral stabs were performed so that the incision would be on the primary plane of motion for tail discs. A number 11 blade was inserted 1.5 mm into the disc to depressurize the nucleus. A clamp was placed on the blade to prevent the blade from penetrating the disc more than 1.5 mm and radiographic images were captured to ensure the blade was parallel to the endplates to avoid endplate damage. The blade was then removed and the tail skin was closed using interupted stitches.

*Histology*

*Protocol:* Discs and adjacent vertebrae were harvested, fixed in formalin, decalcified in formic acid, dehydrated, and embedded in paraffin. Six-micron sections were cut through the nucleus pulposus parallel to the direction of the stab. Sections were stained with Safranin-O, fast green, and hematoxylin.

*Specimen groups:* Groups for histology were: control (n=5), stab 4-day recovery (4), stab 7-day recovery (5), stab 14-day recovery (5), stab 28-day recovery (5), stab 56-day recovery (5) and stab 112-day recovery (5).

*Analysis*: Disc and endplate architecture was examined at 2x magnification. Nuclear and annular cellular and extracellular aspects were analyzed using 20x magnification.

*Immunohistochemistry*

*Protocol*: Sections were prepared as described in the histology protocol. Sections stained for TNF-α and IL-1β were treated for 20 minutes at 90ºC in Tris HCL (pH 8.6) followed by 20 minutes of room temperature cooling. Sections were blocked for 30 minutes with 10% goat or rabbit serum and then quenched for 15 minutes in 3% hydrogen peroxide. Primary antibody sources were goat (TNF-α; R&D Systems, Minneapolis, MN: and IL-6; Santa Cruz Biotechnology; Santa Cruz, CA) and rabbit (IL-1β; Santa Cruz Biotechnology; Santa Cruz, CA: and KC (rat homologue for IL-8); BioVision, Mountain View, CA). Biotinylated secondary antibodies against the species in which the primary antibody was made were used with a Vector ABC Elite kit (Vector

Laboratories, Burlingame, CA). Staining was visualized using DAB. For negative control sections, rabbit or goat IgG was used at the same concentration as the primary antibody. Sections were counterstained using hematoxylin.

*Specimen groups*: Each disc analyzed for cytokine immunohistochemistry was stained for IL-1β, IL-6, IL-8, and TNF-α. Groups for immunohistochemistry were 4–day recovery (3), 14-day recovery (3), 28-day recovery (3), and 56–day recovery (3). Two control, uninjured discs were also analyzed for each cytokine.

*Analysis*: To observe cellular and extracellular staining, sections were analyzed at 4x and 20x magnification.

*Cytokines*

*Protocol:* Complete discs were harvested, frozen in liquid nitrogen, pulverized, and digested in liquid buffer. Levels of TNF-α, IL-1β, IL-6, and KC (the murine homologue to IL-8) were determined using enzyme linked immunosorbent assays (ELISAs) according to the manufacturer's protocols (R&D Systems, Minneapolis, MN). The limit of detection was 10 pg/ml. Cytokine levels were normalized to tissue wet weight and expressed as ng/g tissue.

*Specimen groups:* Groups for each cytokine were: control (10), stab 4-day recovery (10), stab 7-day recovery (10), stab 14-day recovery (10), and stab 28-day recovery (10).

*Analysis:* A one-way analysis of variance (ANOVA) was used to assess temporal changes for each cytokine. Significance was set at $p<0.05$.

*Biomechanics*

*Protocol*: A bending test was performed in the plane of the stab incision to evaluate the mechanical properties of each spinal unit (vertebra-disc-vertebra). Spinal units were harvested and the soft tissue was removed. While the inferior vertebra was held in place, a metal pin inserted longitudinally into the superior vertebra was deflected by a servo-hydraulic testing machine (MTS Systems Corporation, Eden Prairie, MN) under force control (Figure 2.1). Each specimen was preconditioned for ten cycles at 0.05 Hz before collecting the moment/deflection angle curve. Spinal unit bending test limits were set at 0.01 Nm in both directions of lateral bending. Preliminary data suggested this was this was the range in which the behavior was recoverable.

*Specimen groups:* Disc groups for biomechanics were stab 28-day recovery (9) and sham surgery 28-day recovery (11).

*Analysis*: The loading portion of the moment/deflection angle curve of each specimen was fit to a 5th order polynomial [138]. The first derivative of the curve represented the spinal unit bending stiffness (SUBS). The SUBS (Nm/°) was noted at 0.0075 Nm in both directions of lateral bending. The neutral zone (NZ) was defined as the angle of rotation corresponding to a SUBS under 0.001 Nm/º. Two-sample t-tests were used to compare biomechanical data between sham and stab groups. Significance was set at $p<0.05$.

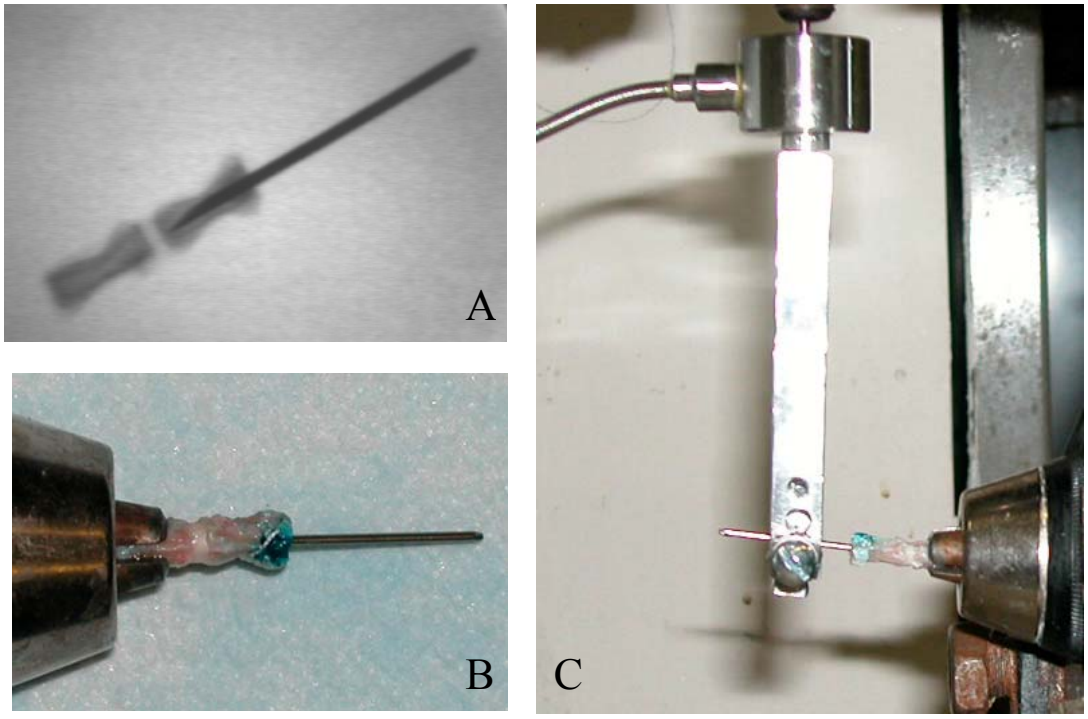


**Figure 2.1** Biomechanical testing. A) Pin longitudinally placed in superior vertebra B) Spinal unit in clamp C) Testing device attached to MTS

*MRI*

*Protocol:* At the 28 day time point, rats were anesthetized with inhaled gas (5% isoflurane in 100% oxygen to induce a surgical plane of anesthesia, 1.5-2.5% thereafter to maintain anesthesia). Rats were placed supine on a plexiglass platform and warmed with a water-recirculated heat pad. The rat's tail was placed in a birdcage radiofrequency coil (3.2 cm diameter, 3.7 cm long), and the apparatus placed in a 2 Tesla magnet (Omega CSI, Bruker Instruments, Fremont, CA) for MRI examination. T2-weighted sagittal images of the three stabbed discs were obtained with a field of view of 4.5 cm, an image matrix of 128 X 128, a slice thickness of 1.5 mm, a repetition time (TR) of 2000 msec, and an echo time (TE) of 60 msec.

*Specimen groups:* Disc groups for MRI analysis were stab 28-day recovery (6) and control (3).

*Analysis:* Images were analyzed according to the methods outlined by Sobajima et al [120] using Image J Software (NIH, Bethesda, MD). The nucleus pulposus of each disc was outlined on the screen to define a region of interest. The area and average signal intensity of the region of interest was computed using Image J. An MRI index (the product of the area and average signal intensity) was calculated for each disc. A two sample t-test was used to compare the MRI indexes of the control and stabbed disc groups. Significance was set at $p<0.05$.

## 2.3 Results

*Histology (Figures 2.2 and 2.3)*

All control discs had a rounded nucleus pulposus which comprised at least one-half of the disc area in midsagittal sections. Nuclear cells were mostly stellar shaped and exhibited normal staining (green). Nuclear cell clusters were centralized with proteoglycan matrix located at the periphery. The endplates were continuous. The annulus consisted of well-organized collagen lamellae and fibroblastic cells.

At the 4-day time point, the nucleus pulposus from the stabbed discs was approximately one-half of the disc area. It was rounded in one case, but irregularly shaped due to inward annular bulging in the three other cases. Nuclear cells were mostly stained green, but two specimens also had some rounded cells containing proteoglycan (stained red). The endplates were continuous. The stab was visible in the annulus in two specimens. Annular cells were fibroblastic.

At the 7-day time point, the nucleus pulposus of the stabbed discs had decreased to approximately one-fifth of the total disc area. Inward bulging of the inner annulus was present in four of five specimens. Nuclear cells were stellar and green in one sample, rounded and green in two samples, and a combination of both types in two samples. Nuclear cells were evenly distributed throughout the nucleus in all specimens. The stab incision was visible in four samples. A herniation of the nucleus into the annulus was present in one sample. One disc had concentric tears in the annulus. Annular cells were fibroblastic with no proteoglycan staining in two of five samples. In the other three specimens, annular cells were approximately half fibroblastic and half chondrocytic with little extracellular proteoglycan.

At the 14-day time point, the nucleus pulposus was acellular, irregularly shaped, poorly stained, and corresponded to one-eighth of the disc area in two of five samples. The endplates were disrupted in one of these two samples. In the three other specimens, the nucleus pulposus corresponded to one-fourth of the total disc area, with the inner annulus systematically bulging inward. Nuclear cells were large, rounded, contained proteoglycan, and were organized into clusters in two samples. Cells were smaller, and formed no clusters in the third sample. The stab was present in one sample and visible but healed in another. Between collagen lamellae, annular cells were approximately half chondrocytic with proteoglycan in and around them, and half fibroblastic.

At the 28-day time point, the nucleus pulposus had disappeared in two of five specimens. In the two specimens with no nucleus, the endplates were discontinuous. The area where the nucleus had been contained only disorganized collagen and fibroblasts. In the three other specimens, the nucleus pulposus represented about one-fourth to one-third of the disc area. The nucleus was not rounded due to inward bulging of the inner annulus. Nuclear cells were mostly rounded and large with proteoglycan in the cytoplasm. Nuclear cells were grouped into clusters and separated by dense areas of proteoglycan. Two of these three cases had a nuclear tissue hernia through the annulus. A radial tear corresponding to the stab incision was present in one case and a scar had formed in the other two cases. Annular cells appeared chondrocytic with intra and extra cellular proteoglycan. The endplates were continuous in these three specimens.

At the 56-day (8 week) time point, all discs contained a nucleus pulposus that represented one-fourth to one-half of the disc area. The endplates in all samples were continuous. The nuclear cells appeared chondrocytic and were surrounded by large

amounts of proteoglycan and the annulus contained both chondrocytic and fibroblastic cells. Proteoglycan production was observed between the lamellae of the annulus. Bone tissue adjacent to the discs appeared normal.

At the 112-day (16 week) time point, all discs had continuous endplates and contained a nucleus pulposus which represented one-fourth to one-half of the disc area. The annulus contained proteoglycan between collagen lamellae and annular cells were both chondrocytic and fibroblastic. The nucleus contained large amounts of proteoglycan with clusters of chondrocytic cells. Bone tissue adjacent to the discs appeared normal.

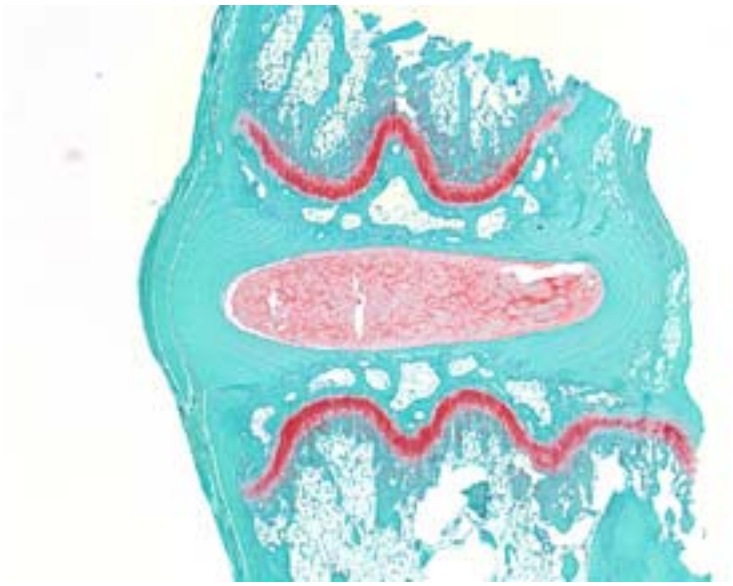

**Figure 2.2** Sagittal image of a control disc stained with Safranin-O and fast green (2x). Collagen lamellae are neatly arranged in concentric circles surrounding the nucleus pulposus.

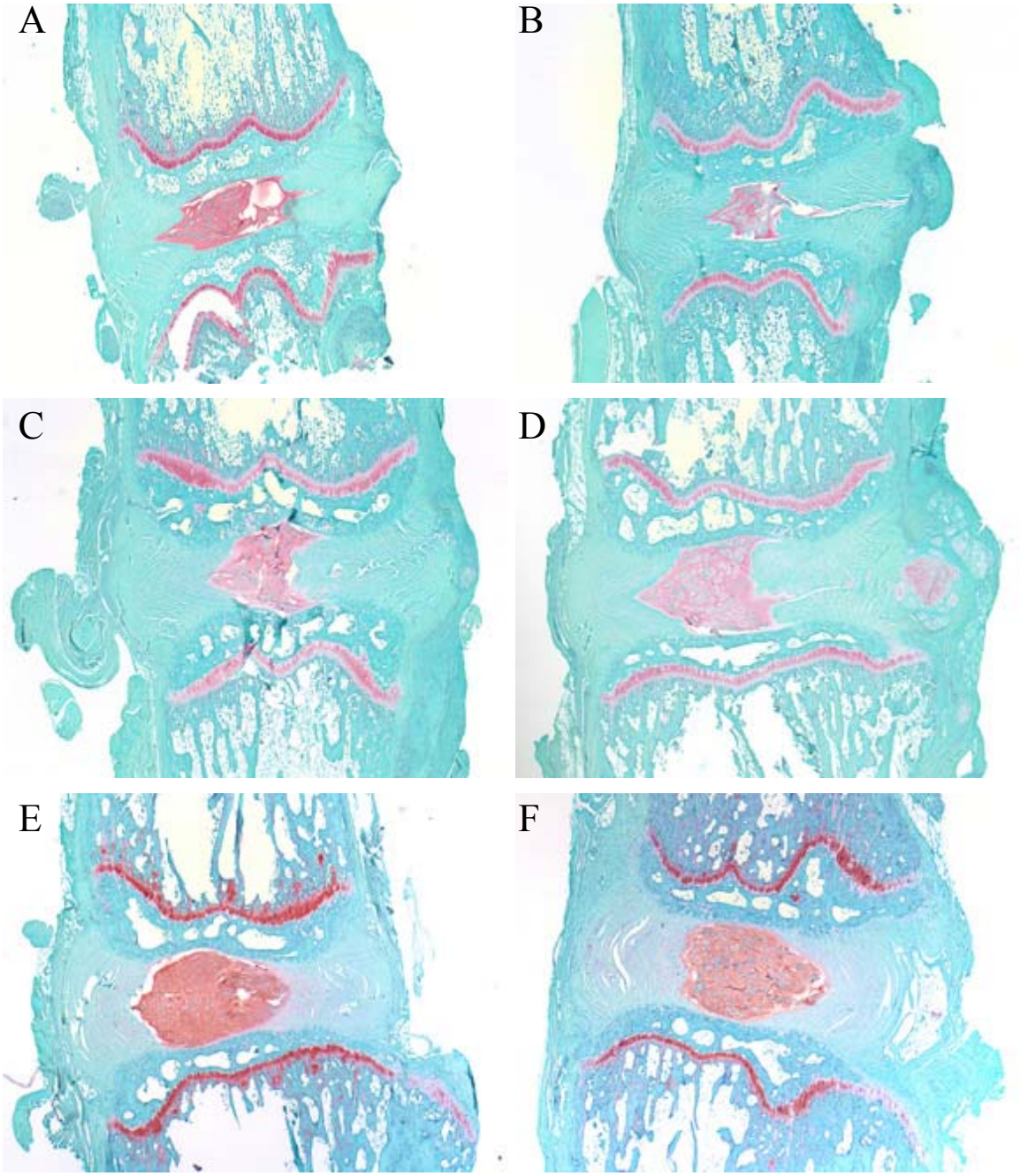


**Figure 2.3** Safranin-O and fast green stained sagittal sections. A) Stab 4-day recovery; B) Stab 7-day recovery; C) Stab 14-day recovery; D) Stab 28-day recovery E) Stab 56-day recovery; F) Stab 112-day recovery.

*Immunohistochemistry (Figures 2.4 and 25)*

No positive staining was observed in the negative control sections using goat and rabbit IgG at the same concentration as the primary antibodies.

In the control discs, most annular cells were negative for IL-1β, TNF-α, and IL-6 and stained positive for IL-8. Nucleus pulposus cells were negative for IL-1β and TNF-α. Many control disc nuclear cells were positive for IL-6 and IL-8 and heavy extracellular IL-6 staining was observed in the nucleus.

At the 4 and 14-day time points, annular cells were positive for TNF-α along the wound tract and a few positive cells were located throughout the annulus. At the 28 and 56-day time points, most annular cells were negative for TNF-α throughout the disc. Nuclear cells were negative for TNF-α at all time points.

At the 4 and 14-day time points, some discs had annular staining for IL-1β on the side of the stab and some did not. More cells were positive for IL-1β on the side of the disc containing the stab incision than on the opposite side of the disc. Little annular cell staining for IL-1β was observed at the later time points. Nucleus pulposus cells did not stain positive for IL-1β.

At the 4 and 14-day time points, most annular cells were negative for IL-6 in some discs and most annular cells were positive in other discs. At the 28 and 56-day time points, annular cells were approximately half positive and half negative. Heavy extracellular staining was present in the nucleus at the early time points and appeared lighter at later time points.

Most annular cells at all time points stained positive for IL-8. Some nuclear cells were positive while others were negative. The chondrocyte-like cells present in the wound tract were darkly stained for IL-8 in discs where the wound tract was visible.

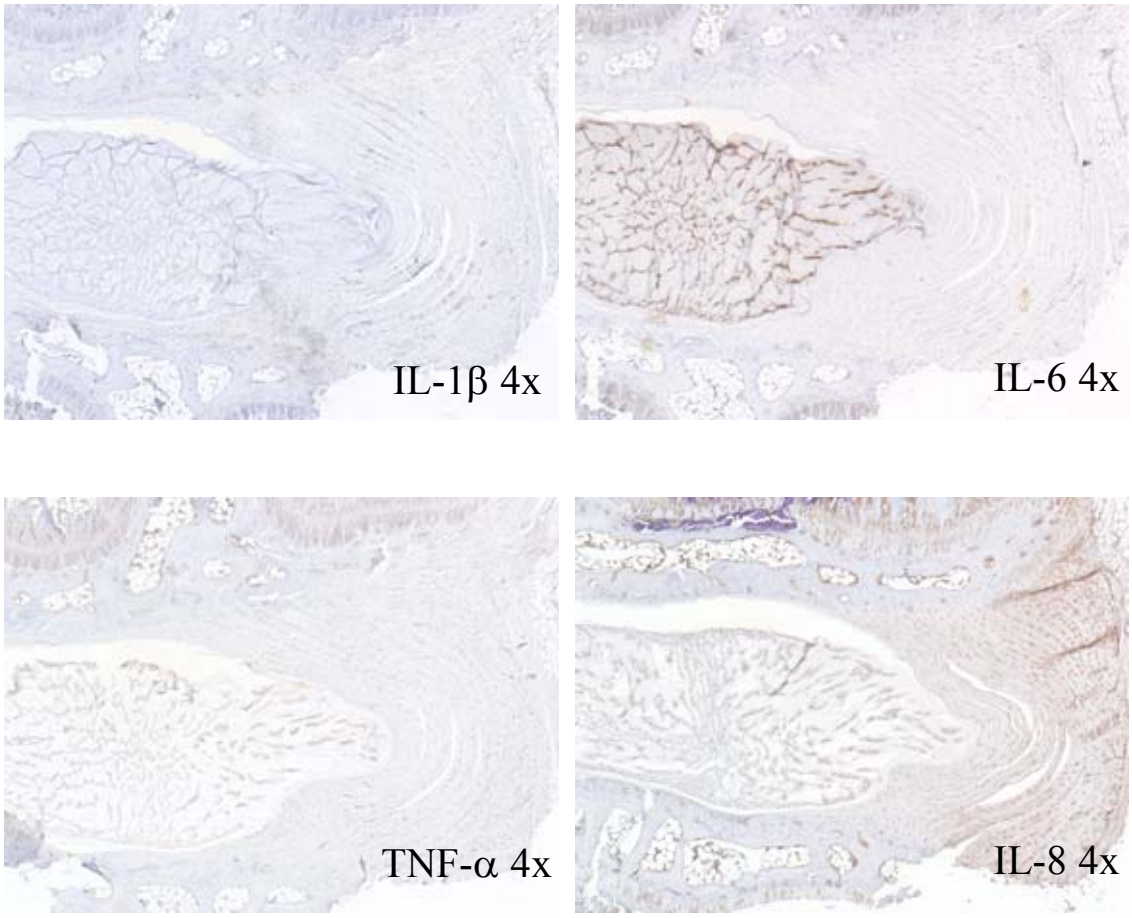


**Figure 2.4** Control disc immunohistochemistry. Little staining for IL−1β and TNF-α was observed. Annular cells stained positive for IL-8 and nuclear cells stained positive for IL-6.

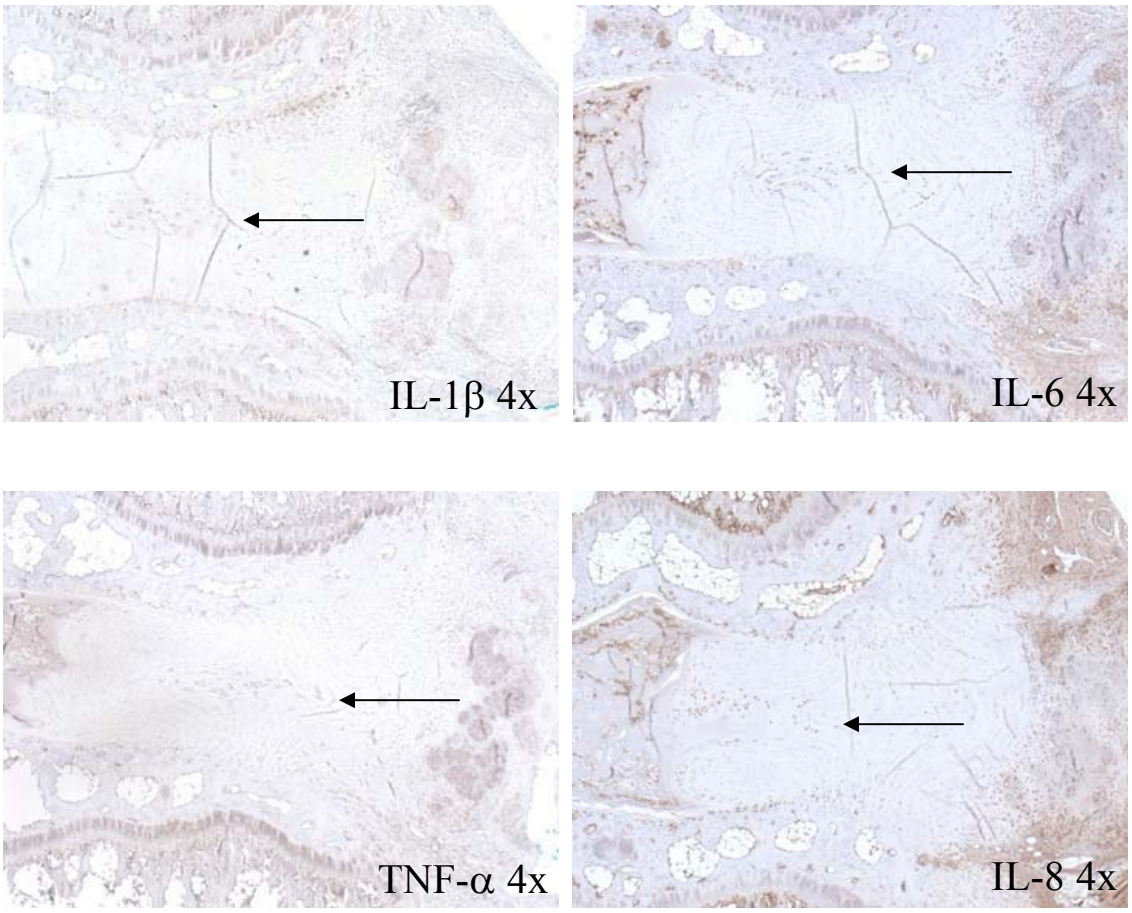


**Figure 2.5** Single-stab cytokine immunohistochemistry after 28-day recovery period. Cells stained positive for IL-1β, IL-8, TNF-α, and IL-6 in the wound tract as indicated by the arrows.

*Cytokines (Figures 2.6-2.9)*

IL-1β levels peaked at day 4, reaching 8.1 ng/g which was significantly different from the concentration at all other time points (p=0.006). TNF-α levels did not significantly differ from control levels at any time point (p=0.491). IL-8 levels peaked 4 days following surgery at 11.3 ng/g, but was not quite significant (p=0.052). IL-6 levels did not significantly change over time (p=0.075).

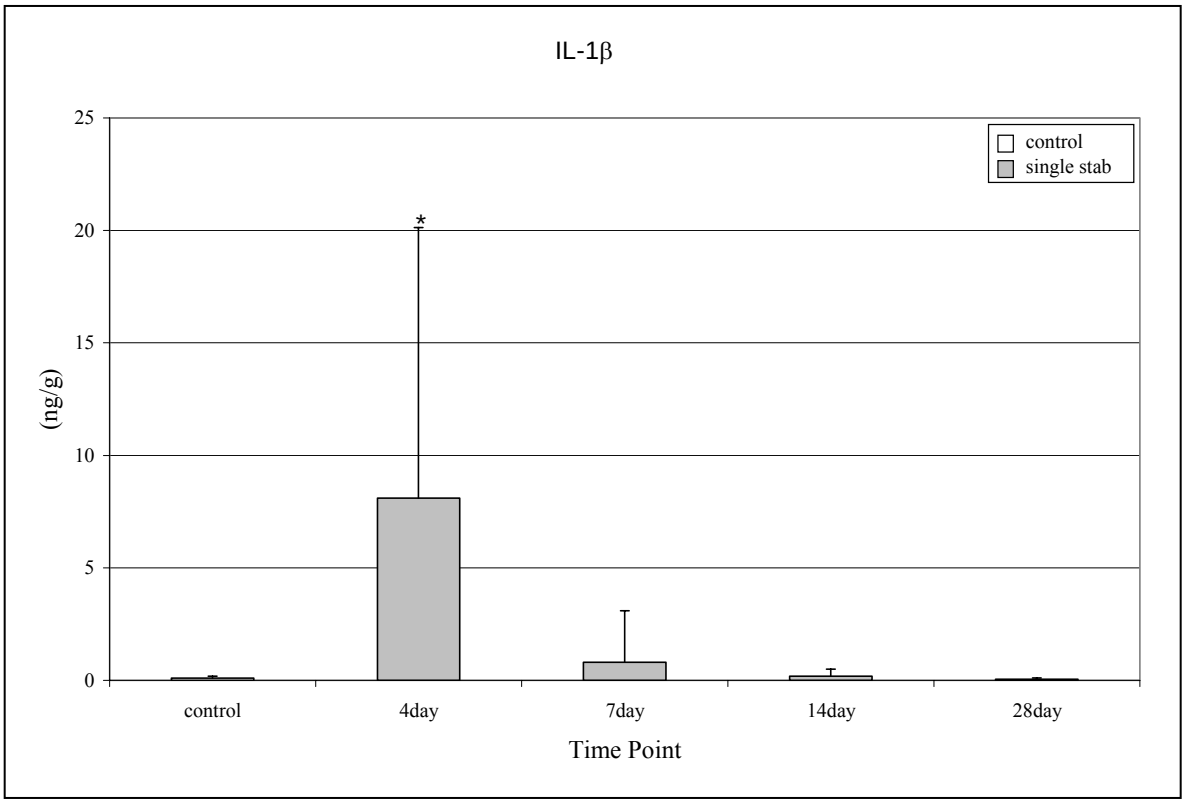


**Figure 2.6** Concentration of IL-1β present in the disc following single-stab annular injury. * = significantly greater than control (p<0.05).

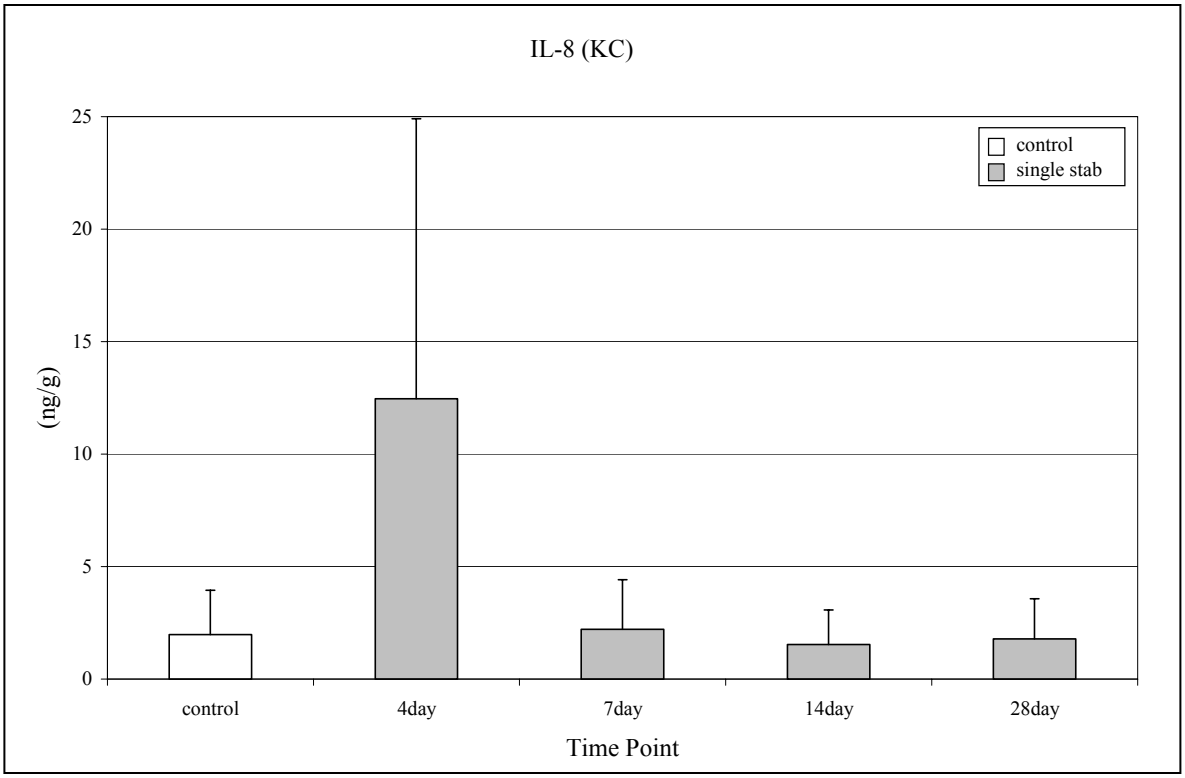


**Figure 2.7** Concentration of IL-8 present in the disc following single-stab annular injury. Although a large increase in IL-8 was observed four days following injury, this increase was not statistically significant (p=0.052).

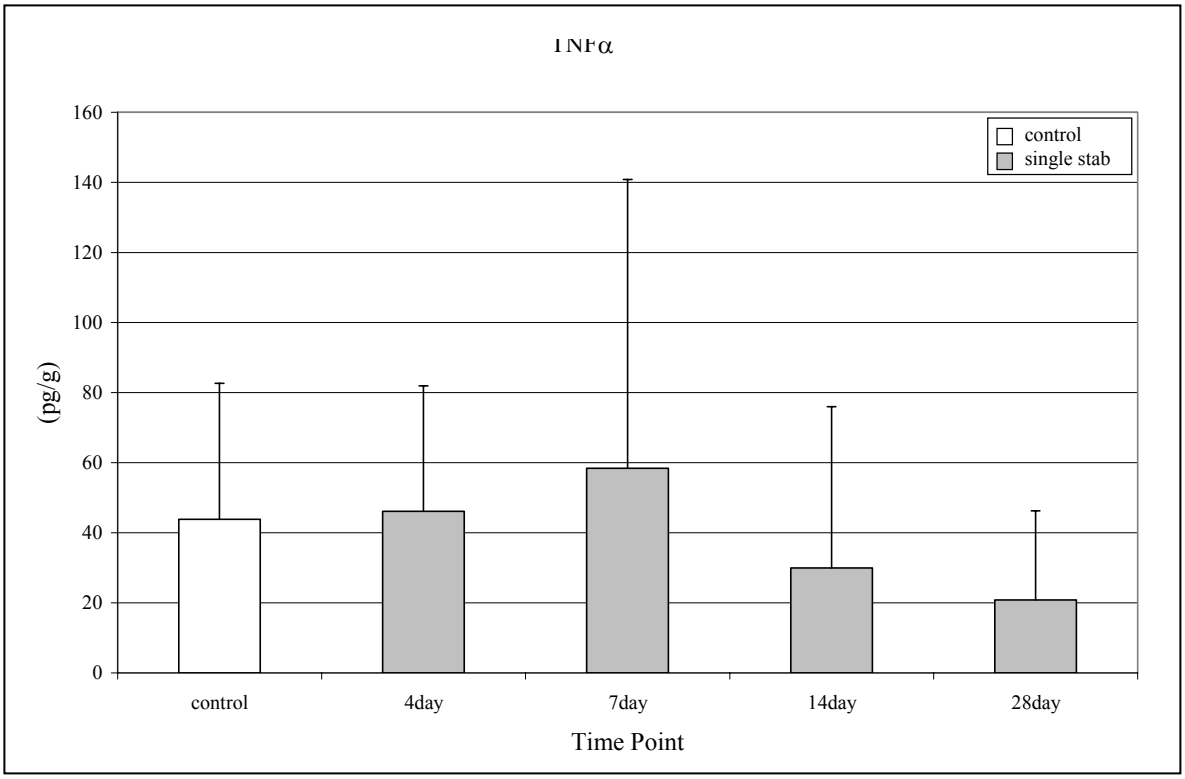


**Figure 2.8** Concentration of TNF-α present in the disc following single-stab annular injury. No statistically significant changes were observed.

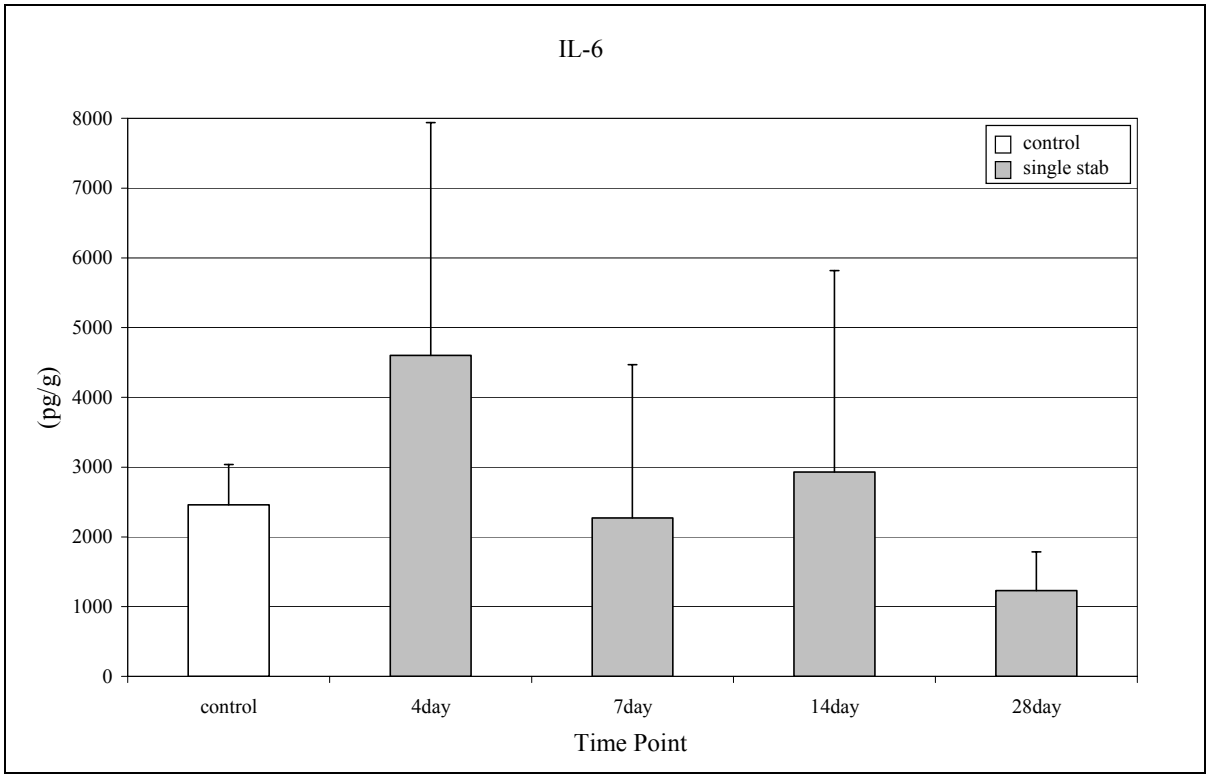


**Figure 2.9** Concentration of IL-6 present in the disc following single-stab annular injury. No statistically significant changes were observed.

*Biomechanics*

The neutral zone and SUBS on both sides of the elastic zone were not significantly different in the sham and stab groups.

*MRI*

The MRI index was not significantly different in the control and stabbed disc groups ($p=0.938$).

## 2.4 Discussion

The goal of this study was to evaluate a rodent tail stab model of degenerative disc disease. The results demonstrate that stab injury to the rat-tail intervertebral disc

induces early, transient elevations in IL-1β and IL-8 and morphological signs of degeneration within 7 days. Despite histologic evidence of degeneration, tail discs did not demonstrate significant differences in bending behavior or MRI index after stab injury.

The degenerative changes that we observed in the rat model are similar to those described for human disc degeneration [21, 139]. Architectural and cellular changes involved both the nucleus pulposus and the annulus fibrosis. Nuclear depressurization led to annular layer disorganization, inward bulging of the inner annulus, and concentric and radial annular tears. A compensatory proteoglycan production was observed in both the nucleus and annulus, similar to what has been reported for stabbed rabbit discs [109]. In the rat, this was associated with cellular modifications: green quiescent stellar cells turned to large rounded chondrocyte-like cells, similar to what has been noted previously in a rat spondylosis model [140]. Compensatory nuclear proteoglycan production was coincident with nuclear cell cluster formation. Despite the injury-stimulated proteoglycan production, nuclear size decreased and reached complete disappearance with associated endplate disruption at 28 days. This indicates a failure in disc repair mechanisms as described in rabbit disc degeneration [109]. Similar to human disc degeneration data [14], the proteoglycan content time course was different in the annulus and the nucleus pulposus, showing an increase of proteoglycan in the annulus in moderately degenerated discs but a continuous decrease in the nucleus. Between 28 days of recovery and 112 days of recovery, few morphological changes were observed indicating that further degeneration of the disc extracellular matrix was not occurring.

By 28 days after stab incision, cytokine expression in the annulus was primarily localized to the wound tract and adjacent tissue. This restricted staining indicates that a wound healing response is occurring at the incision site rather than a degenerative response involving the entire disc. This localized healing response in the rat is similar to that observed following an ovine annular lesion where healing is confined to the annular tissue surrounding the wound and not observed elsewhere in the disc [141].

IL-1β, IL-6, IL-8, and TNF-α have been detected in herniated human discs [42, 45] and can sensitize dorsal root nociceptivity [59]. It is unclear whether the high levels of IL-1β and IL-8 we observed were produced by cells associated with granulation tissue formation or by disc cells. IL-1β has been shown to stimulate matrix metalloproteinases, nitric oxide, IL-6, and prostaglandin $E_2$ production in human disc cells *in vitro* [51]. IL-8 is associated with acute inflammation, the development of radicular pain, increased nerve sensitivity, and vessel growth [66]. Our histology and cytokine data suggest that transient IL-1β and IL-8 elevation are involved the in the pro-inflammatory cascade leading to disc degeneration after the stab injury, perhaps by sensitizing disc cells to shear stress [142]. The absence of cytokine elevation after four weeks is consistent with observations in larger animals [122], and suggests that in a stab model, cytokine elevation is transiently associated with granulation tissue formation and wound tract healing, rather than resulting from chronic cytokine production by disc cells [143]. Our immunohistochemistry staining confirms that after a 28-day recovery period, cytokine production is limited to the tissue surrounding the wound tract. Levels of TNF-α were minimal, as reported in human and murine disc cell culture, even after LPS stimulation [143, 144] and in human disc biopsies [145]. Taken together, these results suggest that

chronic cytokine elevation may be associated with an ongoing process of peripheral annular repair, perhaps stimulated by damage accumulation from mechanical instability and aberrant tissue stress [104].

Although the stab injury induced histological changes and transiently activated pro-inflammatory factors in the discs, the disc biomechanical properties were unaffected. Neither the neutral zone length nor the SUBS of the stabbed discs and non-stabbed discs were significantly different. This may be due to a rapid peripheral granulation tissue formation that effectively seals the disc and helps maintain nuclear pressure. Subsequently, residual disc cells can synthesize nuclear matrix and reconstitute disc height similar to that observed after chemonucleolysis [104]. This observation suggests that progressive degeneration after stab injury may be partially dependent on disc size. That is, a slower healing rate for larger discs may allow more damage accumulation under physiologic loads.

Surprisingly, the MRI index was not significantly affected by the annular injury. Because the size of the nucleus is a factor in MRI index calculation, it would be expected that as the nuclear size decreases, so too would the MRI index. Researchers using rabbits [120] and dogs [123] observed decreases in MRI index and signal intensity following an annular stab incision. The low sample size of imaged discs and the small volume of a rat disc nucleus pulposus may have limited our ability to detect differences.

Rodent models for disc degeneration may serve as convenient tools to screen novel treatments. For example, successes at recovering morphology and reducing inflammation in the tail model could lead to efficacy studies in more challenging and costly model systems. In this regard, tail discs may be used as a platform to investigate

approaches meant to recover morphology such as delivery of growth factors, bio-inductive matrices, or cells. More aggressive degeneration inducing measures may be required to observe the chronic inflammation present in human degenerated discs.

In summary, a single stab injury was successful in creating rapid histologic changes in rat tail discs. Nuclear size decrease, annular layer disorganization, and cellular changes were consistent with human degenerative discs. Further, we demonstrated that some cytokines noted in human herniated discs (IL-1β, IL-6, IL-8, and TNF-α) were either unaffected or only transiently elevated after stab injury.

## Chapter 3 Analysis of a Triple Annular Stab to Induce Chronic Intervertebral Disc Inflammation

### 3.1 Introduction

Low back pain causes tremendous health and economic problems that are compounded by uncertainty surrounding risk factors and underlying etiologies. The precise relationship between disc pain and disc degeneration is unclear. There is growing evidence; however, that painful disc degeneration differs from asymptomatic disc degeneration by the presence of pro-inflammatory cytokines. Disc tissue excised from painful human discs has elevated levels of certain cytokines compared to tissue from asymptomatic discs. These cytokines associated with painful disc degeneration include interleukin-1 (IL-1), interleukin-6 (IL-6), interleukin-8 (IL-8), and tissue necrosis factor-alpha (TNF-$\alpha$) [44, 71, 81]. In addition to possible production by the granulation tissue present in degenerative discs, *in vitro* studies have demonstrated that disc cells themselves are capable of producing these cytokines [42, 43, 47, 49]. Pro-inflammatory cytokine production by disc cells may be stimulated by abnormal loads [8, 51], fragments of degraded matrix materials [146], and other cytokines [43, 44]. These pro-inflammatory cytokines are involved both in the process of disc matrix degeneration and in the genesis of pain through nerve contact [41].

Animal models of disc degeneration are essential for evaluating the efficacy and safety of novel treatment ideas and should closely mimic the morphological and biochemical conditions of a human symptomatic degenerated disc [102]. Most animal models developed to date lack inflammation, which is sometimes associated with painful human disc degeneration. For example, annular injury to rat discs induces only transient inflammation, and these discs heal within several weeks to recover normal inflammatory

factor levels and morphologic features [147]. Alternatively, animal models with repetitive aberrant disc loading demonstrate significant inflammation and peripheral annular damage [148, 149]. This observation is consistent with epidemiologic evidence that indicates that repetitive biomechanical stress is an important risk factor for work-related musculoskeletal disorders, of which low back pain is one [150]. Cumulative trauma leading to degenerative disorders suggests that repeated application of low magnitude force leads to a vicious cycle of inflammation and matrix damage [151]. Analogous situations have been described for other chronic inflammatory diseases, where the application of a single noxious insult can be accommodated without long-term consequences, whereas repeated dosing leads to chronic inflammation [152]. For example, lung tissue can heal after experiencing one to two injuries. After three or more injuries, however, the tissue is wounded such that the damage progressively increases in extent and severity [153] . These studies suggest that a single-stab annular injury may be insufficient to induce the chronic inflammation associated with human disc degeneration and repetitive injuries may be necessary.

To better clarify the processes that differentiate an acute wound healing response to annular injury from a chronic degenerative response, a triple-stab rat-tail model for disc degeneration was investigated. Morphologic, biochemical, and immunohistological outcome measures were used to compare and contrast the disc's response to a triple-stab and a single-stab to determine whether cumulative disc injuries will induce a chronic inflammatory response mimicking that of human disc degeneration.

## 3.2 Methods

*Animals*

Three month-old Sprague Dawley rats were used. All procedures were approved by the Institutional Animal Care and Use Committee of the University of California at San Francisco. Because rats reach skeletal maturity before 3 months of age, animal growth did not interfere with IVD remodeling [137].

*Surgical Approach*

General anesthesia was administered using ketamine (90 mg/kg IP) and xylazine (10 mg/kg IP). Buprenorphine (0.01 mg/kg SQ) was administered once before recovery and then as needed to control postoperative pain. Atipamezole HCL (0.2 mg/kg IP) was used for anesthesia reversal. Food, drink, and activity were unrestricted post-operatively.

A 2.5 cm longitudinal incision was made along the tail to expose the lateral portion of tail discs Co5/Co6, Co6/Co7, and Co7/Co8. Lateral stabs were performed so that the incision would be on primary plane of motion for tail discs. A number 11 blade was inserted 1.5 mm into the disc to depressurize the nucleus. A clamp was placed on the blade to prevent the blade from penetrating the disc more than 1.5 mm and radiographic images were captured to ensure the blade was parallel to the endplates to avoid endplate damage. The blade was then removed and the tail skin was closed using separated stitches. Discs were then percutaneously stabbed with a 23-gauge needle at three days and again at six days after the initial blade injury. The three and six day time points were chosen to coincide with the peak inflammatory response observed after single-stab injury. The discs were re-injured at the same location as the original blade

stab. Fluoroscopic guidance was used to ensure proper needle placement and to control needle depth (1.5 mm into the disc). Recovery times for the triple-stab animals were measured from the time of the initial blade injury. Triple-stab discs were examined 9, 14, 28, and 56 days after the initial injury.

*Histology*

*Protocol:* Discs and adjacent vertebrae were harvested, fixed in formalin, decalcified in formic acid, dehydrated, and embedded in paraffin. Six micron sagittal sections were cut through the disc parallel to the direction of the stab. Sections were stained with Safranin-O, fast green, and hematoxylin.

*Specimen groups:* Disc groups were: 9-day recovery (5), 14-day recovery (5), 28-day recovery (5) and 56-day recovery (4). Five uninjured discs were also analyzed.

*Analysis*: Disc and endplate architecture was examined at 2x magnification. Nuclear and annular cellular and extracellular aspects were analyzed using 20x magnification.

*Immunohistochemistry*

*Protocol*: Sections were prepared as described in the histology protocol. Sections stained for TNF-α and IL-1β were treated for 20 minutes at 90ºC in Tris HCL (pH 8.6) followed by 20 minutes of room temperature cooling. Sections were blocked for 30 minutes with 10% goat or rabbit serum and then quenched for 15 minutes in 3% hydrogen peroxide. Primary antibody sources were goat (TNF-α; R&D Systems, Minneapolis, MN: and IL-6; Santa Cruz Biotechnology; Santa Cruz, CA) and rabbit (IL-

1β; Santa Cruz Biotechnology; Santa Cruz, CA: and KC (rat homologue for IL-8); BioVision, Mountain View, CA). Biotinylated secondary antibodies against the species in which the primary antibody was made were used with a Vector ABC Elite kit (Vector Laboratories, Burlingame, CA). Staining was visualized using DAB. For negative control sections, rabbit or goat IgG was used at the same concentration as the primary antibody. Sections were counterstained using hematoxylin.

*Specimen groups*: Each disc analyzed for cytokine immunohistochemistry was stained for IL-1β, IL-6, IL-8, and TNF-α. Disc groups were 9-day recovery (3), 14-day recovery (3), 28-day recovery (3), and 56-day recovery (3). Two control, uninjured discs were also analyzed for each cytokine.

*Analysis*: To observe cellular and extracellular staining, sections were analyzed at 4x and 20x magnification.

*Cytokines*

*Protocol:* Complete discs were harvested, frozen in liquid nitrogen, pulverized or homogenized, and digested in liquid buffer. Levels of TNF-α, IL-1β, IL-6, and KC (the murine homologue to IL-8) were determined using enzyme linked immunosorbent assays (ELISAs) according to the manufacturer's protocols (R&D Systems, Minneapolis, MN). The limit of detection was 10 pg/ml. Cytokine levels were normalized to tissue wet weight and expressed as ng/g tissue.

*Specimen groups:* Triple-stab disc groups were: 9-day recovery (10), 14-day recovery (10), 28-day recovery (10), and 56-day recovery (8). Ten uninjured discs were also analyzed for each cytokine.

*Analysis:* One-way analysis of variance (ANOVA) was used to assess temporal changes in cytokine levels in the triple-stab discs. Cytokine concentrations at certain time points were compared to those from a single-stab model [147]. Single-stab and triple-stab discs at corresponding time points (14 and 28-day recovery) were compared using two-sample t-tests. Significance was set at $p<0.05$.

## 3.3 Results

*Histology (Figure 3.1)*

All control discs had a rounded nucleus pulposus which comprised at least one-half of the disc area in midsagittal sections. Nuclear cells were stellar shaped and cell clusters were centralized with proteoglycan matrix located at the periphery. The endplates were continuous. The annulus consisted of well-organized collagen lamellae and fibroblastic cells.

At the 9-day time point, the nucleus was replaced in two discs with a void and in three discs with disorganized collagen fibers. Disc cells were chondrocytic in the nucleus pulposus and inner annulus, and fibroblastic near the edges of the disc where aligned collagen lamellae were present.

At the 14-day time point, the nucleus pulposus of two discs contained voids, two discs contained disorganized collagen fibers, and one disc contained nuclear tissue representing approximately one-eighth of the disc area. The nuclear tissue contained chondrocytic cells surrounded by large areas of proteoglycan. The endplates were continuous in three samples and disrupted in two samples. Annular cells were both chondrocytic and fibroblastic.

At both the 28-day and 56-day time points, all discs contained disorganized collagen fibers where the nucleus had been and all discs had continuous endplates. Cells were both chondrocytic and fibroblastic. Very little proteoglycan was present in the discs. Marrow spaces in adjacent vertebrae were filled with granulation tissue that contained blood vessels, fibroblasts, and osteoblasts adjacent to bony trabeculae. Osteophytes were present at the vertebral margins.

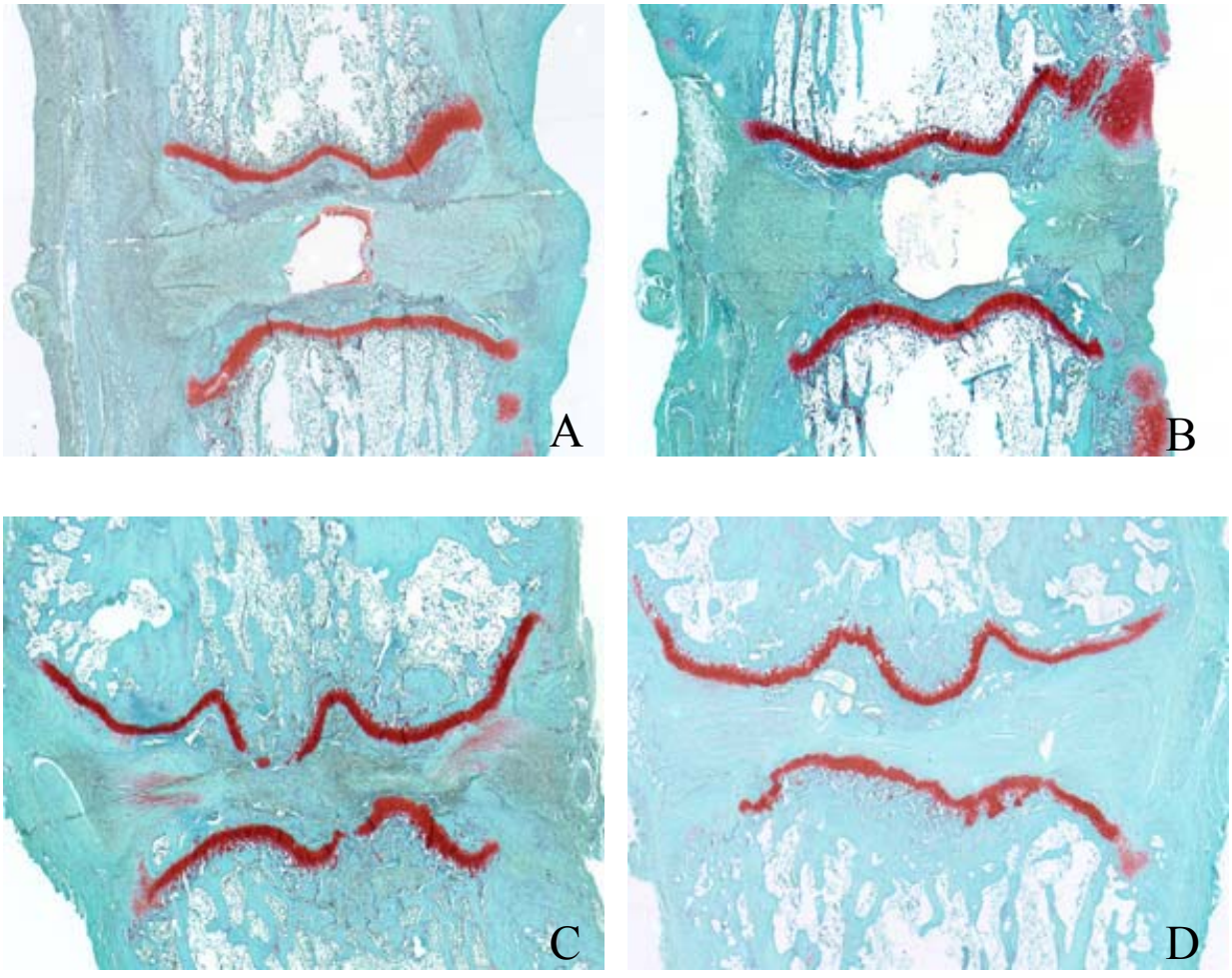


**Figure 3.1** Saffranin-O and fast green stained sagittal sections of triple-stab discs. A) 9-day recovery; B) 14-day recovery; C) 28-day recovery; D) 56-day recovery. For comparison, an uninjured control disc is shown in Figure 2.2 of Chapter 2.

*Immunohistochemistry (Figure 3.2)*

No positive staining was observed in the negative control sections using goat and rabbit IgG at the same concentration as the primary antibodies.

In control discs, most annular cells were negative for IL-1β, TNF-α, and IL-6 and stained positive for IL-8. Nucleus pulposus cells were negative for IL-1β and TNF-α. Many nuclear cells were positive for IL-8, and heavy extracellular IL-6 staining was observed in the nucleus.

At the 9 and 14-day time points after triple-stab injury, most annular cells stained positive for TNF-α. At the 28 and 56-day time points, most cells on the side of the disc that was stabbed stained positive for TNF-α while cells on the opposite side of the disc were approximately half positive and half negative. Cells throughout the discs were approximately half positive and half negative for IL-1β and IL-6 at all time points. Nearly all disc cells stained positive for IL-8 at all time points.

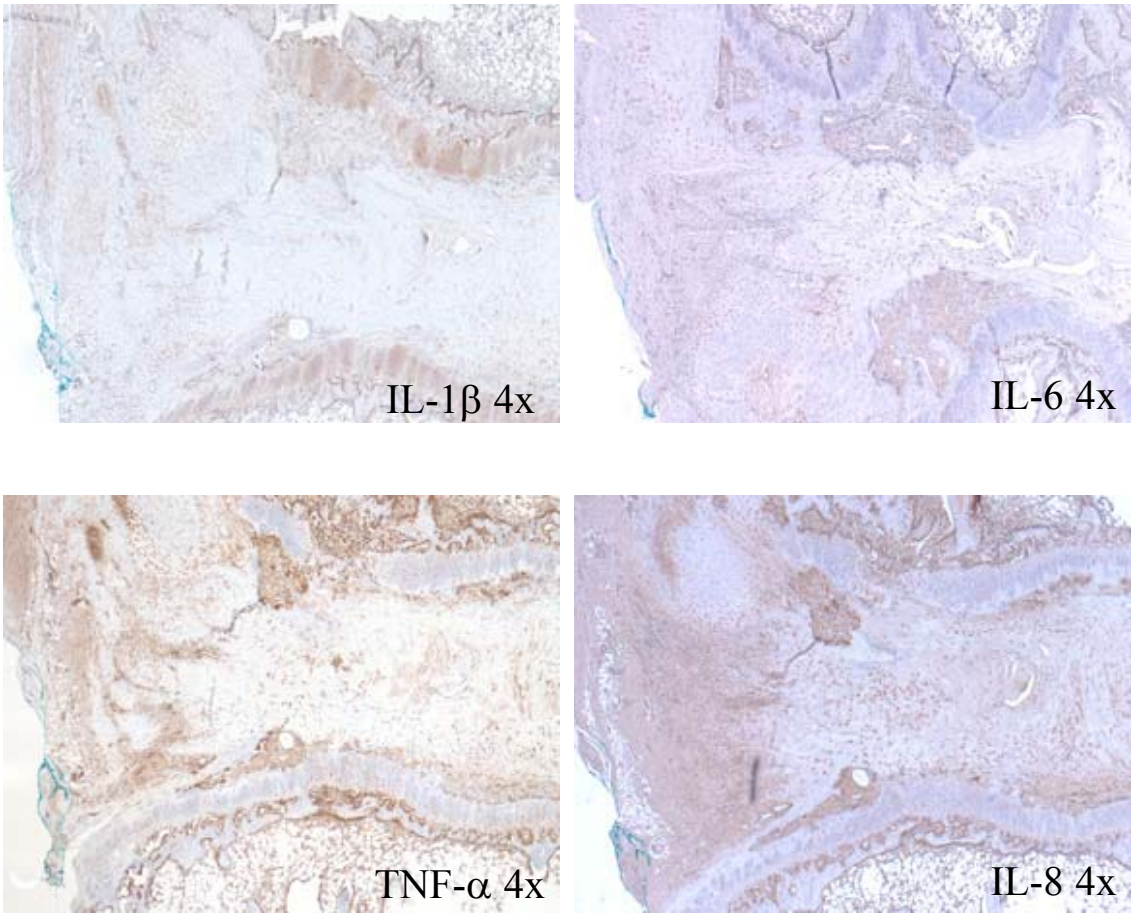


**Figure 3.2** Cytokine immunohistochemistry after 28-day recovery period. Cells stained positive for IL-1β, IL-8, TNF-α, and IL-6 can be observed throughout the disc. For comparison, uninjured control disc immunohistochemistry is shown in Figure 2.4 of Chapter 2. Single-stab immunohistochemistry 28 days after surgery is shown in Figure 2.5 of Chapter 2.

*Cytokines (Figures 3.3, 3.4, 3.5, 3.6)*

In the triple-stab discs, IL-1β levels were significantly higher than control levels at 9 and 14 days after surgery. TNF-α levels were significantly higher than control levels at all time points. IL-8 levels peaked at day 9 reaching 34.5 ng/g, which was significantly higher than the concentration at any other time point ($p<0.001$). IL-6 levels did not significantly change over time.

TNF-α, IL-1β, and IL-8 levels were significantly higher in the triple-stab discs than in the single-stab discs at both 14 and 28 days. IL-6 levels were not significantly different at these time points.

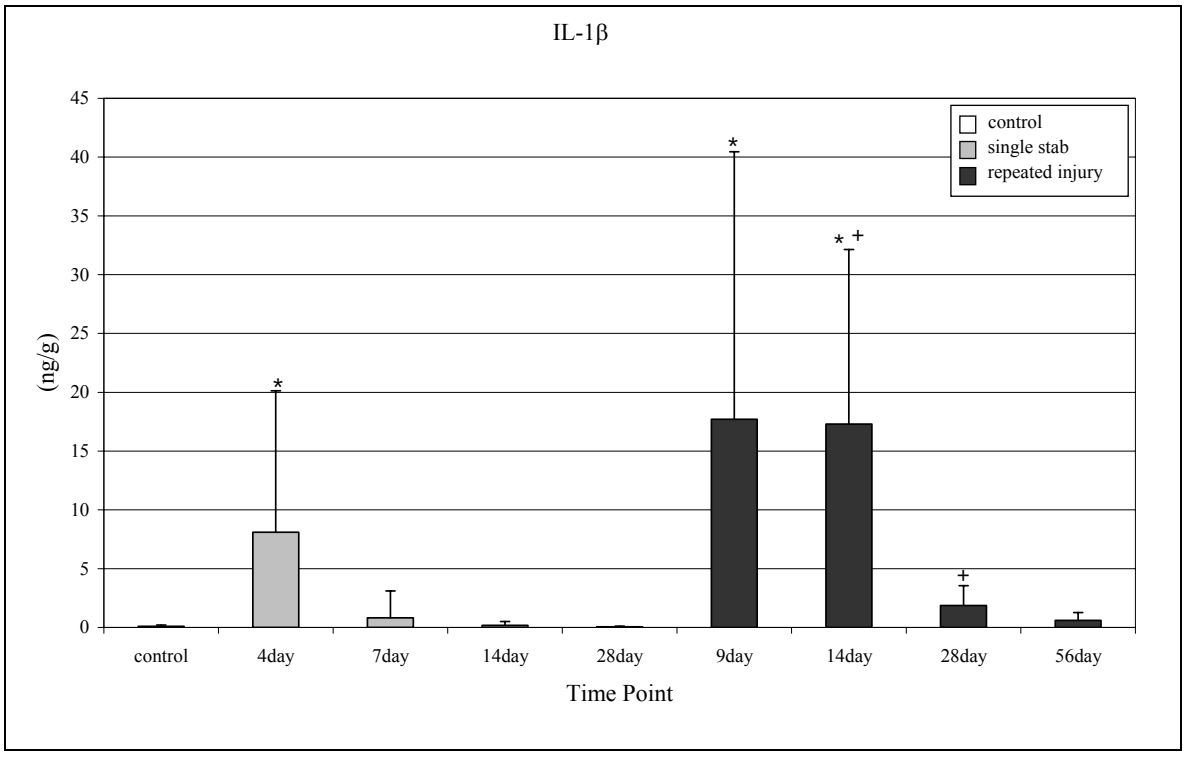


**Figure 3.3** Concentration of IL-1β present in the disc following single-stab and triple-stab annular injury. * = significantly greater than control ($p<0.05$); + = significantly greater than corresponding time point following single-stab.

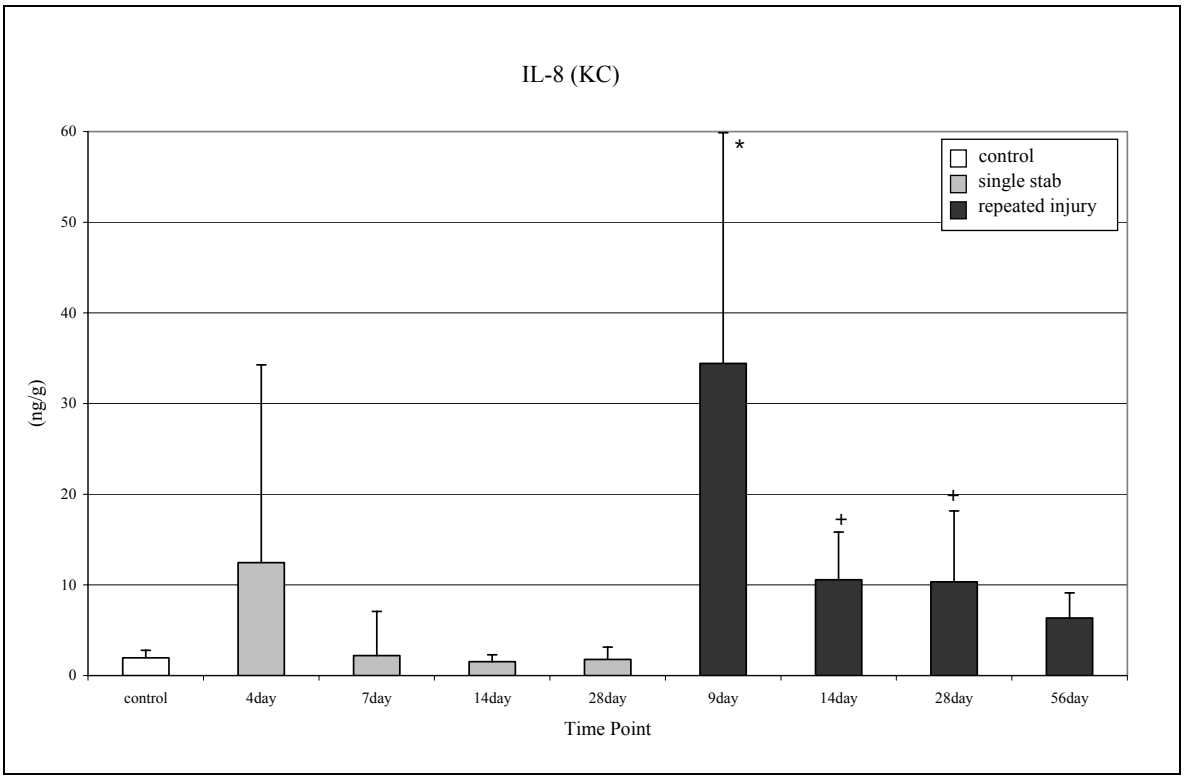


**Figure 3.4** Concentration of IL-8 present in the disc following single-stab and triple-stab annular injury. * = significantly greater than control ($p<0.05$); + = significantly greater than corresponding time point following single-stab.

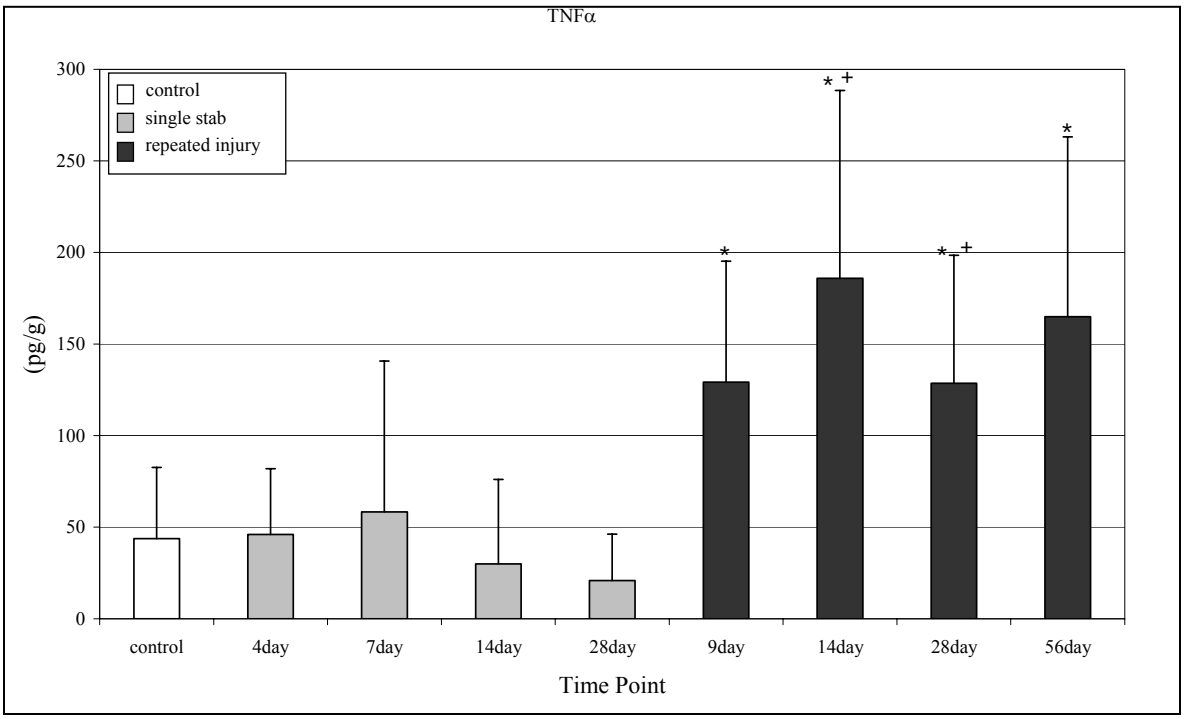


**Figure 3.5** Concentration of TNF-α present in the disc following single-stab and triple-stab annular injury. * = significantly greater than control ($p<0.05$); + = significantly greater than corresponding time point following single-stab.

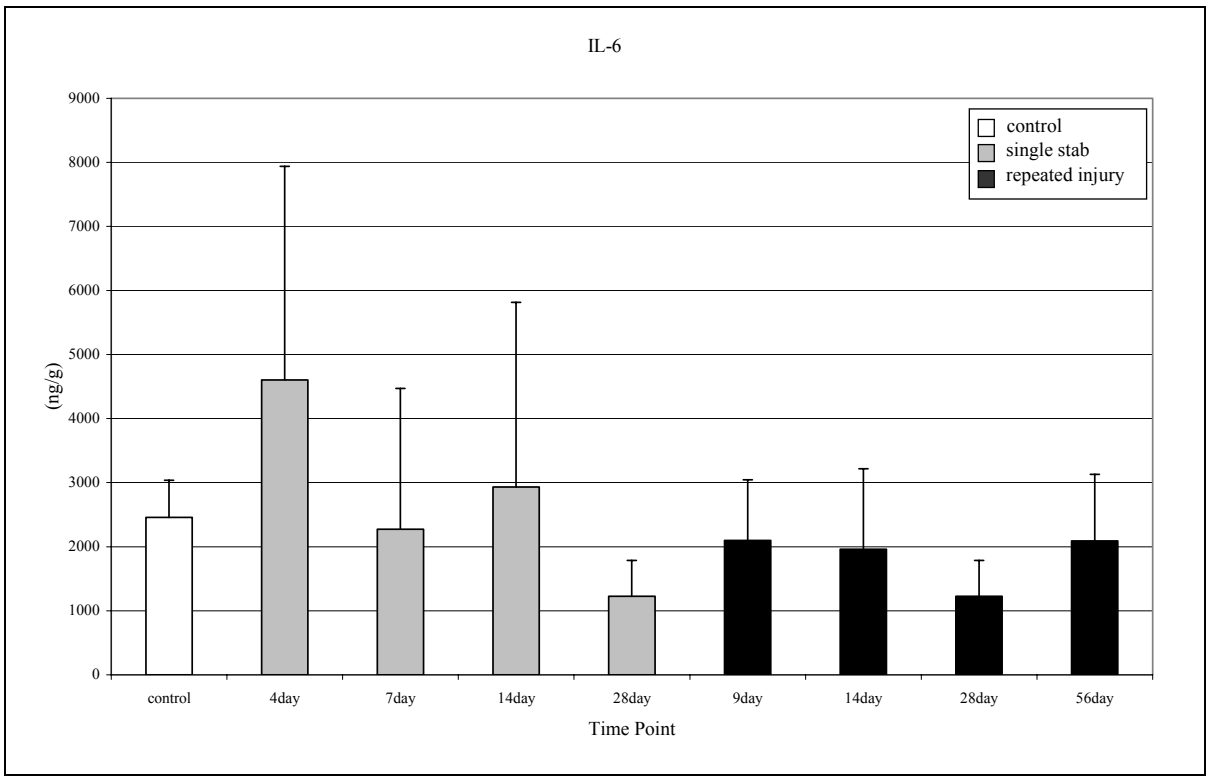


**Figure 3.6** Concentration of IL-6 present in the disc following single-stab and triple-stab annular injury. * = significantly greater than control ($p<0.05$); + = significantly greater than corresponding time point following single-stab.

### 3.4 Discussion

These results demonstrate that repeated injury leads to chronic inflammation and enhanced disc degeneration. While a single-stab disc degenerates with time, it only exhibits transient inflammation that is limited to the wound tract and associated peripheral granulation tissue [147]. By contrast, a triple-stab leads to increased inflammation that continued over the 56-day recovery period and was present throughout the annulus fibrosis. In addition to chronic inflammation, human-like degenerative features were observed in disc morphology after the triple-stab injuries, including a complete disappearance of normal nuclear matrix by 28 days.

The triple-stab injury leads to a distinct disc phenotype distinguished by diffuse pro-inflammatory factor production by activated annular fibroblasts. It has been reported for other tissues that fibroblasts can regulate a progression from acute to chronic inflammation [154]. In the case of acute inflammation and wound repair, activated fibroblasts synthesize IL-1, IL-6 and TNF-α [155]. These cytokines were only present in the wound tract and surrounding tissue in the single-stab discs indicating that a local healing response was occurring at the incision site. The widespread presence of these cytokines throughout the annulus in the triple-stab discs indicates that degenerative changes are affecting the entire disc rather than a localized area surrounding the wound.

Levels of IL-1β, IL-8, and TNF-α were significantly higher at both 14 and 28 days following injury in the triple-stab discs than in the single-stab discs. The ELISA data was supported by immunohistochemistry, which showed a diffuse disc response following triple-stab at 14 and 28 days compared to the local wound healing response surrounding the incision that was observed after single-stab.

While both single and triple-stab disc degenerate, important differences in disc morphology were noted. In triple-stab discs, the nucleus pulposus was replaced by disorganized collagen fibers, very little proteoglycan was present throughout the disc, and annular layers were disordered at 56 days. These changes are consistent with those observed in human disc degeneration [20]. The elevated levels of TNF-α, IL-1β, and IL-8 found in the triple-stab discs may contribute to their pronounced degenerative appearance since these cytokines stimulate production of aggrecanses, matrix metalloprotinases, and other factors involved in tissue breakdown. For example, TNF-α

and IL-1β suppress proteoglycan and collagen production and accelerate the breakdown of proteoglycan [43, 44].

This repeated-injury model provides a convenient system to test the efficacy of anti-inflammatory or regenerative treatments. Clinically relevant outcomes include morphological disruption and inflammation, both of which are associated with painful disc degeneration in humans. Although, we do not have measures that assess animal discomfort, prolonged cytokine production is a feature linked to back pain in humans [71]. IL-1β, IL-8, and TNF-α all increase nerve sensitivity [41, 59, 66], so a reduction in these cytokines may lead to pain relief. The 56-day period of elevated cytokine levels provides a convenient temporal window within which the impact of anti-inflammatory treatments can be assessed.

In summary, these data demonstrate that repeated disc injury that occurs within a period of active healing causes persistent inflammation and enhanced morphological sings of degeneration. Because the human disc is avascular and heals slowly, there may be situations where the rate of tissue damage due to repeated mechanical loading outpaces subsequent attempts to heal. In these cases, this data suggests that degeneration may become pathologic with elevated levels of pro-inflammatory factors, and supposedly increased risk of discogenic pain. If this is true, therapies aimed at both strengthening matrix and quieting inflammation may be particularly effective for treating discogenic pain.

## Chapter 4 Effects of Sublethal Heat on Intervertebral Disc Cells

### 4.1 Introduction

There is growing evidence that painful disc degeneration and asymptomatic disc degeneration can be distinguished by the presence of pro-inflammatory cytokines. Disc tissue excised from painful human discs has elevated levels of certain cytokines compared to tissue from asymptomatic discs. These cytokines associated with painful disc degeneration include interleukin-1 (IL-1), interleukin-6 (IL-6), interleukin-8 (IL-8), and tumor necrosis factor-alpha (TNF-$\alpha$) [44, 71, 81]. These pro-inflammatory cytokines are involved both in the process of disc matrix degeneration and in the genesis of pain through nerve contact [41].

Several low back pain treatments involve procedures which produce heat in the intervertebral disc: intradiscal electrothermal therapy (IDET), percutaneous intradiscal radiofrequency thermocoagulation (PIRFT), and nucleoplasty [100, 156, 157]. Possible therapeutic mechanisms for these procedures include collagen denaturation, cell ablation, tissue breakdown, nerve tissue coagulation, and pro-inflammatory factor reduction [89, 100, 156, 157]; however, the precise mechanism or combination of mechanisms is not known. In addition, the thermal exposures (temperature-time relationships) necessary to achieve these effects are not well defined and the optimal size of the treated region has not been investigated. These treatments target high temperatures, ranging from 70ºC to 90ºC [100, 156-159], in order to denature collagen, ablate nerve fibers, and cause cell necrosis. The disc tissue adjacent to these high temperature regions is exposed to sublethal thermal doses. The effects of sublethal heat on intervertebral disc cells are unclear.

Sublethal temperatures may affect disc cells though the induction of a heat shock protein (HSP) response. HSPs are a group of highly conserved stress proteins that play important physiological roles under both normal and stressed cellular conditions. HSP production can be induced by many stressors, including hyperthermia, hypothermia, hypoxia, acidosis, reactive oxygen species, and reactive nitrogen species [160]. The most temperature sensitive and easily induced HSPs are those of the 70kDa HSP family [161]. The HSP70 family includes four proteins that share common protein sequences and are present in the cytosol, nucleus, and mitochondria of cells [160]. HSP70 can alter cell function through its involvement in protein folding, protein maintenance, refolding of misfolded proteins, movement of proteins across membranes, prevention of protein aggregation, and degradation of unstable proteins [161]. By influencing protein formation and function, HSP70 can affect both the cellular production of and the cellular response to cytokines. HSP70 has been shown to inhibit the production of and decrease the sensitivity to certain cytokines in several cell types [162-164]; however, its effects on disc cell inflammation are unclear.

HSP70 is present in endplate chondrocytes and nucleus pulposus cells during gestation and then decreases in concentration with aging [165]. As discs degenerate, increased expression of HSP70 is observed in the cytoplasm of endplate chondrocytes and nucleus pulposus cells. In addition, HSP70 has been identified in the nucleus of both annulus fibrosis and nucleus pulposus cells in degenerated discs [165]. These observations indicate that discs cells are capable of producing HSP70 and may do so when exposed to stressful conditions. If HSP70 production is increased by intervertebral

disc cells in response to sublethal heat, disc cell function may be affected by reducing cytokine production.

The goal of this project was to investigate the anti-inflammatory effects of sublethal heat on intervertebral disc cells. Rat annulus fibrosis and nucleus pulposus cells were cultured separately and treated with IL-1α to induce a cytokine response. The cells were then heated for one hour at 40ºC or 43ºC. Levels of TNF-α, IL-8, IL-6, NO, $PGE_2$, and HSP70 were analyzed and compared one, four, and seven days after heat treatment.

## 4.2 Methods

The cell isolation and cell culture methods used in this study were developed based on the protocols specified by others examining intervertebral disc cells in alginate bead culture [166].

*Disc Cell Isolation*

Cells were isolated from adult, male Sprague-Dawley rats. Immediately following sacrifice, the eight largest tail discs from each rat were excised. Annulus fibrosis tissue and nucleus pulposus tissue were pooled separately. Both tissues were digested in a 0.4% pronase solution for one hour at 37ºC followed by digestion in a 0.025% collagenase solution overnight at 37ºC. The enzyme solutions were made using DMEM/F-12 containing fetal bovine serum (FBS) and antibiotics. Following digestion, the solutions were passed through a 100 μm cell strainer, rinsed several times with cell dissociation buffer, and centrifuged to separate a cell pellet.

*Cell Culture in Alginate Beads*

Cells were counted and resuspended in an appropriate volume of 1.2% alginate solution to make a concentration of $1x10^6$ cells/mL. Alginate beads were produced by dropping the alginate solution into a 102 mM $CaCl_2$ solution through a 22 gauge needle. After curing for ten minutes at room temperature, ten beads were added to each well of a 24-well plate containing 1 mL of DMEM/F-12 with FBS and antibiotics. The cells were cultured for three days at 37ºC and 5% $CO_2$. Three wells containing 10 beads each were analyzed for nucleus cells and annulus cells for each treatment (control, IL-1α treated, IL-1α + 40ºC, and IL-1α + 43ºC) and each time point (1 day, 4 days, and 7 days).

After three days, the media was changed for all treatment groups. The control wells were cultured in 1 mL of control media (without IL-1α) for the entire study. Wells in the IL-1α, IL-1α + 40ºC, and IL-1α + 43ºC treatment groups were cultured in 1 mL of media containing 10ng/mL of IL-1α (Sigma; St. Louis, MO) for the remainder of the study. Media was replaced every three days for all treatment groups for the rest of the study. Three days after the initial addition of the IL-1α media, the media was replaced, and cells in the IL-1α + 40ºC and IL-1α + 43ºC groups were thermally treated. All groups were cultured at 37ºC and 5% $CO_2$ for the entire study except during media changes and during heat treatment for the thermal therapy groups.

*Thermal Treatment*

During heat treatment, the 24-well plates were placed in an incubator set to either 40ºC or 43ºC for 60 minutes. These temperature and time combinations have been used in other studies to investigate the HSP response of various cell types, including

chondrocytes [167-169]. In the incubator, the plates were placed on aluminum blocks sized slightly smaller than the bottom of the 24-well plates so that the bottom of each well would have direct contact with the aluminum block. This method of heating allowed the cells to reach the target temperature rapidly while avoiding the risk of contamination associated with water bath heating [170]. The blocks had been placed in the incubator at the target temperature at least 48 hours prior to treating the cells to allow them to equilibrate to the incubator temperature. Following 60 minutes of heat treatment, the plates were returned to the 37ºC incubator.

*Sample Collection*

Twenty-four hours before terminating the study of each well, the media was changed so that each sample would contain substances that had been produced by the cells in the preceding 24 hours. One, four, or seven days after heat treatment, the media from each well was collected and stored at -80ºC. The beads were dissolved in a sodium citrate solution (150 mM NaCitrate, 10 mM EDTA, 150 mM NaCl) for 20 minutes at room temperature. The solution was then centrifuged, and the cell pellet and supernatant were stored separately at -80ºC.

*DNA Content*

Cell content was determined by quantifying the DNA in each well. Cell pellets were suspended in TE buffer and DNA was quantified using a PicoGreen assay according to the manufacturer's instructions (Invitrogen; Carlsbad, CA). The results were compared to a standard curve made using DNA from calf thymus of a known

concentration. The amount of DNA in each well was used to calculate the number of cells per well. Cell viability was determined using one alginate bead from each treatment group following the manufacturer's protocols for the Live/Dead Cell Viability Kit (Invitrogen; Carlsbad, CA).

*HSP70 and Inflammatory Factor Analysis*

The concentrations of TNF-α, IL-6, and KC (the murine homologue to IL-8) in the media samples were determined using enzyme linked immunosorbent assays (ELISAs) (R&D Systems, Minneapolis, MN). The concentrations of $PGE_2$ in the media samples were quantified using a competitive binding assay (R&D Systems; Minneapolis, MN). Nitric Oxide (NO) was measured indirectly by quantifying the levels of nitrite in the media samples using a Griess reagent (Sigma; St. Louis, MO). Nitrite concentration was determined using a standard curve made from known concentrations of sodium nitrite. The amount of HSP70 in the cell lysate was quantified using an ELISA kit (Assay Designs; Ann Arbor, MI). All assays were performed according to the manufacturers' protocols. All results (TNF-α, IL-6, IL-8, NO, $PGE_2$, and HSP70) were normalized to the amount of DNA in each well.

*Statistical Analysis*

Results for each treatment group (control, IL-1α, IL-1α + 40ºC, and IL-1α + 43ºC) were compared at each time point (1 day, 4 days, and 7 days) using an one-way analysis of variance (ANOVA). Temporal changes within each treatment group were also compared using an ANOVA. Significance was set at $p<0.05$.

## 4.3 Results

*DNA Content*

DNA content was 7.47 ± 4.8 ng DNA/bead for annulus cells and 9.4 ± 4.4 ng DNA/bead for nucleus cells. Cell viability was estimated at ~90% for both nucleus and annulus cells and remained consistent throughout the study.

*HSP70 (Figure 4.1)*

Stimulation with IL-1α generated significantly more HSP70 at the one-day and four-day time points in nucleus cells. Nucleus cells treated at 40ºC and 43ºC produced significantly less HSP70 than those treated with IL-1α alone at the one-day time point. Four days after thermal therapy, the nucleus cell 43ºC treatment group had significantly more HSP70 than any other four-day group. This was similar to what was observed in annular cells; the 43ºC treatment group had significantly higher concentrations of HSP70 than any other group one, four, and seven days after heat treatment.

*TNF-α (Figure 4.2)*

Stimulation with IL-1α significantly increased TNF-α levels at the one-day and four-day time points in nucleus cells. Less TNF-α was produced by nucleus cells treated at 40ºC than by cells in the IL-1α treatment group at all time points; however, the difference was only significant at the one-day time point. Treatment at 43ºC did not significantly affect TNF-α levels in nuclear cells. Annular results differed from nucleus results. In the annular cells, IL-1α significantly increased TNF-α production at the one-

day time point. While cells treated at 43ºC produced significantly less TNF-α at the one-day time point than the IL-1α treated cells, treatment at 40ºC had no effect. At seven days, both the 40ºC and 43ºC treatment groups had significantly higher TNF-α levels compared to the IL-1α treated cells and the control cells.

*IL-6 (Figure 4.3)*

Stimulation with IL-1α caused a significant increase in IL-6 levels at the one-day and four-day time points in both nucleus and annulus cells. Less IL-6 was produced by nucleus cells treated at 40ºC than by cells in the IL-1α group at all time points; however, the difference was only significant at the four-day time point. Thermal treatment at 43ºC increased IL-6 at the one-day and four-day time points in both nucleus and annulus cells; however, the changes were only significantly different than the IL-1α treatment levels at the one-day time point for the annulus cells. No significant changes were observed in either nucleus cell groups or annulus cell groups at the seven-day time point.

*IL-8 (Figure 4.4)*

Stimulation with IL-1α caused a significant increase in IL-8 levels at the one-day and four-day time points in both nucleus and annulus cells. In nucleus cells exposed to 40ºC, IL-8 production was significantly less than that observed in IL-1α treatment alone and significantly higher than control levels at the one and four-day time points. Nuclear cells exposed to 43ºC had significantly less IL-8 production at the four-day time point compared to that of the IL-1α treatment group. At the one-day and four-day time points, annular cells treated at 43ªC produced significantly more IL-8 than annular cells

stimulated with IL-1α only. No significant changes were observed in either nucleus cell groups or annulus cell groups at the seven-day time point.

*$PGE_2$ (Figure 4.5)*

Stimulation with IL-1α caused a significant increase in $PGE_2$ levels at the one-day and four-day time points in both nucleus and annulus cells. Thermal treatment at 43ºC caused a significant increase in $PGE_2$ levels compared to the IL-1α only group at the one-day time point for both cell types. A decrease in $PGE_2$ levels compared to the IL-1α only group was observed in the 40ºC treated nucleus cells at each time point; however, this change was only significant at the four-day time point. No significant changes were observed in nucleus cells or annulus cells at the seven-day time point.

*NO (Figure 4.6)*

No significant changes were observed in the nucleus cells at any time point. The 43ºC treatment for annular cells significantly increased the concentration of NO one day following treatment. No changes in NO levels were observed at the four-day or seven-day time points in annular cells.

*Temporal Changes*

Following seven days in cell culture, control cells expressed higher concentrations of cytokines compared to control levels at earlier time points. Nucleus cells produced significantly more IL-8, $PGE_2$, and TNF-α, and annular cells produced significantly more IL-8, $PGE_2$, and HSP70 at the seven-day time point.

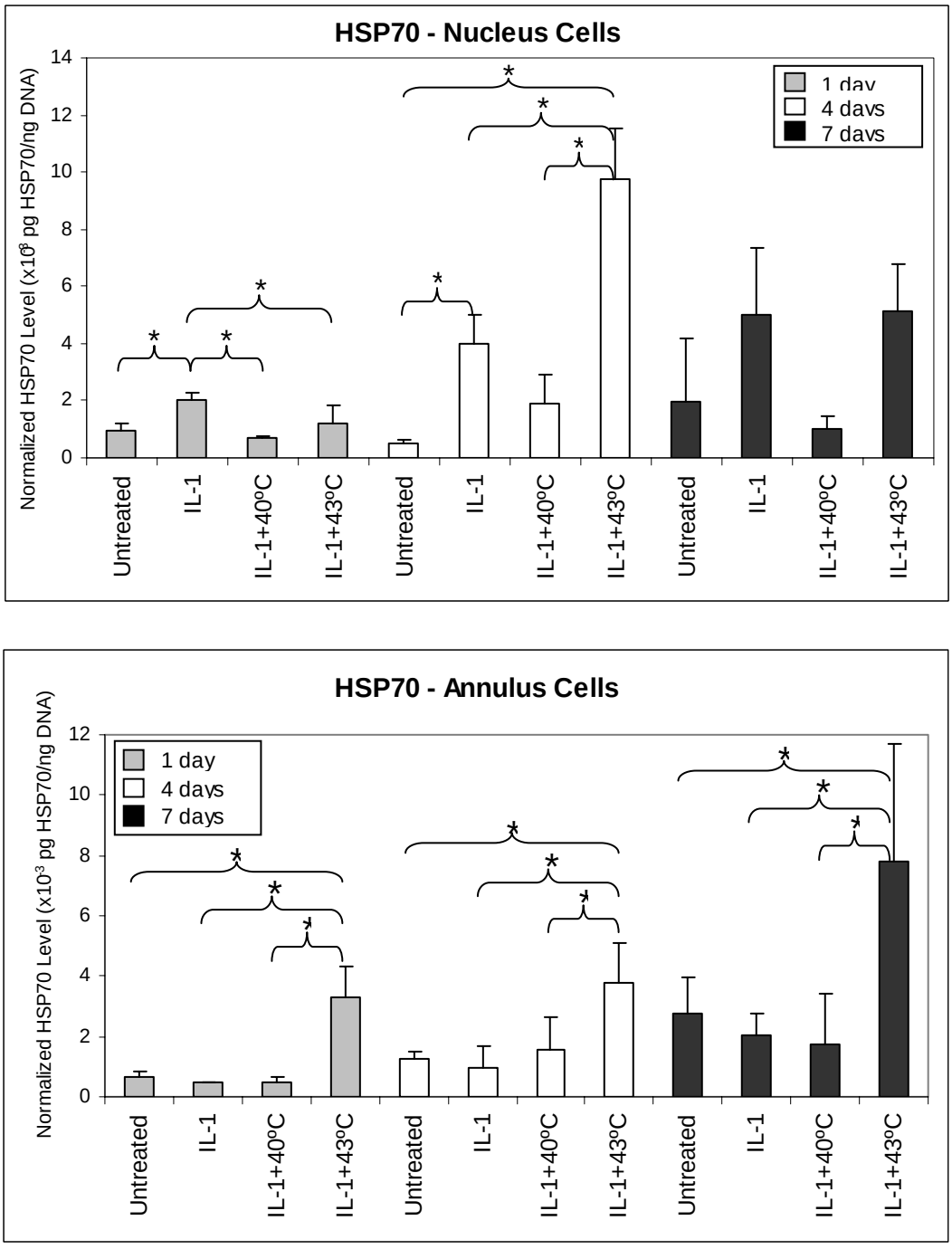


**Figure 4.1** HSP70 levels in culture medium normalized to the DNA content in each corresponding well. * = statistically significant difference ($p<0.05$).

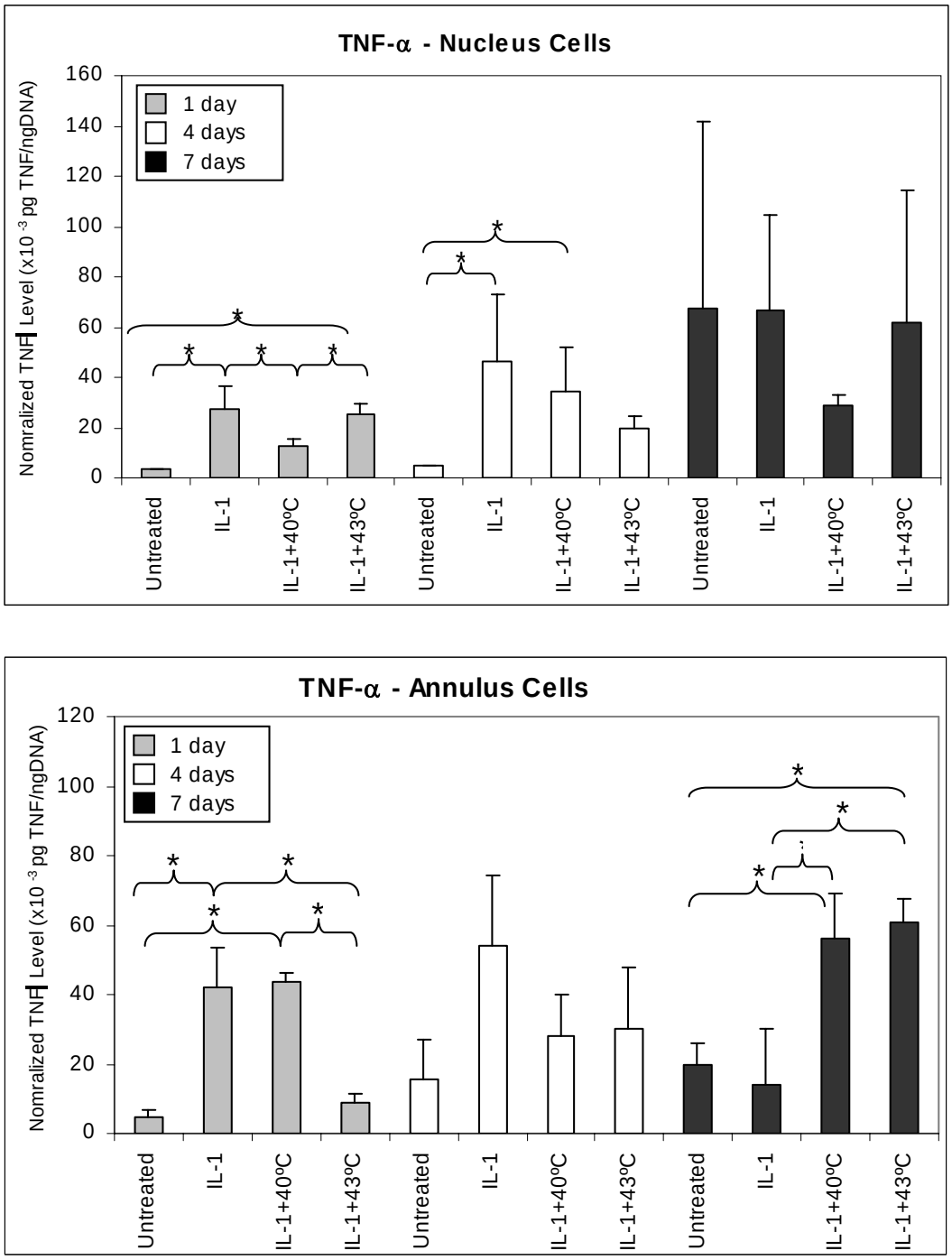


**Figure 4.2** TNF-α levels in culture medium normalized to the DNA content in each corresponding well. * = statistically significant difference ($p<0.05$).

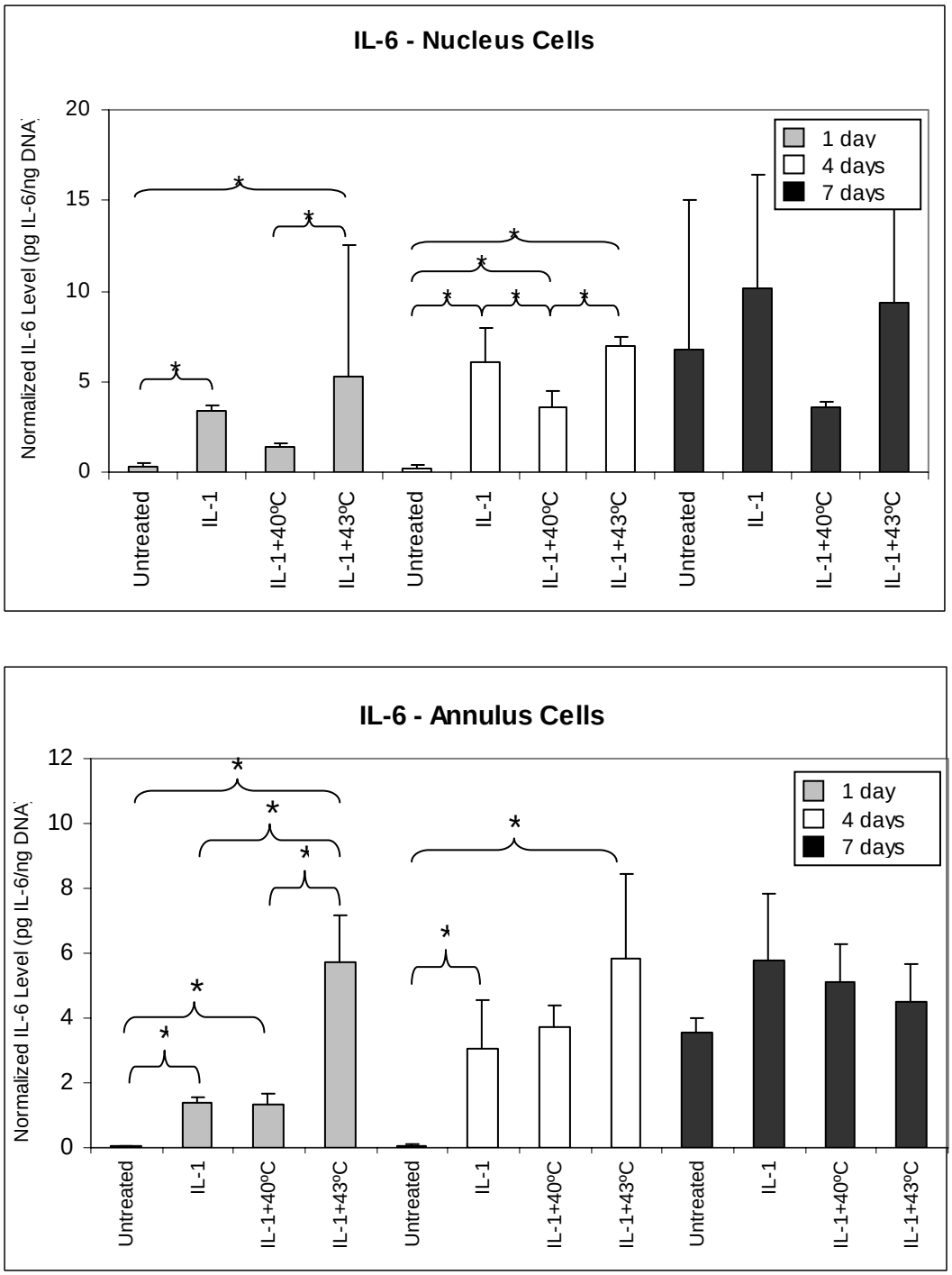


**Figure 4.3** IL-6 levels in culture medium normalized to the DNA content in each corresponding well. * = statistically significant difference ($p<0.05$).

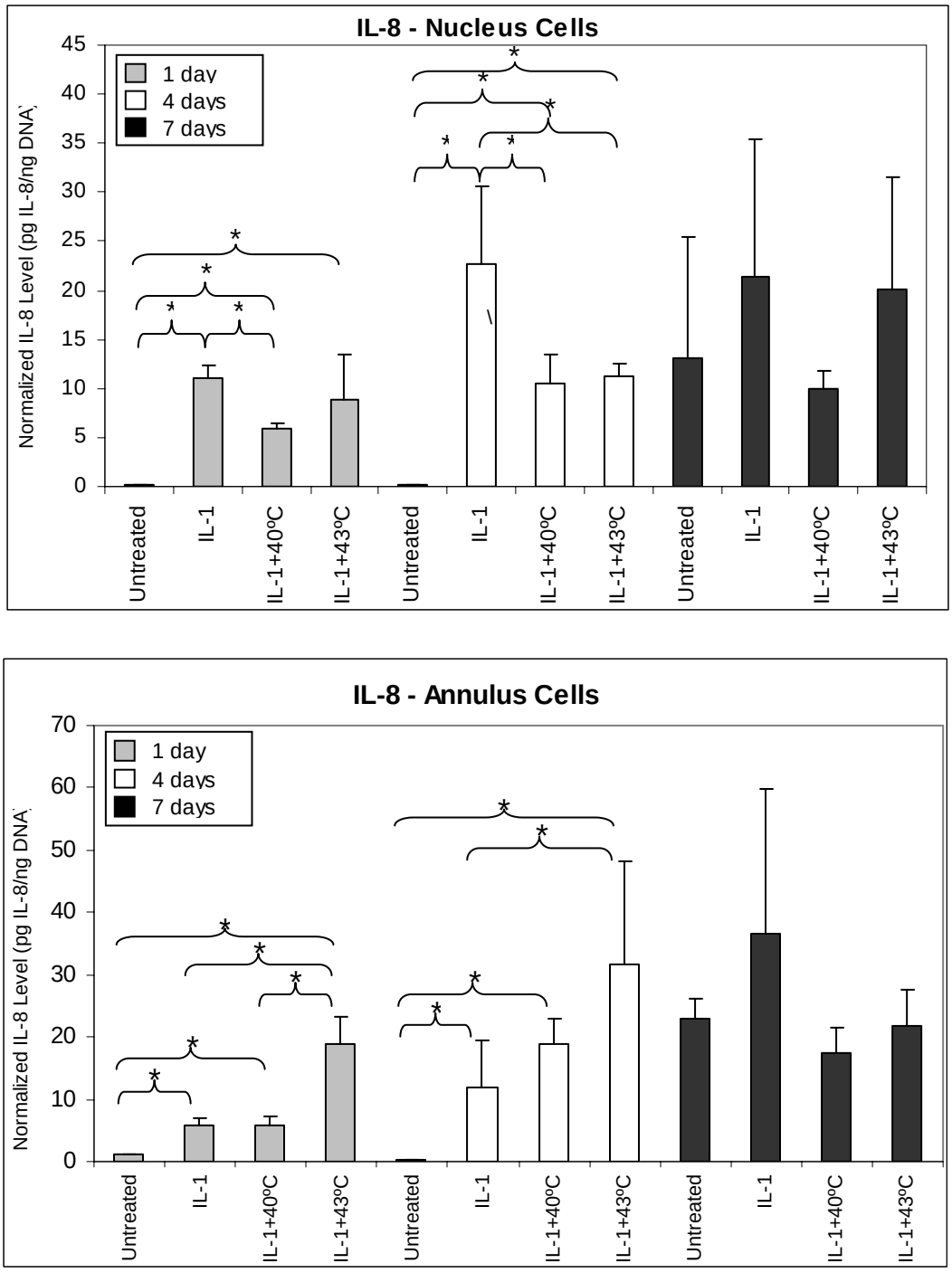


**Figure 4.4** IL-8 levels in culture medium normalized to the DNA content in each corresponding well. * = statistically significant difference ($p<0.05$).

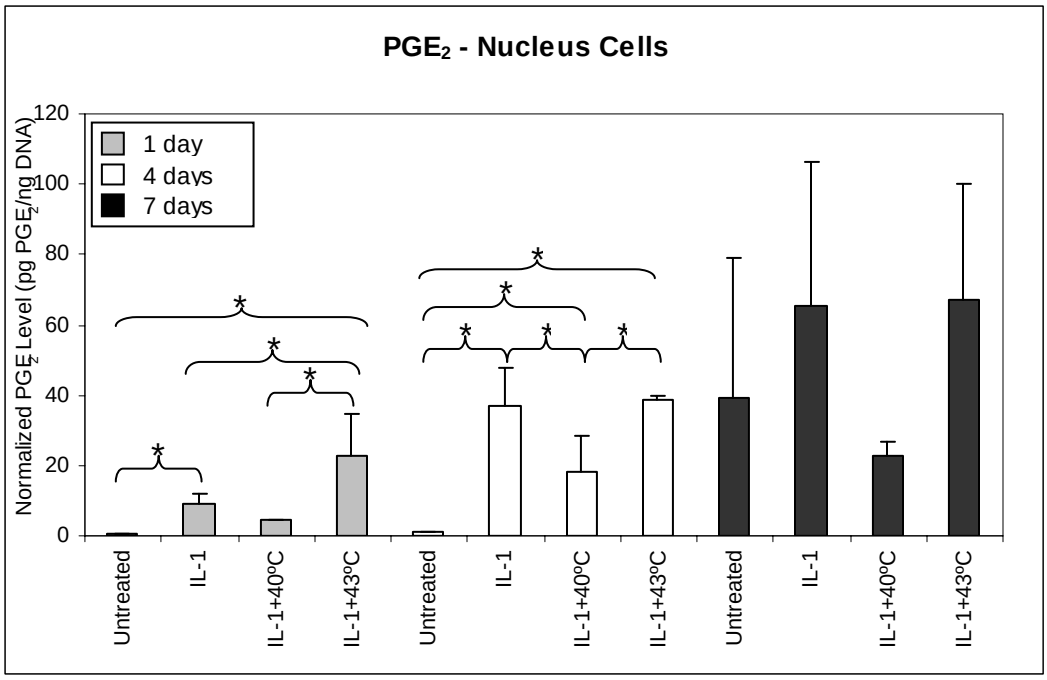


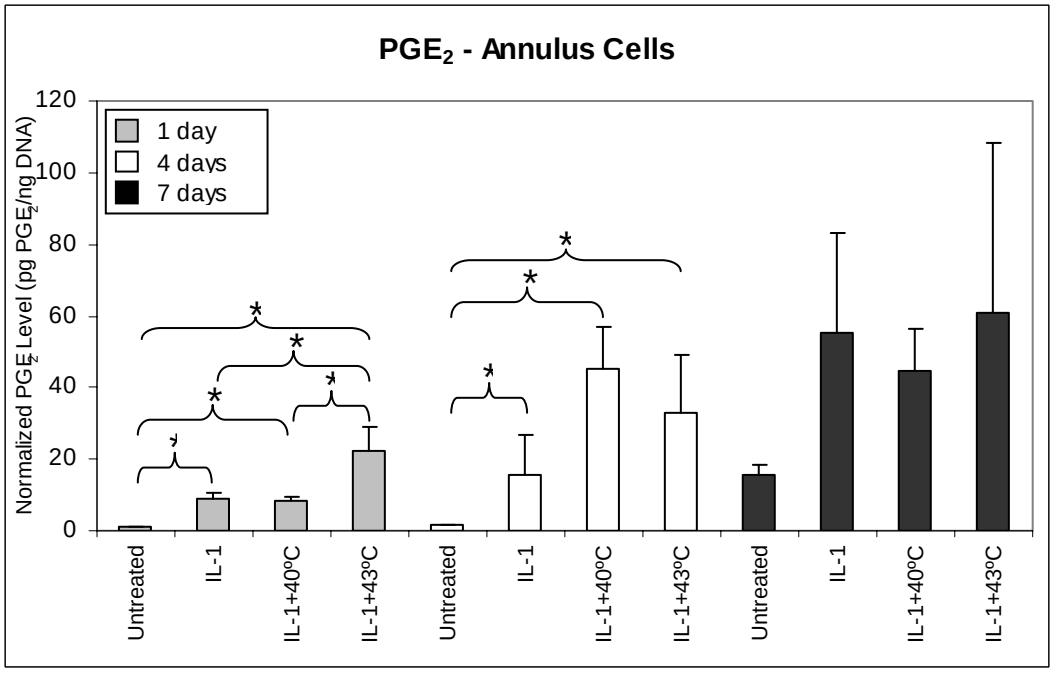


**Figure 4.5** $PGE_2$ levels in culture medium normalized to the DNA content in each corresponding well. * = statistically significant difference ($p<0.05$).

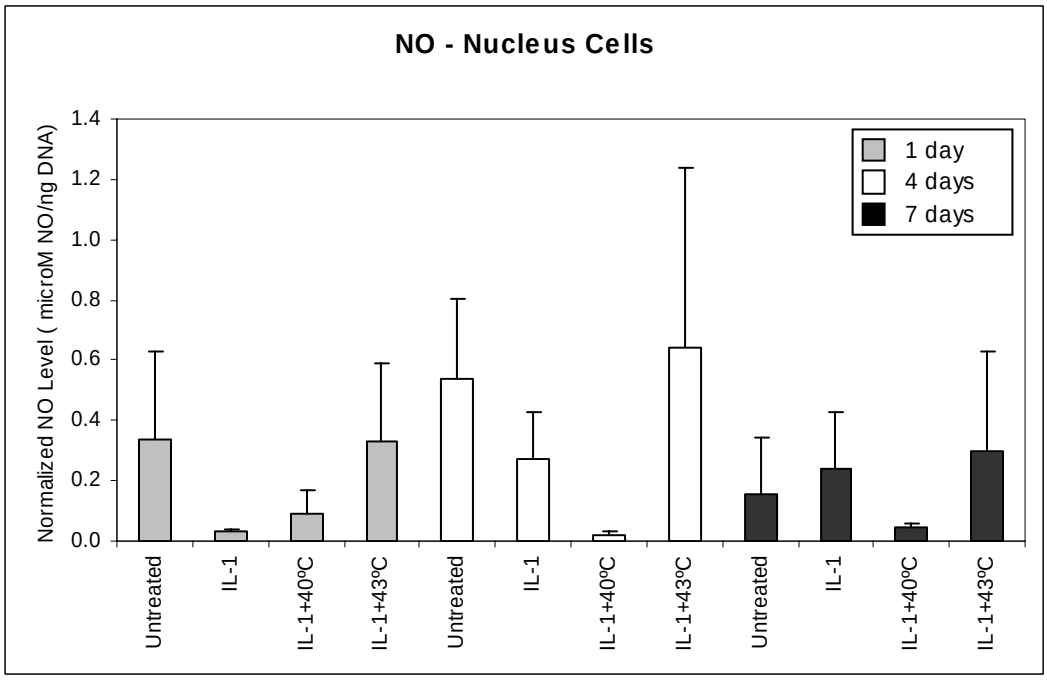


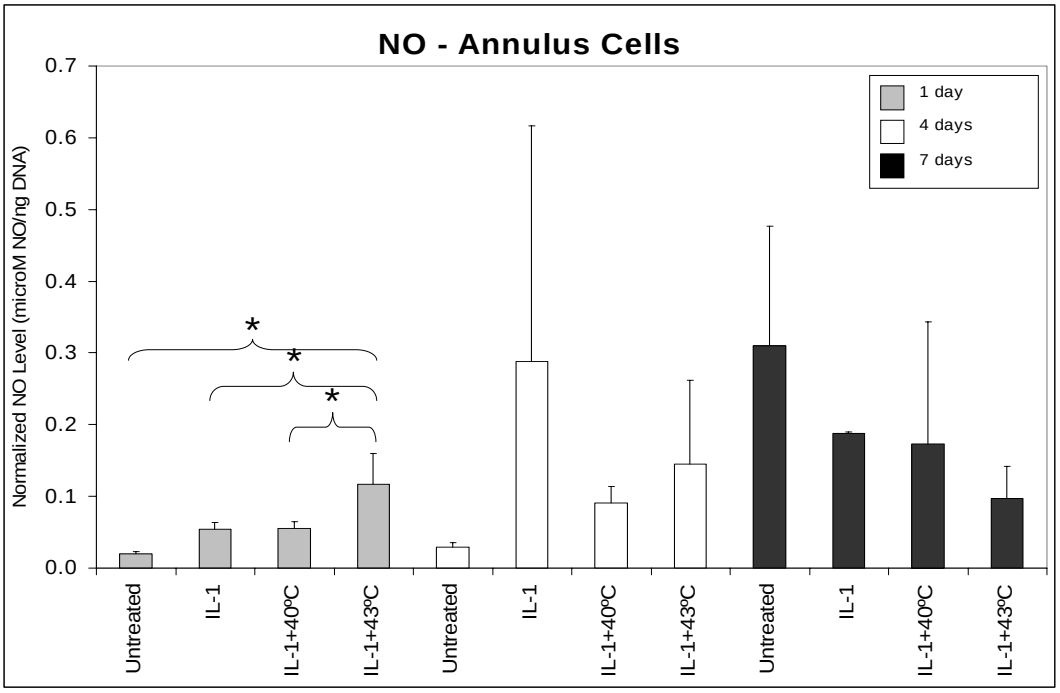


**Figure 4.6** NO levels in culture medium normalized to the DNA content in each corresponding well. * = statistically significant difference ($p<0.05$).

## 4.4 Discussion

In this study, nucleus and annulus cells were thermally treated at two different exposures following stimulation with IL-1α. Treatment with IL-1α increased the production of most cytokines in both cell types. HSP70 levels were significantly elevated in annular cells at all time points following treatment at 43ºC, but were unaffected by the 40ºC treatment. An increase in HSP70 was also observed in nuclear cells at the four-day time point following treatment at 43ºC. The cellular cytokine response to thermal therapy varied between cell types and was dependent upon thermal dose. Thermal therapy significantly elevated the concentration of some cytokines while significantly lowering the concentration of others. These results indicate that the cellular response to thermal therapy may differ between nucleus and annulus cells, and that the production of some cytokines may be more affected by thermal therapy than others.

Following simulation with IL-1α, a significant elevation of pro-inflammatory factor levels ($PGE_2$, IL-8, IL-6, TNF-α) was observed at the one-day and four-day time points for both nucleus and annulus cells. This inflammatory response is consistent with the observations of others [51, 166] and indicates that the cells are producing and surrounded by pro-inflammatory factors as they are in degenerative discs [44, 71]. HSP70 levels were also elevated in nucleus cells following stimulation with IL-1α as has been observed in other cell types [168]. Cytokine levels were elevated in control cells at the seven-day time point. This elevation of control cell cytokine levels at seven days indicates that the cells were responding their culture environment by producing inflammatory factors and rationalizes why few significant changes due to thermal treatment were observed at this time point.

Similar to these findings using both annulus and nucleus cells, others have observed that temperatures ranging from 41ºC to 43ºC for one hour are necessary to induce a heat shock response whereas treatments at or below 40ºC fail to induce one [169]. The HSP response is dependent upon both treatment temperature and duration of exposure [171]. In this study, the shortest endpoint following thermal treatment was 24 hours. Other studies have identified HSP peaks at shorter time points indicating that HSP production could have spiked and then started to recovered before the first measurement [172], so the values reported in this study may not be indicative of the maximal heat shock response. For example, following chondrocyte incubation at 42.5ºC for one hour, the maximal levels of RNA for HSP were observed one hour after heat shock [168].

Thermal treatment significantly affected cytokine production in both nuclear and annular cells. Elevated HSP70 production may have caused the observed changes in cytokine levels. HSP accumulation can inhibit both pro-inflammatory cytokine transcription and secretion [160, 162, 163, 173]. When under stress, cells prioritize which genes are expressed and can inhibit the production of certain proteins to accommodate the upregulation of others. This indicates that the reduction of pro-inflammatory cytokines associated with hyperthermia could be due to increased HSP production at the expense of cytokine production [174]. HSPs may also inhibit cytokine production through the inactivation of transcription factor NF-κB. Since the transcription of IL-6, IL-8, TNF-α and iNOS involves activation of NF-κB, it is likely that blocking this transcription factor results in lowered cytokine expression [169, 174]. Besides affecting cytokine production and release, a heat shock response can inhibit inducible nitric oxide synthase (iNOS) production, which is involved in the production of NO

[169]. Other studies; however, indicate that HSP70 induces NO production which leads to further upregulation of HSP70 production [175]. Increased HSP70 levels have also been shown to increase production of cyclooxygenase-2 (COX-2), which serves to induce $PGE_2$ production [176].

In this study, significantly increased levels of HSP70 were associated with a reduction of TNF-α levels and an increase in IL-6 levels; however, the differences were only significant at the one-day time point for annular cells. A significant increase in HSP70 levels also corresponded to an increase of IL-8 in nucleus cells and a decrease of IL-8 in annulus cells. $PGE_2$ and NO levels were significantly elevated when associated with a HSP response one day following thermal treatment. As observed in other studies, the effect of HSP on cells varies between cytokines and cell type. For example, TNF-α, but not IL-6, production is reduced by hyperthermia and the associated presence of HSP70 in macrophages [162]. Others observed that heat shock increases IL-8 production and reduces IL-6 production [177]. Still another study observed that heat shock increases the release of IL-6, but does not affect TNF-α or IL-1 [178].

Although HSP70 levels were unaffected by the 40ºC treatment for one hour, this exposure led to several significant changes in cytokine levels in nucleus cells. TNF-α, IL-6, IL-8, and $PGE_2$ were all significantly lower following the 40ºC treatment at one or more time points. This could be explained by the heat itself, rather than the presence of HSP70, affecting cytokine production [179]. Several studies have demonstrated that thermal doses insufficient for inducing HSPs may inhibit cytokine production through the degradation of mRNA [169, 180].

As established by others investigating the effects of HSPs and cytokines, the precise effects of hyperthermia and HSPs on cytokine production are unclear due to the high degree of redundancy and cross-talk among cytokine induction pathways and the paradoxical effects of HSPs [51, 164]. The temporal response of cytokine production varies as a result of thermal dose [181], cytokine production varies between different cell types exposed to the same hyperthermic conditions [164, 173], and the response of the same cell type to the same hyperthermic conditions depends on numerous other environmental conditions [182]. Additional complicating factors relate to the timing of heat shock induction with respect to cell cycle and the differing effects of intracellular and extracellular HSP70 [164]. In addition, HSP production can be induced by a number of factors other than hyperthermia, including TNF-α, IL-1, IL-6, and NO, which were all present in this study [160, 173]. A further confounding factor of using heat to induce a HSP response is that the thermal doses necessary to induce HSP production cause some level of cellular damage [175]. The beneficial and protective effects of elevated HSP levels are balanced by the hyperthermia-related cellular injury [175].

Currently available intradiscal thermal therapies create a region of lethal temperatures in the disc which is surrounded by regions of sublethal heat. Besides affecting cytokine production in disc cells, the induction of HSP70 could protect disc cells through thermotolerance, which is the cell's ability to withstand an otherwise lethal thermal challenge [173]. This increased tolerance occurs within hours of heating and can last three to five days [160]. Cells given a mild heat shock are less susceptible to other toxic agents and protected against further environmental insults [161]. HSPs can also mitigate the deleterious effects of inflammatory cytokines by increasing the cell's

resistance to these factors [173]. HSP70 has been shown to suppress the apoptotic and necrotic effects of TNF-α and IL-1 [160, 164, 183]. HPS70 may also contribute to cellular repair processes following hyperthermia through the activation and inactivation of certain proteases [160]. Induction of an HSP70 response can increase cellular tolerance to subsequent stressors such as hypoxia [184], ischemia [185], acidosis [186], and energy depletion [187]. Since many of these conditions are present in the disc cellular environment, the protective effects of HSPs may benefit disc cells following thermal therapy.

In conclusion, this study has demonstrated that sublethal heat can affect cytokine production in disc cells either with or without an accompanying HSP70 response. A thermal dose of 43ºC for one hour was sufficient to induce a HSP response in both nucleus and annulus cells and this response could impact the *in vivo* disc cellular environment by altering cytokine production, mitigating deleterious effects of cytokines, or protecting cells through thermotolerance. Thermal doses lower than those necessary to induce a HSP response may affect cytokine concentrations through the breakdown of cytokine mRNA. Further studies are necessary to determine whether the effects observed here mimic the *in vivo* effects of sublethal heat. In addition, the duration of the effect on cytokine levels has not been determined, so it remains unclear whether sublethal heat would be helpful for chronic disc pain management. These observations from this study, coupled with further analysis, could indicate whether it is advantageous to limit or expand regions of sublethal heat during thermal therapy, or whether a stand alone sublethal heat treatment could decrease back pain.

## Chapter 5 Heating Probe Development and Characterization

### 5.1 Introduction

It has been suggested that thermal therapy has a healing effect on collagenous tissues [188], and this modality has been incorporated into several minimally invasive back pain treatments. Possible therapeutic mechanisms include collagen denaturation, cell ablation, nerve tissue coagulation, and pro-inflammatory factor reduction [89, 100]; however, the precise mechanism or combination of mechanisms is not known. In addition, the thermal exposures (temperature-time relationships) necessary to achieve these effects are not well defined and the optimal size of the treated region has not been investigated.

Numerous studies have emphasized the need for further basic science research into the potential therapeutic mechanisms of thermal therapy on degenerative discs [89, 189-191]. Elucidating the therapeutic mechanisms and optimizing treatment regimens requires an understanding of the disc's biologic response to thermal therapy over time. Rodent tail discs provide an efficient model to understand how different thermal dosing regimens affect architecture, cellularity, and biochemical behavior. Although cell death or collagen denaturation in a portion of the disc may have a healing effect, it is likely that killing most disc cells or denaturing large amounts collagen will accelerate degeneration. Therefore, it is important to control of the size of the treated region. Precise control of the size and shape of the thermal lesion in the disc will allow different potential therapeutic mechanisms to be analyzed: sublethal thermal exposures to cells may cause a reduction of inflammation through heat shock protein release, lethal thermal exposures

could ablate nerve cells, and high thermal exposures could induce a remodeling response through collagen denaturation.

Heat can limit cell viability by affecting membrane function, altering cytoskeletal proteins, disrupting nuclear structure and function, and hindering cell metabolism [192]. The precise thermal dose required to necrose cells is affected by many factors including: species, cell type, and cell phase. In addition, environmental conditions such as oxygen concentration, nutrient availability, and pH can change the thermal sensitivity of a certain cell type [192, 193]. Lethal thermal doses have been reported ranging from 20-30 minutes at 43ºC for brain, liver, and colon tissue while doses up to 240 minutes at 43ºC are required for muscle and fat tissue [193]. The thermal dose necessary to necrose rat intervertebral disc cells has not been studied; however, doses of 120-210 minutes at 43ºC have been reported for rat cartilaginous tissue and skin [193]. In addition to killing cells, thermal therapy can damage cells adjacent to the treatment area leading to apoptosis, which peaks in chondrocytes approximately three days after heat treatment [194].

Collagen denatures when the heal-liable intramolecular bonds which stabilize its triple helical structure break resulting in a transition from a highly ordered structure to a random gelatinous state [195]. The temperature at which this transition occurs is affected by many factors including: species, age [196], fiber orientation [197], and pH [99]. Denaturation temperature can also be affected by the mechanical stress state and hydration level of the tissue [198]. The typical temperature at which collagen denatures ranges from 60-65ºC, but temperatures ranging from 45-90ºC have been reported to induce denaturation [199]. The tissue shrinkage that accompanies collagen denaturation results from the unwinding of the triple helix and the tension in the remaining heat-stable

intermolecular crosslinks [200]. The remodeling response and tissue shrinkage resulting from collagen denaturation could both contribute to the therapeutic effect of thermal therapy on collagenous tissues.

Radiofrequency (RF) current probes are popular for focal destruction of tissue since they have precise control over the size and location of the thermal lesion [201]. Because temperature falls off rapidly as the distance from the probe increases, RF heating probes are effective for delivering precisely controlled thermal lesions to small volumes of tissue [188]. Lesion size and shape can be controlled by varying several different probe design parameters, such as tip exposure and gauge, to obtain a desired lesion volume [202]. In addition, the lesion size and shape can be further contoured by adjusting the time of treatment and the temperature of the probe tip [202]. Studies performed to evaluate the thermal properties of intervertebral disc tissue and examine spatial heat profiles produced by an RF probe confirm that RF heating is an appropriate method to heat a small volume of disc tissue [201].

The goal of this study was to develop a miniature RF heating probe and use rat tail intervertebral discs to demonstrate that it is possible to limit and target the effects of thermal therapy at a variety of thermal exposures in a small animal model. The effects of thermal treatment at seven distinct thermal exposures on the extent of cell death and denaturation in an *in vivo* murine model were quantified seven days after treatment. The purpose of these measurements was to determine whether the relative areas of cell death and collagen denaturation could be controlled so that their independent effects on disc remodeling could be studied. The seven day time point was selected so that the delayed apoptosis associated with heat damage would be included when quantifying cell death.

## 5.2 Methods

*Probe Design*

An RF probe was designed and built to heat a small volume of disc tissue to high temperatures without damaging adjacent tissue. To investigate collagen denaturation as a potential therapeutic mechanism of intradiscal thermal therapy, temperatures of approximately 60ºC to 65ºC had to be generated in the disc. Because rat-tail intervertebral discs are small (approximately 3 mm diameter and 1.5 mm thick) and killing cells throughout the entire disc would accelerate in disc degeneration, the temperatures in the disc had to fall steeply within short distances from the probe.

RF probes were assembled using a 30-gauge needle (outer diameter 0.30 mm). Each probe tip contained a type T thermocouple made of 0.001 inch diameter manganin and constantin wires. The thermocouple was insulated with polyimide tubing (0.0031 inch inner diameter; 0.00050 inch wall thickness (A-M Systmes Inc; Carlsborg, WA)) and placed inside the needle so that the junction of the thermocouple was just inside the beveled tip of the needle. The non-junction portion of the thermocouple was glued to the polyimide tube and the polyimide tube was glued to the needle so that the junction would remain in place at the tip of the needle. The outside of the needle was lined with polyimide tubing (0.0133 inch inner diameter; 0.00050 inch wall thickness) leaving only the distal 0.9 mm of the tip exposed (Figure 5.1). The non-junction ends of the thermocouple wires were then soldered to miniature thermocouple connectors (Physitemp; Clifton, NF) and used to record probe tip temperature. Polyethylene tubing (0.030 inch diameter) lined the length of the thermocouple between the needle and thermocouple connectors.

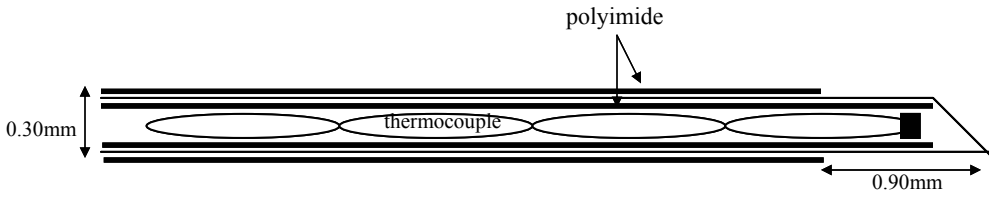


**Figure 5.1** Schematic of RF probe tip.

*Probe Characterization*

Cadaver rat tails were used to map temperatures across the intervertebral disc. Tail discs Co5/Co6, Co6/Co7, and Co7/Co8 were studied. During heating, the temperature was monitored in the distal portion of the needle and represented the maximum temperature in the disc. A copper return electrode lined with conductive gel was placed adjacent to the tail. Less than 2 Watts of monopolar RF energy were required to produce probe tip temperatures up to 80ºC.

The heating probe was placed in the annulus on one side of the disc and heated to either a high temperature (70ºC) or a low temperature (50ºC). These two temperatures were evaluated since the high temperature would cause collagen denaturation and cell death and the low temperature would cause cell death while avoiding collagen denaturation. During each trial, the target temperature was maintained for ten minutes and the temperature at nine different locations throughout the disc was recorded using thermocouples. In addition, the temperature was recorded in both vertebral endplates adjacent to the treated disc to determine if the endplates would be damaged during intradiscal thermal treatment. Five trials were run at the high temperature and one at the low temperature.

*In-Vivo Analysis*

All procedures were approved by the Intuitional Animal Care and Use Committee at the University of California at San Francisco. Three-month old Sprague Dawley rats were used for this study. Forty-five murine tail intervertebral discs were treated. Each rat was anesthetized using intraperitoneal injections of ketamine (90 mg/kg) and xylazine (10 mg/kg). Buprenorphine (5 mg/kg, SQ) was administered once prior to surgery and on an as needed basis to control for post-operative pain. Atipamezole HCL (0.2 mg/kg, IP) was used for anesthesia reversal.

The tail skin was lined with a conductive gel and a copper return electrode was placed next to the tail. The heating probe was placed in the lateral portion of the annulus using fluoroscopic guidance to ensure that the highest temperatures were in the annulus fibrosis (Figure 5.2). Tail discs Co5/Co6, Co6/Co7, and Co7/Co8 were used for treatment. Five discs were treated at each of seven thermal exposures: 80ºC for 10 minutes, 80ºC for 1 minute, 75ºC for 5 minutes, 62ºC for 10 minutes, 55ºC for 15 minutes, 48ºC for 15 minutes, and 48ºC for 5 minutes. During treatment, power was adjusted as necessary to maintain a constant temperature at the probe tip. A sham treatment (insertion of heating probe but no heat treatment) was applied to five discs, and five discs were used as controls. Following surgery, the animals were allowed unrestricted food, drink, and activity.

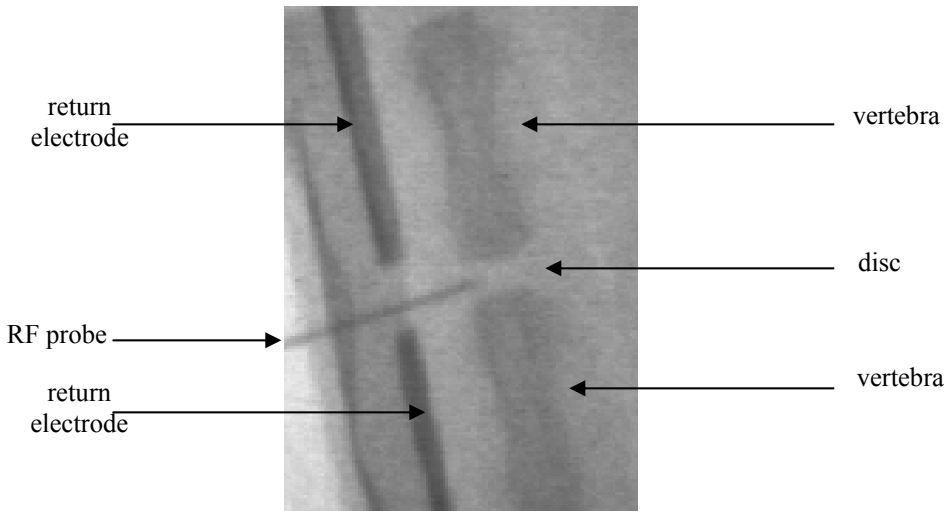


**Figure 5.2** Fluoroscopic image showing location of heating probe in disc. The heating probe is placed in the annulus so that the highest temperatures are in the annulus and are confined to one side of the disc.

*Post Treatment Analysis*

Seven days after treatment, the rats were sacrificed and the treated discs were removed along with half of the vertebral bone above and below the treated disc. All discs were fixed in formalin, decalcified in EDTA, dehydrated using alcohol solutions, and embedded in paraffin. Discs were sectioned transversely into six micron sections and stained using Safranin-O, fast green, and hematoxylin. Discs architecture was examined to identify the section most affected by thermal treatment. An adjacent section was then assessed for apoptosis by the fluorescein-tunel method (In Situ Cell Death Detection Kit; Roche; Mannheim, Germany) and cellularity by DAPI staining (Vectasheild with DAPI; Vector Labs; Burlingame, CA). The denatured area (defined as non-birefringent area under polarized light) and the cell death area (combined apoptotic area and acellular area) were measured by manually tracing the affected region on digitized microscopic images (Figures 5.3 and 5.4). The areas affected by collagen denaturation and cell death were

normalized to the total area of the disc to find the percentage of the disc cross-section that was affected. Differences in the percent of the disc areas affected by both denaturation and cell death were compared using a one-way analysis of variance (ANOVA). Post hoc tests were performed with an LSD adjustment. Significance was set at $p<0.05$.

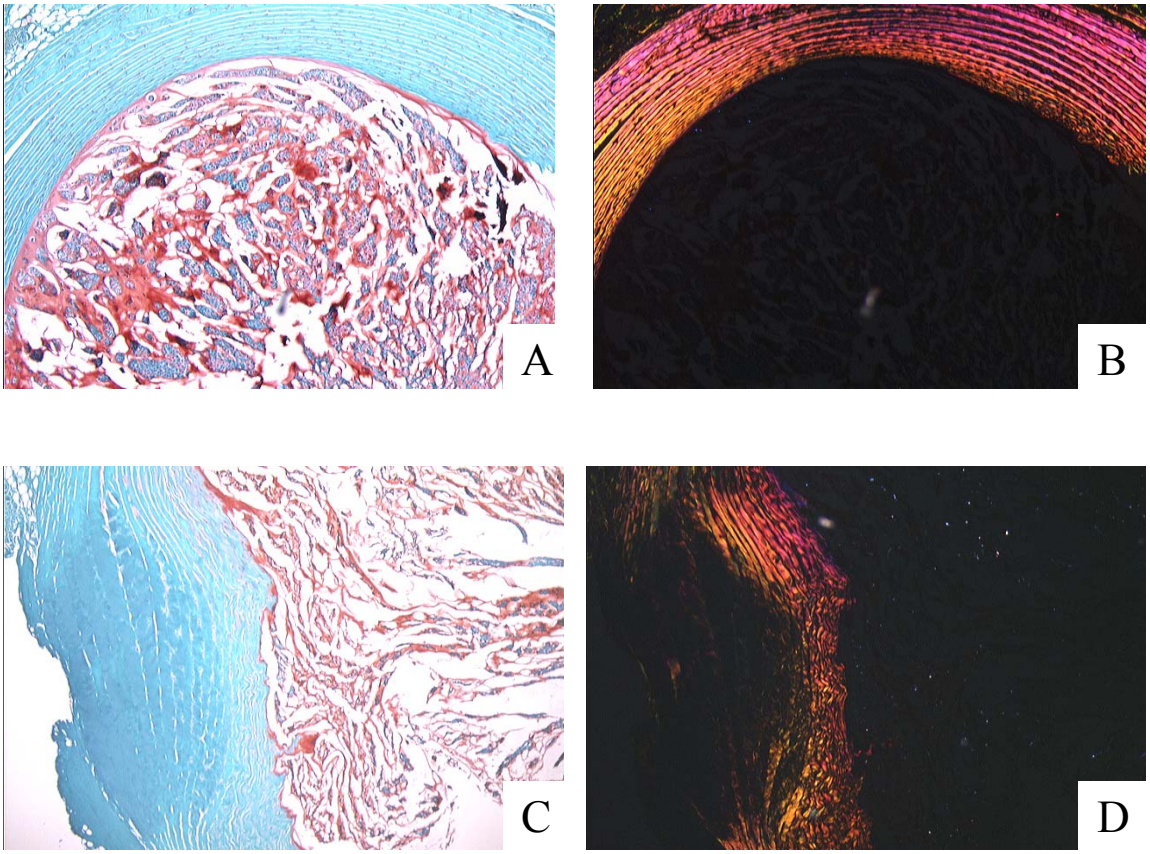


**Figure 5.3** (A) Control disc stained with Safranin-O and fast green under white light. (B) Control disc under polarized light. (C) Thermally treated (80ºC for 10 min) disc stained with Safranin-O and fast green under white light. (D) Thermally treated disc under polarized light. The thermally treated disc no longer exhibits birefringence where collagen was denatured.

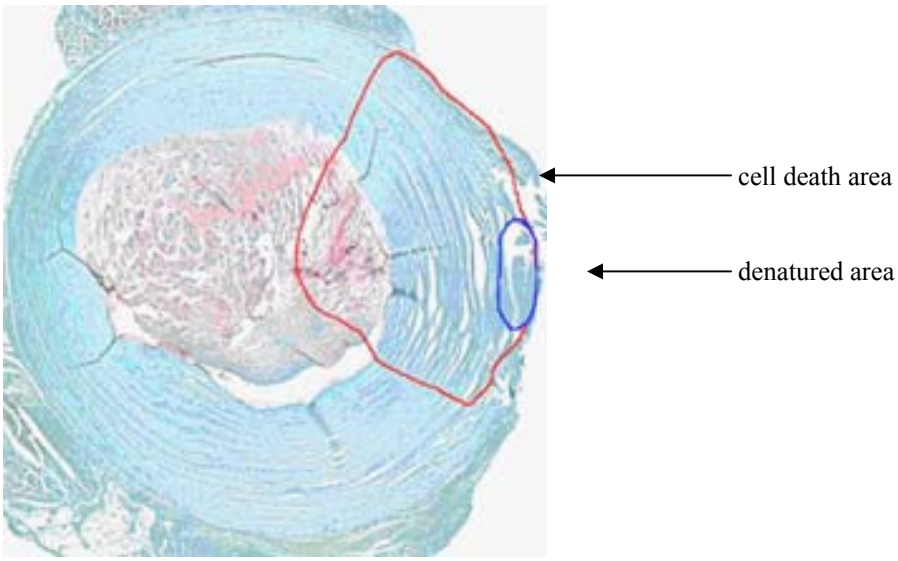


**Figure 5.4** Thermally treated disc (62ºC for 10 min) under 2X objective showing areas of cell death and collagen denaturation. Cell death area was found using an adjacent section stained for cellularity and apoptosis and magnified with a 10X objective. Collagen denatured areas were found using the 2X objective and polarizing filters. These areas were then normalized by the area of the entire disc to find the percent area affected by both collagen denaturation and cell death.

## 5.3 Results

*Probe Characterization Results*

For both the high temperature and low temperature trials, the temperature on the side of the disc farthest from the heating probe remained below 40ºC (Figures 5.5 and 5.6). The temperature in the adjacent endplates remained below 43ºC during both the high temperature and low temperature trials that lasted for 10 minutes. The heating probe rapidly reached the target temperature and then remained within approximately one degree of the target temperature throughout the trial.

This heating modality produces high temperatures in close proximity to the needle with a steep radial falloff. The probes created an elliptical temperature distribution that

expanded with time at a given temperature. Even in the high temperature trials, the temperature on the side of the disc farthest from the heating probe remained cool enough to allow for cell survival. Temperature measurements indicated that following the high temperature treatment, approximately half of the disc cells would survive to induce a remodeling response following treatment.

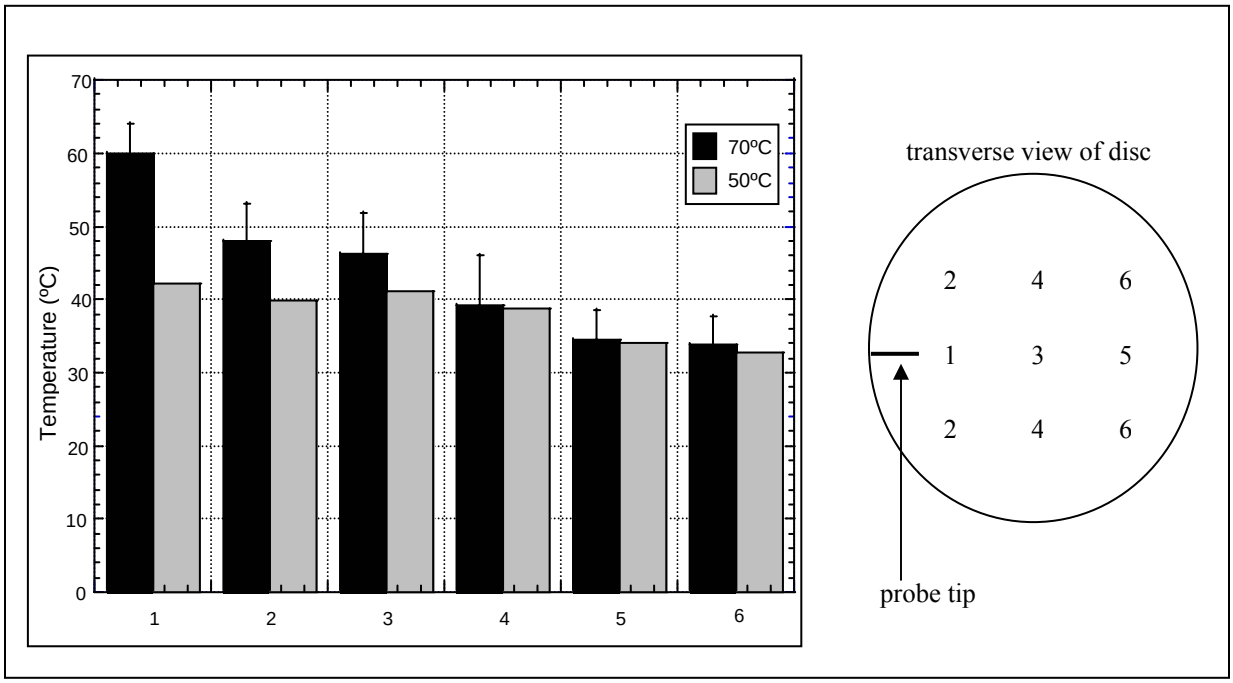


**Figure 5.5** The disc schematic shows the location of the nine temperature measurements that were recorded during each trial. The graph shows the average temperature reached during both the high (70ºC) and low (50ºC) temperature trials at each location after 10 minutes of heating. Locations that were equidistant from the temperature probe were combined to give an average for that location (locations 2, 4, and 6).

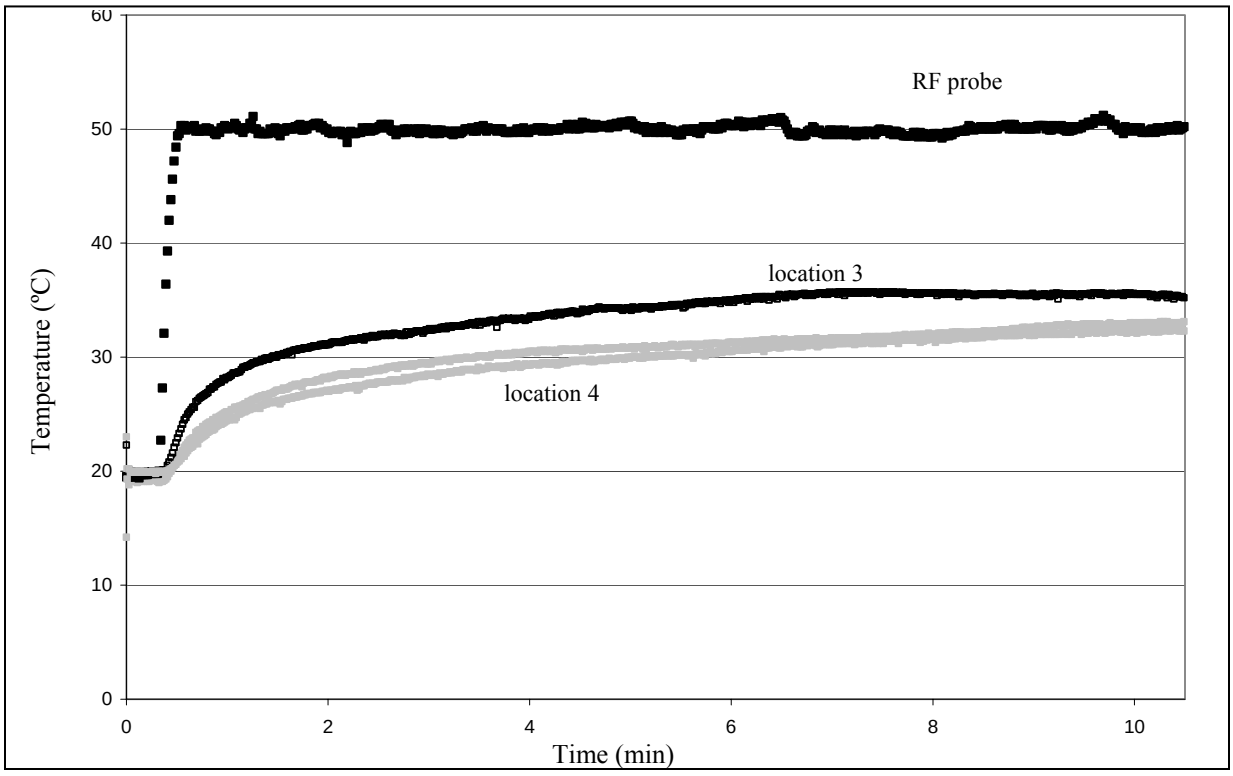


**Figure 5.6** Temperature of the heating probe at three locations in the disc during a 10 minute trial. The location numbers correspond to the disc schematic in Figure 5.5. The heating probe rapidly reached the target temperature and then remained within approximately one degree of the target temperature throughout the trial

*In-Vivo Results*

A region of cell death was observed in all thermally treated discs, with the cell death area greatest in the discs treated for 10 minutes at 80ºC (49% of the disc area) (Figure 5.7). This area was significantly higher than the cell death at the other exposures, which ranged from 6-26% of the disc ($p<0.05$). The cell death areas of the two lowest doses, 48ºC for 5 and 15 minutes (6% and 9% of disc area), were significantly lower than the areas for the five highest doses (80ºC for 10 minutes, 80ºC for 1 minute, 75ºC for 5 minutes, 62ºC for 10 minutes, and 55ºC for 15 minutes) which ranged from 19-49% of the disc ($p<0.05$). There was no region of cell death in either the control or sham discs.

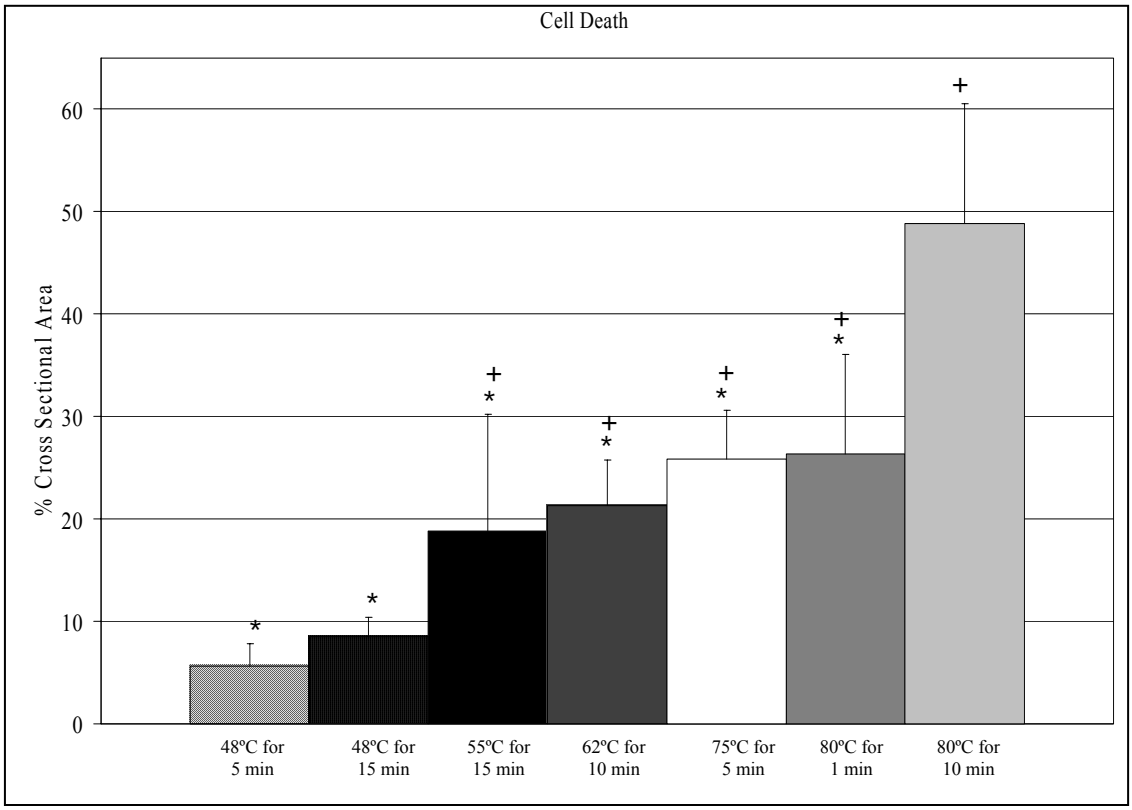


**Figure 5.7** Percent of disc cross-sectional area affected by cell death. The cell death area is defined as the combined area of loss of cellularity and apoptotic cells. There was no region of cell death in either the sham or control discs. (* = different from 80ºC for 10 min, $p<0.05$; + = different from the 48ºC exposures, $p<0.05$)

Denaturation was observed in all treated discs except those treated at 48ºC, two treated to 62ºC for 10 minutes, and one treated to 55ºC for 15 minutes (Figure 5.8). Maximum denaturation area (17% of the disc) was achieved in the discs treated at 80ºC for 10 minutes. This was significantly greater than the four lowest temperature exposures (48ºC for 5 minutes, 48ºC for 15 minutes, 55ºC for 15 minutes, and 62ºC for 10 minutes; $p<0.05$). The denatured areas of the discs treated at 75ºC for 5 minutes, 80ºC for 1 minute, and 80ºC for 10 minutes were significantly higher than the denatured areas of the discs treated to 48ºC for 5 and 15 minutes ($p<0.05$). No collagen denatured region was found in either the sham discs or control discs.

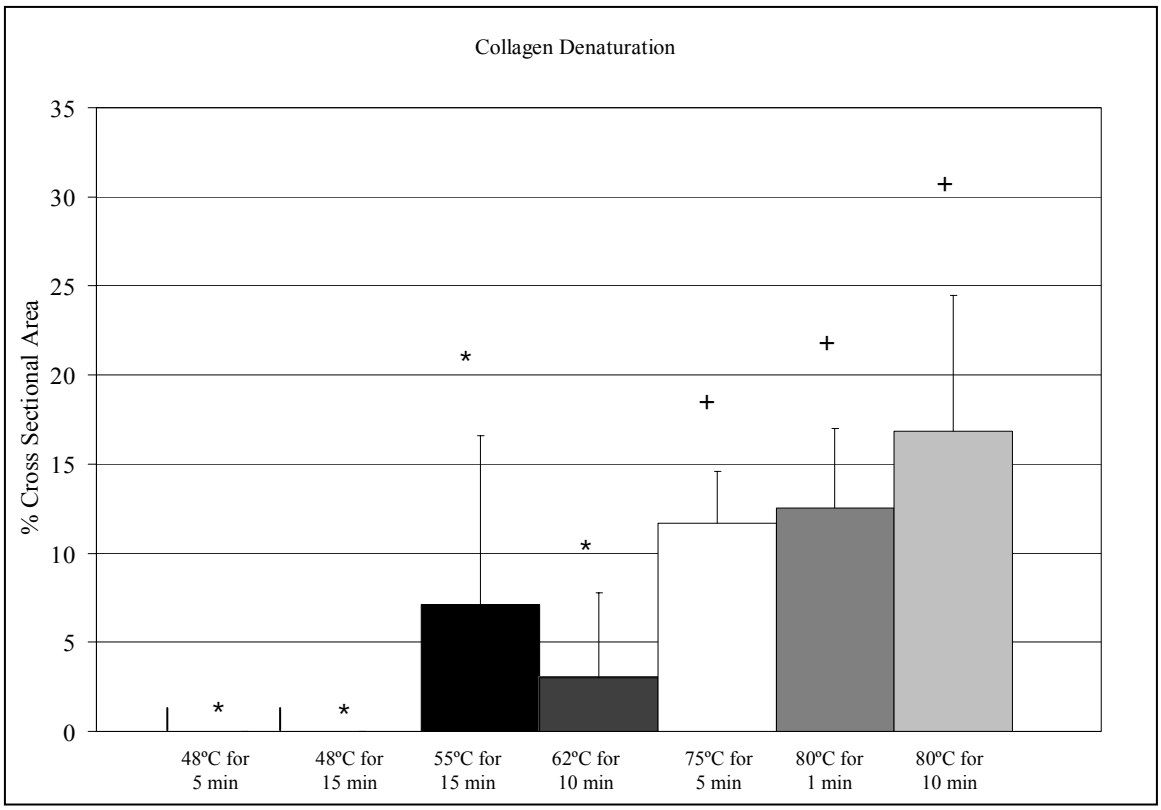


**Figure 5.8** Percent of disc cross-sectional area affected by collagen denaturation. The area of collagen denaturation is defined as the non-birefringent area under polarized light. There was no collagen denatured area in sham discs, control discs, or the discs treated at 48ºC for 5 or 15 min. (* = different from 80ºC for 10 min, $p<0.05$; + = different from the 48ºC exposures, $p<0.05$)

## 5.4 Discussion

The results of this study demonstrate that it is possible to limit and target the effects of thermal therapy to a portion of the murine disc using this RF probe. Due to the steep falloff of temperatures away from the applicator tip and non-linear accumulation of thermal dose with temperature, exposures of 75ºC for 5 minutes and 80ºC for 1 minute both resulted in similar regions of cell death and denaturation: in both cases about one-fourth of the cells were killed and one-eighth of the disc was denatured. The highest exposure, 80ºC for 10 minutes, caused cell death in almost half of the disc. Since both higher temperatures and longer times were necessary to significantly increase the region

of cell death, a wide variety of thermal exposures (temperature and time combinations) can be examined with this probe without inducing the confounding effect of degeneration which may result from killing a large region of cells.

The size of the applicator and the steep falloff in temperature prevented large regions of the disc from being denatured. Interestingly, the temperature at which denaturation was observed was lower than that cited by many investigators examining both stressed and unstressed tissue. While the rat tail annulus in this study, which has been disrupted by the introduction of the heating probe, may be under less stress than an intact disc, studies using Differential Scanning Calorimetry (DSC) to determine peak denaturation temperatures in excised collagenous tissues have observed endothermic peaks at approximately 65ºC. However these studies also indicate that the onset of energy release occurs at lower temperatures [203], and these results are consistent with observations of others who have used polarized light to detect collagen denaturation [204]. To date, the specific denaturation behavior of rat tail intervertebral disc collagen has not been studied.

This model is an important step towards determining the therapeutic mechanisms of thermal therapy in the disc since the thermal dose can be both controlled and quantified, and the remodeling response over time examined. By choosing lower temperatures and longer times, cells in the annulus can be selectively killed and denaturation avoided, so that disc remodeling after nociceptor ablation can be investigated. Conversely, by choosing high temperatures and shorter times, it is possible to denature the annulus without causing significant cell death. In addition, the sublethal effects of heating can be investigated by using temperatures and times below those that

necrose cells. Examining post-treatment remodeling *in-vivo* may help define therapeutic mechanisms and help distinguish the relative merits of two distinct treatment effects: cell ablation and collagen denaturation. In addition, post-treatment biochemical outcomes can be examined to better clarify the cellular inflammatory response to both sublethal and lethal thermal exposures.

## Chapter 6 *In-vivo* Effects of Thermal Therapy on Degenerated Discs

### 6.1 Introduction

Traditionally, patients who fail conservative therapy for discogenic back pain have few treatment options outside of discectomy, disc replacement, or fusion, all of which can result in significant morbidity and variable outcomes [84, 85, 87]. As a result, less invasive techniques are being investigated. Thermal therapy is thought to have a healing effect on collagenous tissues [99, 197], and therefore this modality has been incorporated into several minimally invasive back pain treatments. Possible therapeutic mechanisms include collagen denaturation, cell ablation, nerve fiber destruction, and pro-inflammatory cytokine level reduction [100, 174]; however, the precise mechanism or combination of mechanisms is not known. Optimization of thermal therapies for disc treatment requires an understanding of the mechanisms of thermal therapy, namely, the biologic response in the disc over time.

Intradiscal electrothermal annuloplasty (IDET, Oratec Interventions Inc; Menlo Park, CA) is a minimally invasive surgery used to treat disc pain. The IDET procedure is typically performed under local anesthesia [191]. Using fluoroscopic guidance, a 17-gauge needle is inserted into the center of the disc to be treated. A flexible catheter with a temperature-controlled thermal resistive coil is then passed through the needle and navigated into the inner posterior annulus. The coil temperature is raised to 90ºC over the course of 13 minutes, maintained at 90ºC for 4 minutes, and then removed [100]. A recent review of the IDET procedure estimates that over 60,000 IDET surgeries have been performed worldwide, yet evidence for the efficacy of IDET remains weak and the therapeutic mechanisms remain unclear [91].

Two randomized placebo controlled studies on the effects of IDET have been completed. One study identified a minor improvement in pain scores following IDET [205], while the other observed no major differences between IDET and a placebo procedure [98]. Several observational studies have identified a statistically significant reduction in patient pain levels and improvement of function and quality of life both one year [93, 94, 100] and two years [92, 206, 207] after IDET. Other observational studies have shown no therapeutic benefits following the IDET procedure [95-97, 208].

The increased laxity and decreased height associated with degenerated discs can cause abnormal loads to be placed on disc nerves and other tissues in the joint [11]. Studies investigating thermal therapy on other collagenous tissues, particularly the shoulder, have observed that thermal therapy can stiffen collagen [99]. Consequently, thermal therapy may relieve back pain by stiffening the joint through the shrinkage of disc collagen with denaturation and/or the induction of an extracellular remodeling response, thereby restoring the biomechanical function of the joint [100]. In addition, in patients whose back pain is related to high annular stress concentrations, collagen denaturation may reduce these concentrations through "welding" of the collagen network and healing of annular tears [209, 210].

Collagen denatures at approximately 60ºC-65ºC; however, the precise temperature of denaturation varies with species, tissue stress, and tissue type [198, 199]. Collagen heated to these temperatures can thicken and remodel either with [211] or without the formation of scar tissue [212] leading to stabilization of the joint. Some studies have shown that temperatures necessary to induce collage denaturation are reached in annular tissue during the IDET procedure [208, 211], while others have shown

they are not [101]. It is thought that the therapeutic benefit of denaturing collagen occurs by stabilizing the joint acutely by shrinking disc tissue that is then remodeled and strengthened over time [213].

A second therapeutic mechanism of IDET could be the destruction of sensitive nerve endings and cauterization of vascular ingrowth in the annulus [100, 210]. As discs degenerate, nerve and blood vessel growth into the previously aneural inner annulus and nucleus tissue has been associated with pain generation [31]. Nerve tissue is ablated at 45ºC [214], and temperatures high enough to ablate nerves have been identified at distances ranging from 9 to 14 mm from the IDET heating probe [211]. It has also been suggested that pain relief may be related to partial denervation of the dorsal root ganglion [215]. If denervation were the mechanism for pain relief following IDET, the relief should occur as soon as the temperature of the innervated tissue surpasses 45ºC. Clinical findings, however, indicate a slow improvement with time following surgery. Improvement begins in the second or third month following surgery and continues through six months. This indicates that a mechanism other than nerve fiber ablation is responsible for pain relief and points to collagen modification and remodeling as the mechanism of action [100, 215].

Another possible therapeutic mechanism of IDET may be to alter cytokine production in the disc. Painful discs contain high concentrations of pro-inflammatory cytokines. Disc cells produce many cytokines; however, IL-1, TNF-α, IL-6, and IL-8 have been implicated in the progression of, and pain associated with, disc degeneration [71]. Pro-inflammatory cytokines can sensitize nerve fibers and reduce their threshold for mechanical stimulation. In addition, these cytokines can increase degradative enzyme

activity, slow matrix metabolism, and increase matrix catabolism [216]. Thermal therapy has been shown to inhibit cytokine production in some cell types [174, 217]. Inhibition of pro-inflammatory factor production may be related to a heat shock protein (HSP) response, which is initiated following sublethal thermal stimulation. Thermal therapy in degenerated discs may reduce disc pain by either inhibiting the expression and release of pro-inflammatory cytokines by disc cells or by inducing HSP production which can protect cells from the deleterious effects of cytokines [174, 213].

The success of thermal therapy for the treatment of degenerative disc disease is a subject of controversy [191], and the mechanism of action is still unclear [89]. Numerous authors have emphasized the need for further basic science research into the effects of thermal therapy on degenerative discs [189, 190]. A better understanding of the biologic response to thermal therapy could help elucidate the therapeutic mechanisms of IDET. After the therapeutic mechanisms are understood, patient selection criteria and treatment parameters can be refined to optimize the therapeutic effect.

The goal of this study was to evaluate the *in-vivo* effects of three different thermal exposures on degenerated discs. A triple-stab model of disc degeneration was used to produce degenerative rat tail discs [218], and the discs were treated with thermal therapy using an RF heating probe. A sublethal exposure (43ºC for 15 minutes) was used to investigate the effects of thermal stimulation of cells while avoiding necrosis. A low temperature exposure (48ºC for 15 minutes) was used to investigate the effects of cell ablation while avoiding collagen denaturation. A high temperature exposure (75ºC for 5 minutes) was used to investigate the effects of collagen denaturation. Disc architecture and cytokine concentrations were evaluated 7 and 28 days after thermal therapy.

## 6.2 Methods

*Animals*

Three month-old Sprague Dawley rats were used. All procedures were approved by the Institutional Animal Care and Use Committee of the University of California at San Francisco. Because rats reach skeletal maturity before 3 months of age, animal growth did not interfere with IVD remodeling [137].

*Induction of Disc Degeneration*

General anesthesia was administered using ketamine (90 mg/kg IP) and xylazine (10 mg/kg IP). Buprenorphine (0.01 mg/kg SQ) was administered once before recovery and then as needed to control postoperative pain. Atipamezole HCL (0.2 mg/kg IP) was used for anesthesia reversal. Food, drink, and activity were unrestricted post-operatively.

A 2.5 cm longitudinal incision was made along the tail to expose the lateral portion of tail discs Co5/Co6, Co6/Co7, and Co7/Co8. Lateral stabs were performed so that the incision would be on primary plane of motion for tail discs. A number 11 blade was inserted 1.5 mm into the disc to depressurize the nucleus. A clamp was placed on the blade to prevent the blade from penetrating the disc more than 1.5 mm and radiographic images were captured to ensure the blade was parallel to the endplates to avoid endplate damage. The blade was then removed and the tail skin was closed using separated stitches. Discs were then percutaneously stabbed with a 23-gauge needle at three days and again at six days after the initial blade injury. The three and six day time points were chosen to coincide with the peak inflammatory response observed after single-stab injury. The discs were re-injured at the same location as the original blade

stab. Fluoroscopic guidance was used to ensure proper needle placement and to control needle depth (1.5 mm into the disc).

*Thermal Therapy*

Twenty-eight days after the initial blade incision for the induction of disc degeneration, the degenerated discs were treated with thermal therapy. Each rat was anesthetized using ketamine (90 mg/kg) and xylazine (10 mg/kg). Buprenorphine (0.01 mg/kg) was administered once before recovery and then as needed to control postoperative pain. Atipamezole HCL (0.2 mg/kg) was used for anesthesia reversal. Food, drink, and activity were unrestricted post-operatively.

A 0.30 mm diameter RF heating probe was used to treat each disc. The tail skin was lined with a conductive gel, and a copper return electrode was placed next to the tail. The heating probe was placed in the lateral portion of the annulus using fluoroscopic guidance to ensure that the highest temperatures were in the annulus fibrosis. During treatment, power was adjusted as necessary to maintain a constant temperature at the probe tip. Tail discs Co5/Co6, Co6/Co7, and Co7/Co8 were used for treatment. Fifteen discs were treated at each of three thermal exposures:

Sublethal – 43°C for 15 minutes
Low Temperature -- 48°C for 15 minutes
High Temperature – 75°C for 5 minutes

Previous experiments demonstrated that the 48ºC exposure causes cell death in approximately 10% of the disc, and the 75ºC exposure causes cell death in approximately 25% of the disc and denatures collagen in approximately 10% of the disc.

After treatment, the heating probe was removed and the animals were allowed unrestricted food, drink, and activity. Animals were sacrificed either 7 or 28 days following thermal therapy.

*Histology*

Five discs from each of the three thermal exposures were analyzed at each time point. Five control discs and five untreated degenerated discs 28 days and 56 days after the induction of disc degeneration were also analyzed. Discs and adjacent vertebrae were harvested, fixed in formalin, decalcified in EDTA, dehydrated, and embedded in paraffin. Six micron sagittal sections were cut through the disc parallel to the direction of the stab. Sections were stained using safranin-O, fast green, and hematoxylin to evaluate disc architecture and cellularity. Collagen denaturation was identified by locating non-birefringent collagen using polarized light microscopy.

*Cytokines*

Ten discs from each of the three thermal exposures were analyzed at each time point. Ten control discs and ten untreated degenerated discs 28 days and 56 days after the induction of disc degeneration were also analyzed. Complete discs were harvested, homogenized, and digested in liquid buffer. Levels of TNF-$\alpha$, IL-1$\beta$, IL-6, and KC (the murine homologue to IL-8) were determined using enzyme linked immunosorbent assays (ELISAs) according to the manufacturer's protocols (R&D Systems, Minneapolis, MN). The limit of detection was 10 pg/ml. Cytokine levels were normalized to tissue wet weight and expressed as ng/g of tissue. A one-way analysis of variance (ANOVA) was

used to detect differences between the three different thermal exposures at the 28-day time point, untreated degenerated discs at the same time point (56 days after the induction of degeneration), and control discs. An ANOVA was also used to detect differences in cytokine levels between the three different thermal exposures at the 7-day time point, the 28-day degenerated discs, and the control discs. Significance was set at $p<0.05$.

## 6.3 Results

*Histology (Figure 6.1)*

All control discs had a rounded nucleus pulposus, which comprised at least one-half of the disc area in midsagittal sections. Nuclear cells were stellar shaped and cell clusters were centralized with proteoglycan matrix located at the periphery. The endplates were continuous. The annulus consisted of well-organized collagen lamellae and fibroblastic cells.

A detailed description of the triple-stab model has been presented previously [218]. At both the 28-day and 56-day time points, discs contained disorganized collagen fibers where the nucleus had been and all discs had continuous endplates. Cells were both chondrocytic and fibroblastic. Very little proteoglycan was present in the discs.

*7-Day Sublethal (43ºC for 15 minutes)*

A small acellular area was observed adjacent to the location in the disc where the heating probe was placed in four of five discs. In two of these discs, a region of proteoglycan production was noted surrounding the acellular area, but this was not evident in the two other discs. One disc out of the five 7-day sublethal exposure discs

contained a discontinuous endplate on one side of the disc, was missing the endplate on the other side of the disc, and had blood vessels growing into the disc. The vertebrae adjacent to this disc contained dense bone and the marrow spaces contained osteoblasts and fibroblasts.

*28-Day Sublethal (43ºC for 15 minutes)*

Two discs contained more proteoglycan in the annular tissue on the side of the disc that had been heated than on the opposite side of the discs. Two other discs contained roughly equal amounts of proteoglycan on both sides of the annulus. Four of five discs in this group contained more proteoglycan than the untreated degenerated discs at the corresponding 56-day time point. One disc out of the five 28-day sublethal exposure discs contained discontinuous endplates that were touching in the center of the disc, so very little disc tissue was present. Blood vessels were observed growing into the tissue that remained at the periphery of the disc.

*7-Day Low Temperature (48ºC for 15 minutes)*

An acellular area was observed adjacent to the location in the disc where the heating probe was placed in four of five discs. In three of these discs, a region of proteoglycan production was observed surrounding the acellular area. In the fourth disc, proteoglycan was noted throughout the entire disc. One disc out of the five 7-day low temperature exposure discs had discontinuous endplates and contained disorganized hypercellular fibrous tissue. In this disc, the vertebrae adjacent to the disc contained dense bone with osteoblasts and fibroblasts in the marrow spaces.

*28-Day Low Temperature (48ºC for 15 minutes)*

Two of five discs contained a small acellular region adjacent to where the heating probe had been placed. This region was surrounded by cells producing proteoglycan. In two other discs, an acellular region was not observed, but proteoglycan production was observed in the tissue adjacent to where the probe had been placed. One disc out of the five 28-day low temperature exposure discs had discontinuous endplates and contained disorganized hypercellular fibrous tissue. Two discs in this group, including the one with discontinuous endplates, had dense bone in the adjacent vertebrae and the marrow spaces contained blood vessels, osteoblasts, and fibroblasts.

*7-Day High Temperature (75ºC for 5 minutes)*

One disc contained an area of collagen denaturation adjacent to where the probe had been placed and this denatured region was surrounded by acellular collagen. A second disc contained an acellular region, but an area of collagen denaturation could not be located. Three discs of the five 7-day high temperature exposure discs had discontinuous endplates; two discs contained disorganized hypercellular fibrous tissue and one had bone growing through the endplates. In the vertebrae adjacent to these three discs, dense bone was present and marrow spaces contained blood vessels, osteoblasts and fibroblasts.

*28-Day High Temperature (75ºC for 5 minutes)*

Two discs contained areas of denatured collagen surrounded by an acellular region where the heating probe had been placed. Another disc contained an acellular

region surrounded by a region of proteoglycan production, but no denatured area was observed. Two discs of the five 28-day high temperature exposure discs had broken endplates and contained hypercellular disorganized fibrous tissue. In the vertebrae adjacent to these discs, dense bone was present and marrow spaces contained blood vessels, osteoblasts and fibroblasts.

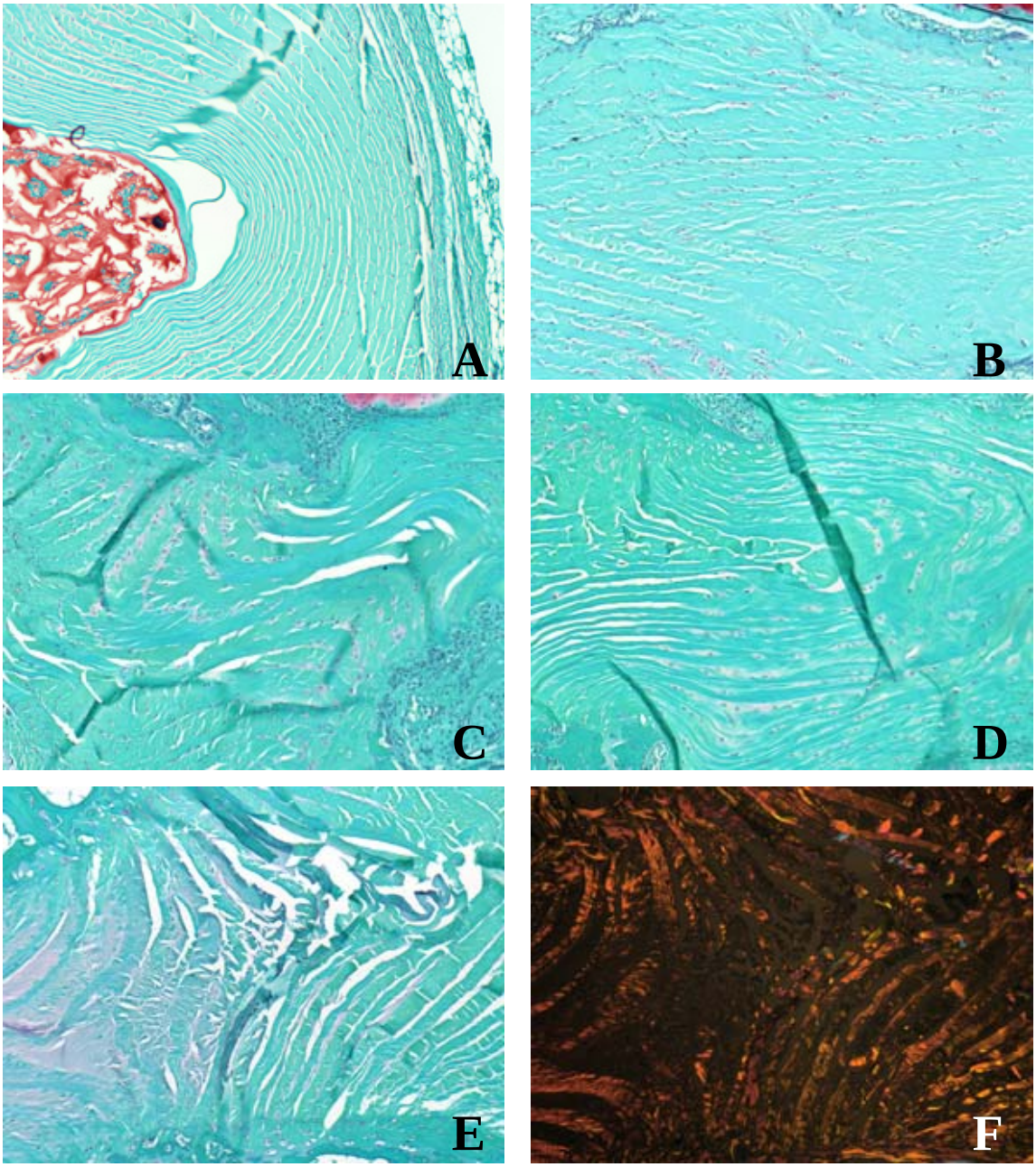


**Figure 6.1** Safrannin O/Fast Green images at 10X. A) Control disc annulus B) 28 day degenerated annulus C) 7 days following 43º for 15 minutes treatment D) 7 days following 48ºC for 15 minutes treatment E) 7 days following 75ºC for 5 minutes F) 7 days following 75ºC for 5 minutes treatment under polarized light

*Cytokines*

*TNF-α (Figure 6.2)*

Degenerated discs produced significantly more TNF−α than the control discs both 28 and 56 days after the induction of degeneration. No significant differences were observed between control discs, untreated discs, and thermally treated discs at the 7-day time point or between thermal exposures at either time point. Twenty-eight days following thermal therapy, discs produced significantly less TNF-α than untreated degenerated discs at the corresponding 56-day time point. This decrease in cytokine production was observed for all three thermal exposures: sublethal, low temperature, and high temperature.

*IL-8 (Figure 6.3)*

Degenerated discs produced significantly more IL-8 than the control discs both 28 and 56 days after the induction of degeneration. Seven days following thermal exposure IL-8 levels were significantly greater in the 75ºC treatment group than the control group, the untreated degenerated 28-day discs, the 43ºC treated discs, and the 48ºC treated discs. Twenty-eight days following thermal therapy, IL-8 levels in the 48ºC treatment discs were significantly lower than the untreated degenerated discs at the corresponding time point. Discs treated at the 43ºC exposure and the 75ºC exposure were not different than the untreated degenerated disc at the 28-day time point, and IL-8 remained significantly higher than the control discs in these treatment groups.

*IL-1β (Figure 6.4)*

No significant differences in IL-1β levels were observed between the degenerated discs at 28 or 56 days following the induction of disc degeneration and the control discs. Seven days following thermal exposure IL-1β levels were significantly greater than the control discs for all three exposures, but were not different than the 28-day untreated degenerated discs. There were no differences in IL-1β levels between the three different thermal exposures at the 7-day time point. Twenty-eight days following thermal exposure IL-1β levels were significantly greater in the 75ºC exposure group than the control group, the untreated degenerated 56-day discs, the 43ºC exposure discs, and the 48ºC exposure discs.

*IL-6 (Figure 6.5)*

No significant differences in IL-6 levels were observed between the degenerated discs at 28 or 56 days following the induction of disc degeneration and the control discs. In addition, no significant changes in IL-6 were observed between control discs, untreated discs, and thermally treated discs at either time point following therapy or between thermal exposures at either time point.

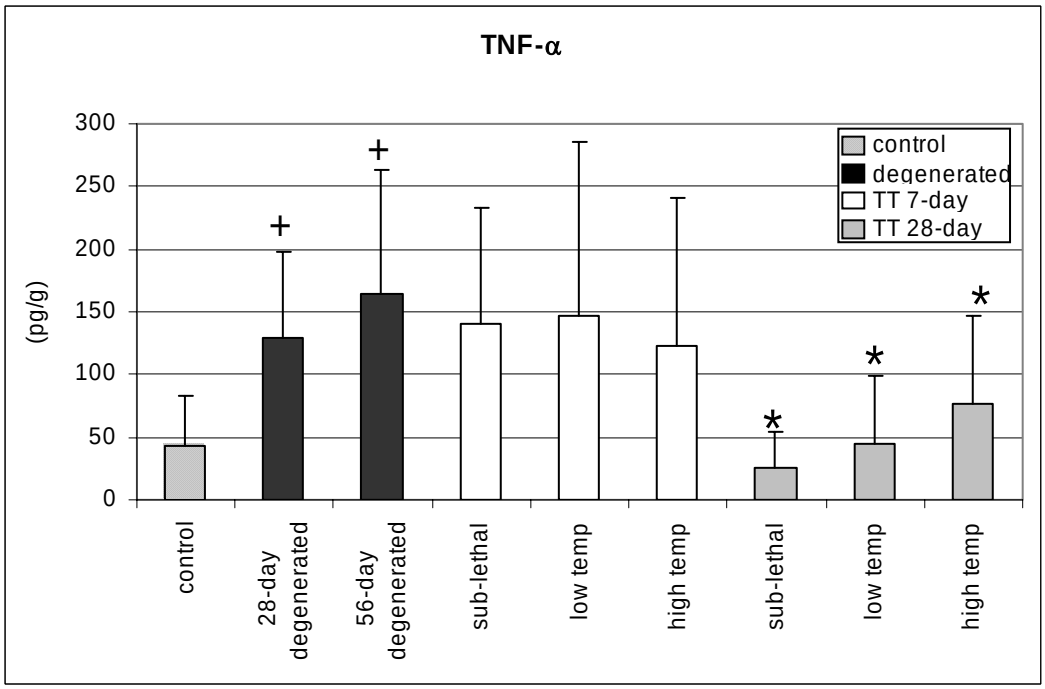


**Figure 6.2** TNF-α levels in control discs, untreated degenerated discs, and thermally treated discs. + = significantly different than control discs; * = significantly different than the corresponding time point untreated degenerated discs

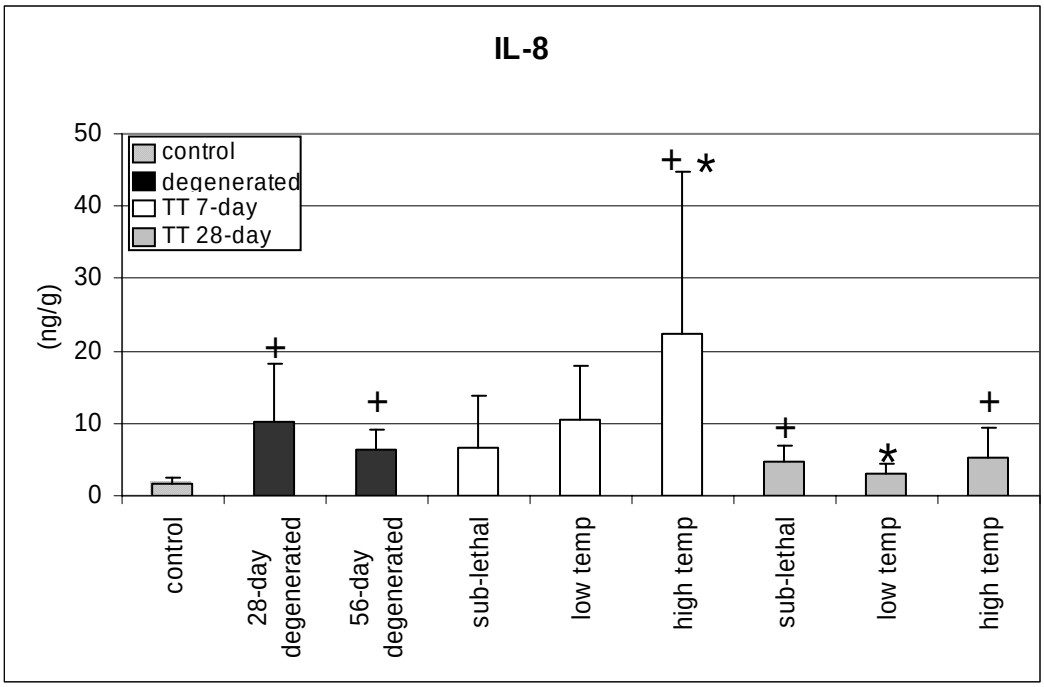


**Figure 6.3** IL-8 levels in control discs, untreated degenerated discs, and thermally treated discs. + = significantly different than control discs; * = significantly different than the corresponding time point untreated degenerated discs

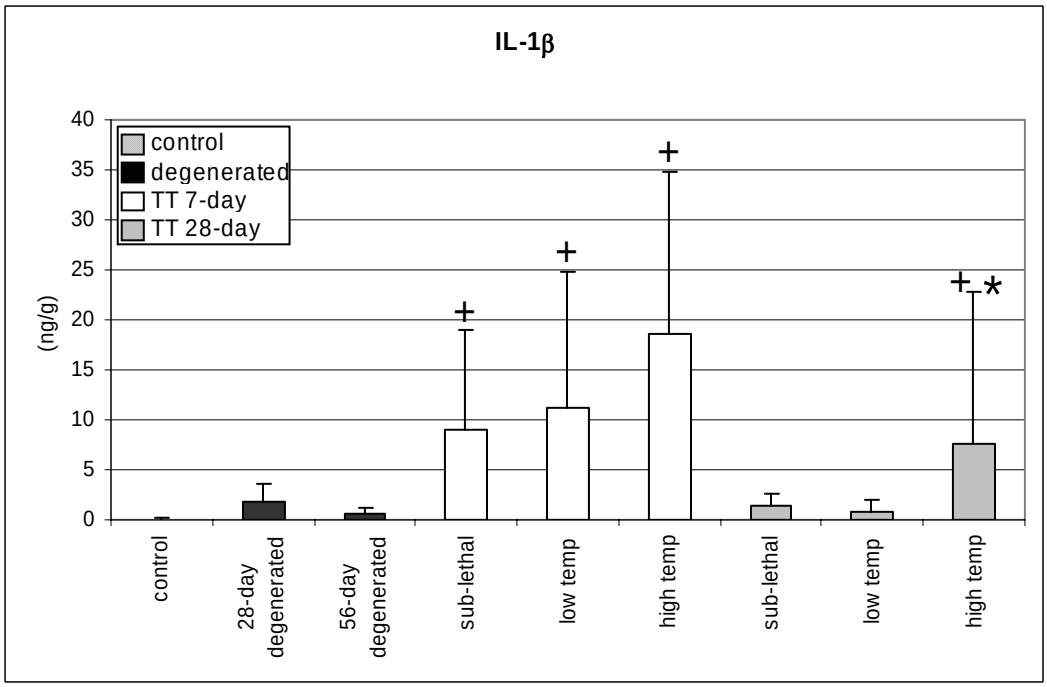


**Figure 6.4** IL-1β levels in control discs, untreated degenerated discs, and thermally treated discs. + = significantly different than control discs; * = significantly different than the corresponding time point untreated degenerated discs

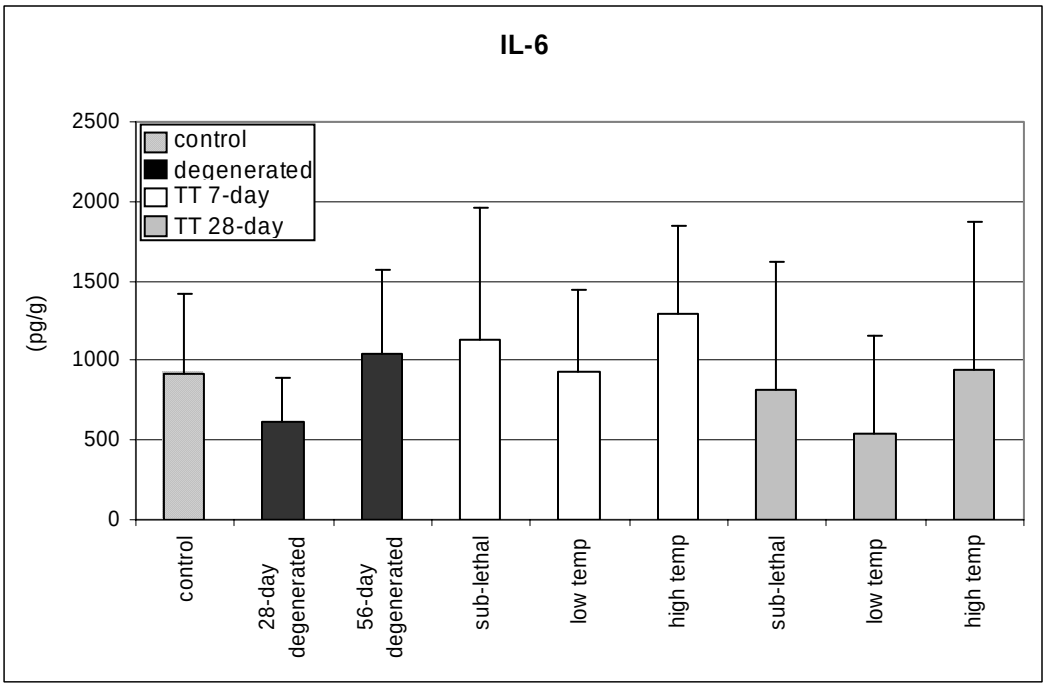


**Figure 6.5** IL-6 levels in control discs, untreated degenerated discs, and thermally treated discs. No significant differences were observed.

## 6.4 Discussion

In this study, the *in vivo* effects of thermal therapy on degenerated intervertebral discs were examined 7 and 28 days after treatment. Three different thermal exposures were examined using histological and biochemical outcome measures. Following thermal treatment, regions of acellularity and proteoglycan production were observed in the treated disc tissue following a 43ºC or 48ºC exposure. Areas of collagen denaturation, acellularity, and proteoglycan production were identified surrounding the treated region of the annulus in the 75ºC treatment groups. The inflammatory response varied between the different cytokines analyzed and the three thermal exposures.

A region of proteoglycan production was observed in most discs following treatment at each of the three thermal exposures. The proteoglycan production was located surrounding the area of acellularity indicating that proteoglycan production was stimulated where sublethal temperatures were present. *In-vitro* studies on chondrocytes confirm that sublethal temperature elevation can induce proteoglycan production [219]. Conversely, proteoglycan loss has been observed following thermal therapy on healthy sheep discs [213]. The different observations between the sheep study and the current study could be related to the health of the treated discs; the sheep study used healthy discs while this study used degenerated discs. In the current study, very little proteoglycan was present in the degenerated discs before thermal therapy, so proteoglycan loss could not be observed and stimulation of proteoglycan may have been more obvious than when treating healthy discs. Because disc degeneration is accompanied by a loss of proteoglycan [14], stimulation of proteoglycan production could help restore disc

function. The region containing increased proteoglycan production was small compared to the size of the disc, so it is unclear whether it would have a clinically meaningful effect on disc function.

Besides areas of increased proteoglycan production, little evidence of matrix remodeling was observed in the discs at the 7-day or 28-day time point. The absence of a remodeling response following therapy is similar to what has been observed in other studies using histology to investigate the *in vivo* effects of thermal therapy. Freeman et al used IDET to treat annular tears in sheep discs and examined disc morphology and nerve immunohistochemistry following the procedure. They observed no signs of disc remodeling or healing and a deterioration of morphologic appearance following the procedure [208]. Bass et al used ultrasound to examine the acute and chronic effects of two different thermal doses on sheep discs using biomechanical and histological outcome measures. No signs of matrix remodeling were observed at any time point following either dose of thermal treatment [213].

Several studies suggest that the therapeutic mechanisms of IDET may be associated with factors other than denervation or post treatment remodeling [89, 208]. Regions of cellular necrosis and sublethal temperature elevation can affect inflammatory factor production and are present during the IDET procedure. Thermally induced necrosis has been shown to increase inflammation [220]. Sublethal thermal exposures can affect cytokine production in both nucleus and annulus cells, with or without an accompanying HSP response. Although both thermal necrosis and sublethal thermal exposures can affect inflammation and inflammation had been implicated in disc pain, the relationship between IDET and disc inflammation is unclear [131].

In this study, treated discs produced significantly less TNF-α in all three thermal exposure groups 28 days after thermal therapy compared to untreated degenerated discs at the corresponding time point. Because all three thermal exposures had reduced TNF-α levels, TNF-α expression or release was most likely affected by the regions of the disc exposed to sublethal heat. An in-vitro study examining the effects of sublethal heat on disc cells confirms that TNF-α levels are affected by sublethal exposures with or without an accompanying HSP response. Because the effects of an HSP response are typically acute, lasting three to five days [160], the mechanism by which IDET could affect TNF-α production 28 days after treatment is unclear.

Because TNF-α can induce inflammatory hyperalgesia [43], endoneuraonal edema, and nerve fiber demyelination, it has been linked to increased nerve sensitivity [44]. In the disc, TNF-α has been shown to increase the mechanosensitivity of lumbar dorsal roots [41], and has been associated with pain related behavior in rat disc herniation models [42]. The reduction of TNF-α levels could be a mechanism for pain relief following IDET. Further studies should be performed to determine whether TNF-α production is reduced longer than the 28 days examined in this study and to investigate the mechanism by which TNF-α production is influenced.

IL-1β levels were significantly elevated following treatment at all three thermal exposures at the 7-day time point. Concentrations of IL-1β returned to normal by 28 days following the 43ºC and 48ºC treatments, but remained significantly elevated in the high temperature exposure group. The IL-1β response following the 43ºC and 48ºC exposures corresponds to what has been observed in discs following a single stab injury; IL-1β is transiently elevated following injury and returns to control levels within 28 days

[147]. A similar transient elevation of IL-8 was observed following the 75ºC treatment and corresponds to the disc's IL-8 response following a single stab injury [147].

The transient elevation of IL-8 following treatment at 43ºC corresponds to observations in an *in vitro* study which investigated the effects of sublethal heat on IL-1α stimulated annulus cells cultured in alginate beads. In the *in vitro* study, one and four days following treatment at 43ºC, IL-8 levels in the culture media of annulus cells were significantly elevated. Following treatment at 43ºC, significant elevations of IL-6 at the one and four-day time points and TNF-α at the seven-day time point were also observed the *in vitro* study but were not observed in this study. Differences between the *in vitro* and *in vivo* environment and the small size of the treatment region in this *in vivo* study compared to the size of the disc may account for the different observations in the two studies. For example, a localized elevation of IL-6 in the tissue surrounding the heating probe may have been masked by using the entire disc for cytokine analysis.

In this study, several discs contained discontinuous endplates with fibrous or bony tissue present in the disc. It is unclear whether this was a result of the methods used to induce disc degeneration, the thermal treatment, or a combination of the two. In these discs, one of the degeneration inducing stabs or the heating probe may have been placed too close an endplate. The occurrence of disturbed endplates was more common in the 75ºC treatment groups than in the 43ºC or 48ºC treatment groups indicating that there may have been less room for error in probe placement in the high temperature group or that the temperature of treatment caused endplate damage. A previous study was performed using the 48ºC for 15 minutes and 75ºC for 5 minutes treatment parameters to examine the temperature distribution in the disc. In the previous study, the high

temperatures were confined to the disc space. This study used healthy discs; however, and the decreased height and varied stress concentrations in the degenerated discs may have affected the heat distribution in the discs.

In addition to the severe degenerative morphological appearance of the discs with discontinuous endplates, the vertebrae adjacent to these discs contained evidence of vertebral remodeling. The bone adjacent to these discs was very dense and the marrow spaces were filled with granulation tissue consisting of new vessels, fibroblasts and osteoblasts. These features of the adjacent vertebrae are similar to those described by Modic [221]. Modic changes are associated with endplate disruption and fissures, vascualarized fibrous tissue in marrow spaces, and inflammation [221, 222]. Further analysis of both the untreated degenerative discs and the heated discs using MRI and histological techniques designed for bone tissue could confirm whether these changes are analogous to the Modic changes observed in painful human degenerative discs.

The results of this study support the findings of others that high temperature doses of thermal energy, which heat a large volume of tissue, can be deleterious to disc healing [213]. Following the 75ºC treatment, many discs contained damaged endplates and fibrous or bony tissue in the disc space at both 7 and 28 days following thermal treatment. Although several 75ºC exposure discs contained areas of denatured collagen, it was not accompanied by an evident remodeling response. In addition, discs continued to exhibit significantly elevated concentrations of IL-1β twenty-eight days after thermal treatment in the 75ºC group. These discs remained inflamed whereas IL-1β levels in the 43ºC and 48ºC treatment groups returned to control levels.

This is the first study to examine the effects of thermal therapy on inflammation in degenerated intervertebral discs. Following thermal therapy, IL-1β was transiently elevated, but returned to control levels by 28 days following treatment in the 43ºC and 48ºC treatment groups. TNF-α levels were significantly lower following thermal therapy at each of the three different exposures, and this may be associated with the reduction of disc pain following thermal therapy. Besides increased proteoglycan production, no evidence of disc remodeling was observed in the discs. In this study, the beneficial effects of proteoglycan production and TNF-α level reduction were observed at all three thermal exposures, and the deleterious effects were primarily associated with the highest temperature exposure. These results, combined with the research of others that observed no denervation or remolding response following high temperature treatments [208, 213], suggest that future research should further investigate the potential therapeutic effects of low thermal doses.

# Chapter 7 Conclusions and Future Directions

## 7.1 Research Summary

The goal of this research was to advance the understanding of disc degeneration and back pain therapy by developing an animal model of disc degeneration and investigating the *in vivo* effects of thermal therapy on degenerated intervertebral discs. The work completed in this thesis has accomplished that goal while generating many ideas for further research.

### *Disc Degeneration Models*

Two models of disc degeneration were characterized using rat tail intervertebral discs. A single-stab incision was successful in creating rapid histologic changes in rat tail discs. Nuclear size decrease, annular layer disorganization, and cellular changes were consistent with human degenerative discs. Cytokines associated with human disc degeneration (IL-1β, IL-6, IL-8, and TNF-α) were either unaffected or only transiently elevated following stab injury. The cytokines present in the disc were primarily located adjacent to the wound tract caused by the stab incision.

After determining that a single-stab annular injury was insufficient to induce the chronic inflammation associated with human disc degeneration, a repetitive injury model was developed. A triple-stab injury to tail discs induced increased inflammation that continued over the 56-day recovery period and was present throughout the annulus fibrosis. In addition to chronic inflammation, human-like degenerative features were observed in disc morphology after the triple-stab injuries, including a complete disappearance of normal nuclear matrix by 28 days. Clinically relevant outcomes include

morphological disruption and inflammation, both of which are associated with painful disc degeneration in humans. The 56-day period of elevated cytokine levels provides a convenient temporal window within which the impact of anti-inflammatory treatments can be assessed. This repeated-injury model provides a simple and cost effective system to test the efficacy of anti-inflammatory or regenerative treatments for disc degeneration.

*Thermal Therapy*

Both *in vitro* and *in vivo* experiments were completed to investigate the effects of thermal therapy on degenerative intervertebral discs. An *in vitro* study was designed and performed to examine the anti-inflammatory effects of sublethal heat on intervertebral disc cells. The study demonstrated that sublethal heat can induce an HSP70 response in disc cells. In addition, sublethal heat can affect cytokine production in both annulus and nucleus cells either with or without an accompanying HSP70 response. The cellular cytokine response to thermal therapy varied between the two cell types and was dependent upon thermal dose. Some inflammatory factor concentrations were elevated following sublethal thermal exposure while others were lowered. Based on these observations, the *in vivo* cytokine response following thermal therapy may depend upon whether primarily nucleus or annulus tissue is subjected to sublethal thermal exposures as well as whether the exposure received is high enough to induce a heat shock response.

In order to investigate the *in vivo* effects of thermal therapy on degenerated discs, a miniature RF heating probe was designed and characterized. The heating probe and treatment protocols were developed to heat a specific region of a rat intervertebral disc while leaving adjacent tissues unaffected. Several different temperature and time

combinations were characterized so that a region of the annulus could be selectively subjected to the thermal conditions necessary to cause collagen denaturation, cell death, or a heat shock response. The ability to heat a portion of the disc in a small animal model is an important step towards determining the therapeutic mechanisms of thermal therapy in the disc since the thermal dose can be both controlled and quantified, and the remodeling and inflammatory responses examined over time.

Finally, the morphological and inflammatory effects of thermal therapy on degenerated discs were examined using the miniature RF heating probe and rat discs degenerated by the triple-stab method. Three thermal exposures were analyzed seven and twenty-eight days following treatment. This was the first study to examine the effects of thermal therapy on inflammation in degenerated intervertebral discs. TNF-α levels in the disc were reduced twenty-eight days following treatment at all three thermal exposures. Besides increased proteoglycan production in the tissue surrounding the treatment region, no evidence of disc remodeling was observed in the discs. Beneficial effects, such as proteoglycan production and TNF-α level reduction, were observed at all three thermal exposures. Deleterious effects observed in the study were primarily associated with the highest temperature exposure. The results of this study suggest that high temperature treatments do not induce a remodeling response and can be harmful to the disc, so future research should further investigate the potential therapeutic effects of low thermal doses.

## 7.2 Future Directions

*Disc Degeneration Model*

Further characterization of the triple-stab model for inducing disc degeneration would provide additional insight into the changes that occur in the disc and adjacent vertebral bodies as the discs degenerate. In several severely degenerated discs, an inflammatory and remodeling response appeared to occur in the vertebral bodies adjacent to the disc. A thorough histological analysis focusing on the adjacent vertebrae using techniques tailored to bony tissue could elucidate the features of the remodeling response. Using MRI to image the discs and adjacent bone could confirm whether the changes occurring in the bone are analogous to the Modic changes observed adjacent to human degenerative discs. In addition, histological staining specific for blood vessels or nerve tissue would determine whether these tissues are present in the triple-stab degenerated discs or increased in the adjacent bone tissue as they are in human degenerated discs.

Further refinement of immunohistochemistry protocols could characterize precisely which cells are producing certain cytokines. For example, it is unclear whether cells are primarily producing one cytokine or if the same cell is producing multiple cytokines simultaneously. Costaining cells for multiple different cytokines would illustrate which cytokines are produced by the same cells. In addition, immunohistochemistry on the vertebral bodies adjacent to the degenerative discs would elucidate which cytokines are involved in the bone remodeling response and localize cytokine production sites in the vertebrae. Finally, additional antibody staining could help to elucidate which pathways are activated during inflammatory factor production in the degenerated discs.

Discontinuous endplates were observed in several severely degenerated discs and not in other discs. It is unclear whether the disruption of the endplate occurred during a

stab incision and accelerated the degenerative process or whether the severe degenerative state of the disc caused discontinuities in the endplate. Because a model should provide a stable platform to evaluate potential therapies, this issue should be resolved to find a way to standardize the condition of the disc before treatment. An imaging protocol could be developed to determine whether or not the endplates remain intact before evaluation of a potential therapy.

Finally, a longer time point should be evaluated to determine the ultimate fate of these degenerated discs. In these studies, a few discs appeared to have bony tissue growing into the disc. This indicates that the joint could be fusing. The analysis of discs several months after the initiation of disc degeneration would determine whether the discs eventually fuse, remain in a static degenerative state, or heal.

*Thermal Therapy*

These studies demonstrated that high temperatures were deleterious to disc structure and several beneficial effects occurred with low temperature treatment. Additional *in vitro* and *in vivo* work could be performed to further elucidate the effects of low temperature thermal therapies on degenerated discs. In this study, low temperature treatments were limited to a portion of the disc. Exposing the entire disc to lethal thermal doses would likely exacerbate degeneration; however, the effects of subjecting the entire disc to sublethal thermal conditions are unknown. Expanding the size of the treatment region for a sublethal exposure treatment, could potentially amplify the beneficial effects of increased proteoglycan production and TNF-$\alpha$ level reduction.

**References:**


1. Borenstein, D.G., *Epidemiology, etiology, diagnostic evaluation, and treatment of low back pain.* Curr Opin Rheumatol, 2001. **13**(2): p. 128-34.
2. Loney, P.L. and P.W. Stratford, *The prevalence of low back pain in adults: a methodological review of the literature.* Phys Ther, 1999. **79**(4): p. 384-96.
3. Deyo, R.A. and Y.J. Tsui-Wu, *Descriptive epidemiology of low-back pain and its related medical care in the United States.* Spine, 1987. **12**(3): p. 264-8.
4. Lee, P., et al., *Epidemiology of musculoskeletal disorders (complaints) and related disability in Canada.* J Rheumatol, 1985. **12**(6): p. 1169-73.
5. Biering-Sorensen, F., *Low back trouble in a general population of 30-, 40-, 50-, and 60-year-old men and women. Study design, representativeness and basic results.* Dan Med Bull, 1982. **29**(6): p. 289-99.
6. Cassidy, J.D., L.J. Carroll, and P. Cote, *The Saskatchewan health and back pain survey. The prevalence of low back pain and related disability in Saskatchewan adults.* Spine, 1998. **23**(17): p. 1860-6; discussion 1867.
7. Hillman, M., et al., *Prevalence of low back pain in the community: implications for service provision in Bradford, UK.* J Epidemiol Community Health, 1996. **50**(3): p. 347-52.
8. Freemont, A.J., et al., *Current understanding of cellular and molecular events in intervertebral disc degeneration: implications for therapy.* J Pathol, 2002. **196**(4): p. 374-9.

9. Katz, J.N., *Lumbar disc disorders and low-back pain: socioeconomic factors and consequences.* J Bone Joint Surg Am, 2006. **88 Suppl 2**: p. 21-4.

10. Roughley, P.J., *Biology of intervertebral disc aging and degeneration: involvement of the extracellular matrix.* Spine, 2004. **29**(23): p. 2691-9.

11. Bibby, S.R., et al., *The pathophysiology of the intervertebral disc.* Joint Bone Spine, 2001. **68**(6): p. 537-42.

12. Walker, M.H. and D.G. Anderson, *Molecular basis of intervertebral disc degeneration.* Spine J, 2004. **4**(6 Suppl): p. 158S-166S.

13. Adams, M.A. and P.J. Roughley, *What is intervertebral disc degeneration, and what causes it?* Spine, 2006. **31**(18): p. 2151-61.

14. Cs-Szabo, G., et al., *Changes in mRNA and protein levels of proteoglycans of the anulus fibrosus and nucleus pulposus during intervertebral disc degeneration.* Spine, 2002. **27**(20): p. 2212-9.

15. Edwards, W.T., et al., *Structural features and thickness of the vertebral cortex in the thoracolumbar spine.* Spine, 2001. **26**(2): p. 218-25.

16. Moore, R.J., *The vertebral endplate: disc degeneration, disc regeneration.* Eur Spine J, 2006. **15 Suppl 15**: p. 333-7.

17. Urban, J.P., S. Smith, and J.C. Fairbank, *Nutrition of the intervertebral disc.* Spine, 2004. **29**(23): p. 2700-9.

18. Fagan, A., et al., *ISSLS prize winner: The innervation of the intervertebral disc: a quantitative analysis.* Spine, 2003. **28**(23): p. 2570-6.

19. Maroudas, A., et al., *Factors involved in the nutrition of the human lumbar intervertebral disc: cellularity and diffusion of glucose in vitro.* J Anat, 1975. **120**(Pt 1): p. 113-30.

20. Roberts, S., et al., *Histology and pathology of the human intervertebral disc.* J Bone Joint Surg Am, 2006. **88 Suppl 2**: p. 10-4.

21. Boos, N., et al., *Classification of age-related changes in lumbar intervertebral discs: 2002 Volvo Award in basic science.* Spine, 2002. **27**(23): p. 2631-44.

22. Guiot, B.H. and R.G. Fessler, *Molecular biology of degenerative disc disease.* Neurosurgery, 2000. **47**(5): p. 1034-40.

23. Gronblad, M., J.N. Weinstein, and S. Santavirta, *Immunohistochemical observations on spinal tissue innervation. A review of hypothetical mechanisms of back pain.* Acta Orthop Scand, 1991. **62**(6): p. 614-22.

24. Bogduk, N., W. Tynan, and A.S. Wilson, *The nerve supply to the human lumbar intervertebral discs.* J Anat, 1981. **132**(Pt 1): p. 39-56.

25. Ahmed, M., et al., *Neuropeptide Y, tyrosine hydroxylase and vasoactive intestinal polypeptide-immunoreactive nerve fibers in the vertebral bodies, discs, dura mater, and spinal ligaments of the rat lumbar spine.* Spine, 1993. **18**(2): p. 268-73.

26. Battie, M.C. and T. Videman, *Lumbar disc degeneration: epidemiology and genetics.* J Bone Joint Surg Am, 2006. **88 Suppl 2**: p. 3-9.

27. Buckwalter, J.A., *Aging and degeneration of the human intervertebral disc.* Spine, 1995. **20**(11): p. 1307-14.

28. Martin, M.D., C.M. Boxell, and D.G. Malone, *Pathophysiology of lumbar disc degeneration: a review of the literature.* Neurosurg Focus, 2002. **13**(2): p. E1.

29. Haefeli, M., et al., *The course of macroscopic degeneration in the human lumbar intervertebral disc.* Spine, 2006. **31**(14): p. 1522-31.

30. Bernick, S., J.M. Walker, and W.J. Paule, *Age changes to the anulus fibrosus in human intervertebral discs.* Spine, 1991. **16**(5): p. 520-4.

31. Freemont, A.J., et al., *Nerve ingrowth into diseased intervertebral disc in chronic back pain.* Lancet, 1997. **350**(9072): p. 178-81.

32. Niosi, C.A. and T.R. Oxland, *Degenerative mechanics of the lumbar spine.* Spine J, 2004. **4**(6 Suppl): p. 202S-208S.

33. Mimura, M., et al., *Disc degeneration affects the multidirectional flexibility of the lumbar spine.* Spine, 1994. **19**(12): p. 1371-80.

34. Umehara, S., et al., *Effects of degeneration on the elastic modulus distribution in the lumbar intervertebral disc.* Spine, 1996. **21**(7): p. 811-9; discussion 820.

35. Lotz, J.C., et al., *Mechanobiology of the intervertebral disc.* Biochem Soc Trans, 2002. **30**(Pt 6): p. 853-8.

36. Blain, E.J., et al., *Up-regulation of matrix metalloproteinase expression and activation following cyclical compressive loading of articular cartilage in vitro.* Arch Biochem Biophys, 2001. **396**(1): p. 49-55.

37. Freemont, A.J., et al., *Nerve growth factor expression and innervation of the painful intervertebral disc.* J Pathol, 2002. **197**(3): p. 286-92.

38. Murata, Y., et al., *Distribution and appearance of tumor necrosis factor-alpha in the dorsal root ganglion exposed to experimental disc herniation in rats.* Spine, 2004. **29**(20): p. 2235-41.

39. Pelletier, J.P., et al., *Are cytokines involved in osteoarthritic pathophysiology?* Semin Arthritis Rheum, 1991. **20**(6 Suppl 2): p. 12-25.

40. Kang, J.D., et al., *Herniated lumbar intervertebral discs spontaneously produce matrix metalloproteinases, nitric oxide, interleukin-6, and prostaglandin E2.* Spine, 1996. **21**(3): p. 271-7.

41. Grang, L., et al., *Intervertebral disk degeneration and herniation: the role of metalloproteinases and cytokines.* Joint Bone Spine, 2001. **68**(6): p. 547-53.

42. Takahashi, H., et al., *Inflammatory cytokines in the herniated disc of the lumbar spine.* Spine, 1996. **21**(2): p. 218-24.

43. Le Maitre, C.L., A.J. Freemont, and J.A. Hoyland, *The role of interleukin-1 in the pathogenesis of human intervertebral disc degeneration.* Arthritis Res Ther, 2005. **7**(4): p. R732-45.

44. Weiler, C., et al., *Expression and distribution of tumor necrosis factor alpha in human lumbar intervertebral discs: a study in surgical specimen and autopsy controls.* Spine, 2005. **30**(1): p. 44-53; discussion 54.

45. Ahn, S.H., et al., *mRNA expression of cytokines and chemokines in herniated lumbar intervertebral discs.* Spine, 2002. **27**(9): p. 911-7.

46. Specchia, N., et al., *Cytokines and growth factors in the protruded intervertebral disc of the lumbar spine.* Eur Spine J, 2002. **11**(2): p. 145-51.

47. Burke, J.G., et al., *Spontaneous production of monocyte chemoattractant protein-1 and interleukin-8 by the human lumbar intervertebral disc.* Spine, 2002. **27**(13): p. 1402-7.

48. Olmarker, K. and K. Larsson, *Tumor necrosis factor alpha and nucleus-pulposus-induced nerve root injury.* Spine, 1998. **23**(23): p. 2538-44.

49. Miyamoto, H., et al., *The role of cyclooxygenase-2 and inflammatory cytokines in pain induction of herniated lumbar intervertebral disc.* Kobe J Med Sci, 2000. **46**(1-2): p. 13-28.

50. Goldring, M.B. and F. Berenbaum, *The regulation of chondrocyte function by proinflammatory mediators: prostaglandins and nitric oxide.* Clin Orthop Relat Res, 2004(427 Suppl): p. S37-46.

51. Kang, J.D., et al., *Toward a biochemical understanding of human intervertebral disc degeneration and herniation. Contributions of nitric oxide, interleukins, prostaglandin E2, and matrix metalloproteinases.* Spine, 1997. **22**(10): p. 1065-73.

52. Rannou, F., et al., *Sensitivity of anulus fibrosus cells to interleukin 1 beta. Comparison with articular chondrocytes.* Spine, 2000. **25**(1): p. 17-23.

53. Schuerwegh, A.J., et al., *Influence of pro-inflammatory (IL-1 alpha, IL-6, TNF-alpha, IFN-gamma) and anti-inflammatory (IL-4) cytokines on chondrocyte function.* Osteoarthritis Cartilage, 2003. **11**(9): p. 681-7.

54. Shen, B., et al., *Induction of matrix metalloproteinase-2 and -3 activity in ovine nucleus pulposus cells grown in three-dimensional agarose gel culture by*

*interleukin-1beta: a potential pathway of disc degeneration.* Eur Spine J, 2003. **12**(1): p. 66-75.

55. Martel-Pelletier, J., J.P. Pelletier, and H. Fahmi, *Cyclooxygenase-2 and prostaglandins in articular tissues.* Semin Arthritis Rheum, 2003. **33**(3): p. 155-67.

56. Maeda, S. and S. Kokubun, *Changes with age in proteoglycan synthesis in cells cultured in vitro from the inner and outer rabbit annulus fibrosus. Responses to interleukin-1 and interleukin-1 receptor antagonist protein.* Spine, 2000. **25**(2): p. 166-9.

57. Sanchez, C., et al., *Differential regulation of chondrocyte metabolism by oncostatin M and interleukin-6.* Osteoarthritis Cartilage, 2004. **12**(10): p. 801-10.

58. Lindholm, D., et al., *Interleukin-1 regulates synthesis of nerve growth factor in non-neuronal cells of rat sciatic nerve.* Nature, 1987. **330**(6149): p. 658-9.

59. Ozaktay, A.C., et al., *Dorsal root sensitivity to interleukin-1 beta, interleukin-6 and tumor necrosis factor in rats.* Eur Spine J, 2002. **11**(5): p. 467-75.

60. Campbell, I.K., D.S. Piccoli, and J.A. Hamilton, *Stimulation of human chondrocyte prostaglandin E2 production by recombinant human interleukin-1 and tumour necrosis factor.* Biochim Biophys Acta, 1990. **1051**(3): p. 310-8.

61. Kuroki, K., A.M. Stoker, and J.L. Cook, *Effects of proinflammatory cytokines on canine articular chondrocytes in a three-dimensional culture.* Am J Vet Res, 2005. **66**(7): p. 1187-96.

62. Olmarker, K., M. Nutu, and R. Storkson, *Changes in spontaneous behavior in rats exposed to experimental disc herniation are blocked by selective TNF-alpha inhibition.* Spine, 2003. **28**(15): p. 1635-41; discussion 1642.

63. Wisithphrom, K. and L.J. Windsor, *The effects of tumor necrosis factor-alpha, interleukin-1beta, interleukin-6, and transforming growth factor-beta1 on pulp fibroblast mediated collagen degradation.* J Endod, 2006. **32**(9): p. 853-61.

64. Flannery, C.R., et al., *IL-6 and its soluble receptor augment aggrecanase-mediated proteoglycan catabolism in articular cartilage.* Matrix Biol, 2000. **19**(6): p. 549-53.

65. Boe, A., et al., *Interleukin 6 knock-out mice are resistant to antigen-induced experimental arthritis.* Cytokine, 1999. **11**(12): p. 1057-64.

66. Moyer, K.E., et al., *Effects of interleukin-8 on granulation tissue maturation.* J Cell Physiol, 2002. **193**(2): p. 173-9.

67. Belperio, J.A., et al., *CXC chemokines in angiogenesis.* J Leukoc Biol, 2000. **68**(1): p. 1-8.

68. Henrotin, Y.E., et al., *Effects of exogenous IL-1 beta, TNF alpha, IL-6, IL-8 and LIF on cytokine production by human articular chondrocytes.* Osteoarthritis Cartilage, 1996. **4**(3): p. 163-73.

69. Torzilli, P.A., et al., *Effects of misoprostol and prostaglandin E2 on proteoglycan biosynthesis and loss in unloaded and loaded articular cartilage explants.* Prostaglandins, 1996. **52**(3): p. 157-73.

70. Choi, Y.A., et al., *Interleukin-1beta stimulates matrix metalloproteinase-2 expression via a prostaglandin E2-dependent mechanism in human chondrocytes.* Exp Mol Med, 2004. **36**(3): p. 226-32.

71. Burke, J.G., et al., *Intervertebral discs which cause low back pain secrete high levels of proinflammatory mediators.* J Bone Joint Surg Br, 2002. **84**(2): p. 196-201.

72. Hauselmann, H.J., et al., *Nitric oxide and proteoglycan biosynthesis by human articular chondrocytes in alginate culture.* FEBS Lett, 1994. **352**(3): p. 361-4.

73. Liu, G.Z., et al., *Nitric oxide mediates the change of proteoglycan synthesis in the human lumbar intervertebral disc in response to hydrostatic pressure.* Spine, 2001. **26**(2): p. 134-41.

74. Rannou, F., et al., *Cyclic tensile stretch modulates proteoglycan production by intervertebral disc annulus fibrosus cells through production of nitrite oxide.* J Cell Biochem, 2003. **90**(1): p. 148-57.

75. Cao, M., et al., *Nitric oxide inhibits the synthesis of type-II collagen without altering Col2A1 mRNA abundance: prolyl hydroxylase as a possible target.* Biochem J, 1997. **324 ( Pt 1)**: p. 305-10.

76. Blanco, F.J. and M. Lotz, *IL-1-induced nitric oxide inhibits chondrocyte proliferation via PGE2.* Exp Cell Res, 1995. **218**(1): p. 319-25.

77. Sasaki, K., et al., *Nitric oxide mediates interleukin-1-induced gene expression of matrix metalloproteinases and basic fibroblast growth factor in cultured rabbit articular chondrocytes.* J Biochem (Tokyo), 1998. **123**(3): p. 431-9.

78. Maneiro, E., et al., *Aceclofenac increases the synthesis of interleukin 1 receptor antagonist and decreases the production of nitric oxide in human articular chondrocytes.* J Rheumatol, 2001. **28**(12): p. 2692-9.

79. Coppes, M.H., et al., *Innervation of "painful" lumbar discs.* Spine, 1997. **22**(20): p. 2342-9; discussion 2349-50.

80. Bogduk, N., *The lumbar disc and low back pain.* Neurosurg Clin N Am, 1991. **2**(4): p. 791-806.

81. Solovieva, S., et al., *Possible association of interleukin 1 gene locus polymorphisms with low back pain.* Pain, 2004. **109**(1-2): p. 8-19.

82. van Tulder, M.W., B. Koes, and A. Malmivaara, *Outcome of non-invasive treatment modalities on back pain: an evidence-based review.* Eur Spine J, 2006. **15 Suppl 1**: p. S64-81.

83. Lee, J., et al., *Stability of the lumbar spine after intradiscal electrothermal therapy.* Arch Phys Med Rehabil, 2001. **82**(1): p. 120-2.

84. Sakalkale, D.P., S.A. Bhagia, and C.W. Slipman, *A historical review and current perspective on the intervertebral disc prosthesis.* Pain Physician, 2003. **6**(2): p. 195-8.

85. Kumar, M.N., F. Jacquot, and H. Hall, *Long-term follow-up of functional outcomes and radiographic changes at adjacent levels following lumbar spine fusion for degenerative disc disease.* Eur Spine J, 2001. **10**(4): p. 309-13.

86. Phillips, F.M., J. Reuben, and F.T. Wetzel, *Intervertebral disc degeneration adjacent to a lumbar fusion. An experimental rabbit model.* J Bone Joint Surg Br, 2002. **84**(2): p. 289-94.

87. Freeman, B.J. and J. Davenport, *Total disc replacement in the lumbar spine: a systematic review of the literature.* Eur Spine J, 2006. **15**(Supplement 15): p. 439-447.

88. Siepe, C.J., et al., *Clinical results of total lumbar disc replacement with ProDisc II: three-year results for different indications.* Spine, 2006. **31**(17): p. 1923-32.

89. Zhou, Y. and S. Abdi, *Diagnosis and minimally invasive treatment of lumbar discogenic pain--a review of the literature.* Clin J Pain, 2006. **22**(5): p. 468-81.

90. Moon, S.H., et al., *Human intervertebral disc cells are genetically modifiable by adenovirus-mediated gene transfer: implications for the clinical management of intervertebral disc disorders.* Spine, 2000. **25**(20): p. 2573-9.

91. Freeman, B.J., *IDET: a critical appraisal of the evidence.* Eur Spine J, 2006. **15**(Supplement 15): p. 448-457.

92. Saal, J.A. and J.S. Saal, *Intradiscal electrothermal treatment for chronic discogenic low back pain: prospective outcome study with a minimum 2-year follow-up.* Spine, 2002. **27**(9): p. 966-73; discussion 973-4.

93. Gerszten, P.C., et al., *A Prospective Outcomes Study Of Patients Undergoing Intradiscal Electrothermy (IDET) For Chronic Low Back Pain.* Pain Physician, 2002. **5**(4): p. 360-4.

94. Karasek, M. and N. Bogduk, *Twelve-month follow-up of a controlled trial of intradiscal thermal anuloplasty for back pain due to internal disc disruption.* Spine, 2000. **25**(20): p. 2601-7.

95. Spruit, M. and W.C. Jacobs, *Pain and function after intradiscal electrothermal treatment (IDET) for symptomatic lumbar disc degeneration.* Eur Spine J, 2002. **11**(6): p. 589-93.

96. Park, S.Y., et al., *Intradiscal electrothermal treatment for chronic lower back pain patients with internal disc disruption.* Yonsei Med J, 2005. **46**(4): p. 539-45.

97. Davis, T.T., et al., *The IDET procedure for chronic discogenic low back pain.* Spine, 2004. **29**(7): p. 752-6.

98. Freeman, B.J., et al., *A randomized, double-blind, controlled trial: intradiscal electrothermal therapy versus placebo for the treatment of chronic discogenic low back pain.* Spine, 2005. **30**(21): p. 2369-77; discussion 2378.

99. Arnoczky, S.P. and A. Aksan, *Thermal modification of connective tissues: basic science considerations and clinical implications.* J Am Acad Orthop Surg, 2000. **8**(5): p. 305-13.

100. Saal, J.A. and J.S. Saal, *Intradiscal electrothermal treatment for chronic discogenic low back pain: a prospective outcome study with minimum 1-year follow-up.* Spine, 2000. **25**(20): p. 2622-7.

101. Kleinstueck, F.S., et al., *Acute biomechanical and histological effects of intradiscal electrothermal therapy on human lumbar discs.* Spine, 2001. **26**(20): p. 2198-207.

102. Singh, K., K. Masuda, and H.S. An, *Animal models for human disc degeneration.* Spine J, 2005. **5**(6 Suppl): p. 267S-279S.

103. An, H.S. and K. Masuda, *Relevance of in vitro and in vivo models for intervertebral disc degeneration.* J Bone Joint Surg Am, 2006. **88 Suppl 2**: p. 88-94.

104. Lotz, J.C., *Animal models of intervertebral disc degeneration: lessons learned.* Spine, 2004. **29**(23): p. 2742-50.

105. Schimandle, J.H. and S.D. Boden, *Spine update. Animal use in spinal research.* Spine, 1994. **19**(21): p. 2474-7.

106. Elliott, D.M. and J.J. Sarver, *Young investigator award winner: validation of the mouse and rat disc as mechanical models of the human lumbar disc.* Spine, 2004. **29**(7): p. 713-22.

107. Hunter, C.J., J.R. Matyas, and N.A. Duncan, *Cytomorphology of notochordal and chondrocytic cells from the nucleus pulposus: a species comparison.* J Anat, 2004. **205**(5): p. 357-62.

108. Aoki, Y., et al., *Disc inflammation potentially promotes axonal regeneration of dorsal root ganglion neurons innervating lumbar intervertebral disc in rats.* Spine, 2004. **29**(23): p. 2621-6.

109. Lipson, S.J. and H. Muir, *1980 Volvo award in basic science. Proteoglycans in experimental intervertebral disc degeneration.* Spine, 1981. **6**(3): p. 194-210.

110. Takaishi, H., et al., *Type-II collagen gene expression is transiently upregulated in experimentally induced degeneration of rabbit intervertebral disc.* J Orthop Res, 1997. **15**(4): p. 528-38.

111. Nomura, T., et al., *Nucleus pulposus allograft retards intervertebral disc degeneration.* Clin Orthop Relat Res, 2001(389): p. 94-101.

112. Anderson, D.G., et al., *Comparative gene expression profiling of normal and degenerative discs: analysis of a rabbit annular laceration model.* Spine, 2002. **27**(12): p. 1291-6.

113. Masuda, K., et al., *A novel rabbit model of mild, reproducible disc degeneration by an anulus needle puncture: correlation between the degree of disc injury and radiological and histological appearances of disc degeneration.* Spine, 2005. **30**(1): p. 5-14.

114. Hampton, D., et al., *Healing potential of the anulus fibrosus.* Spine, 1989. **14**(4): p. 398-401.

115. Osti, O.L., B. Vernon-Roberts, and R.D. Fraser, *1990 Volvo Award in experimental studies. Anulus tears and intervertebral disc degeneration. An experimental study using an animal model.* Spine, 1990. **15**(8): p. 762-7.

116. Moore, R.J., et al., *Remodeling of vertebral bone after outer anular injury in sheep.* Spine, 1996. **21**(8): p. 936-40.

117. Ethier, D.B., et al., *The influence of anulotomy selection on disc competence. A radiographic, biomechanical, and histologic analysis.* Spine, 1994. **19**(18): p. 2071-6.

118. Kaapa, E., et al., *Collagens in the injured porcine intervertebral disc.* J Orthop Res, 1994. **12**(1): p. 93-102.

119. Kanerva, A., et al., *Inflammatory cells in experimental intervertebral disc injury.* Spine, 1997. **22**(23): p. 2711-5.

120. Sobajima, S., et al., *A slowly progressive and reproducible animal model of intervertebral disc degeneration characterized by MRI, X-ray, and histology.* Spine, 2005. **30**(1): p. 15-24.

121. Sobajima, S., et al., *Quantitative analysis of gene expression in a rabbit model of intervertebral disc degeneration by real-time polymerase chain reaction.* Spine J, 2005. **5**(1): p. 14-23.

122. O'Neill, C.W., et al., *Percutaneous plasma decompression alters cytokine expression in injured porcine intervertebral discs.* Spine J, 2004. **4**(1): p. 88-98.

123. Olsewski, J.M., et al., *Magnetic resonance imaging and biological changes in injured intervertebral discs under normal and increased mechanical demands.* Spine, 1996. **21**(17): p. 1945-51.

124. Lotz, J.C., et al., *Compression-induced degeneration of the intervertebral disc: an in vivo mouse model and finite-element study.* Spine, 1998. **23**(23): p. 2493-506.

125. Iatridis, J.C., et al., *Compression-induced changes in intervertebral disc properties in a rat tail model.* Spine, 1999. **24**(10): p. 996-1002.

126. Ching, C.T., et al., *The effect of cyclic compression on the mechanical properties of the inter-vertebral disc: an in vivo study in a rat tail model.* Clin Biomech (Bristol, Avon), 2003. **18**(3): p. 182-9.

127. Court, C., et al., *The effect of static in vivo bending on the murine intervertebral disc.* Spine J, 2001. **1**(4): p. 239-45.

128. Hutton, W.C., et al., *Effect of tail suspension (or simulated weightlessness) on the lumbar intervertebral disc: study of proteoglycans and collagen.* Spine, 2002. **27**(12): p. 1286-90.

129. Cassidy, J.D., et al., *A study of the effects of bipedism and upright posture on the lumbosacral spine and paravertebral muscles of the Wistar rat.* Spine, 1988. **13**(3): p. 301-8.

130. Miyamoto, S., K. Yonenobu, and K. Ono, *Experimental cervical spondylosis in the mouse.* Spine, 1991. **16**(10 Suppl): p. S495-500.

131. Wang, B., et al., *Segmental instability in cervical spondylotic myelopathy with severe disc degeneration.* Spine, 2006. **31**(12): p. 1327-31.

132. Hirakawa, H., et al., *An immunohistochemical evaluation of extracellular matrix components in the spinal posterior longitudinal ligament and intervertebral disc of the tiptoe walking mouse.* J Orthop Sci, 2004. **9**(6): p. 591-7.

133. Norcross, J.P., et al., *An in vivo model of degenerative disc disease.* J Orthop Res, 2003. **21**(1): p. 183-8.

134. Oda, H., et al., *Degeneration of intervertebral discs due to smoking: experimental assessment in a rat-smoking model.* J Orthop Sci, 2004. **9**(2): p. 135-41.

135. Gruber, H.E., et al., *The sand rat model for disc degeneration: radiologic characterization of age-related changes: cross-sectional and prospective analyses.* Spine, 2002. **27**(3): p. 230-4.

136. Sahlman, J., et al., *Premature vertebral endplate ossification and mild disc degeneration in mice after inactivation of one allele belonging to the Col2a1 gene for Type II collagen.* Spine, 2001. **26**(23): p. 2558-65.

137. Hughes, P.C. and J.M. Tanner, *The assessment of skeletal maturity in the growing rat.* J Anat, 1970. **106**(Pt 2): p. 371-402.

138. Thompson, R.E., T.M. Barker, and M.J. Pearcy, *Defining the Neutral Zone of sheep intervertebral joints during dynamic motions: an in vitro study.* Clin Biomech (Bristol, Avon), 2003. **18**(2): p. 89-98.

139. Roberts, S., et al., *Matrix metalloproteinases and aggrecanase: their role in disorders of the human intervertebral disc.* Spine, 2000. **25**(23): p. 3005-13.

140. Nagano, T., et al., *Distribution of the basic fibroblast growth factor and its receptor gene expression in normal and degenerated rat intervertebral discs.* Spine, 1995. **20**(18): p. 1972-8.

141. Melrose, J., et al., *Spatial and temporal localization of transforming growth factor-beta, fibroblast growth factor-2, and osteonectin, and identification of cells expressing alpha-smooth muscle actin in the injured anulus fibrosus: implications for extracellular matrix repair.* Spine, 2002. **27**(16): p. 1756-64.

142. Elfervig, M.K., et al., *IL-1beta sensitizes intervertebral disc annulus cells to fluid-induced shear stress.* J Cell Biochem, 2001. **82**(2): p. 290-8.

143. Burke, J.G., et al., *Human nucleus pulposis can respond to a pro-inflammatory stimulus.* Spine, 2003. **28**(24): p. 2685-93.

144. Rand, N., et al., *Murine nucleus pulposus-derived cells secrete interleukins-1-beta, -6, and -10 and granulocyte-macrophage colony-stimulating factor in cell culture.* Spine, 1997. **22**(22): p. 2598-601; discussion 2602.

145. Nygaard, O.P., S.I. Mellgren, and B. Osterud, *The inflammatory properties of contained and noncontained lumbar disc herniation.* Spine, 1997. **22**(21): p. 2484-8.

146. Oegema, T.R., Jr., et al., *Fibronectin and its fragments increase with degeneration in the human intervertebral disc.* Spine, 2000. **25**(21): p. 2742-7.

147. Rousseau, M.A., et al., *Stab incision for inducing intervertebral disc degeneration in the rat.* Spine, 2007. **32**(1): p. 17-24.

148. Wada, E., et al., *Experimental spondylosis in the rabbit spine. Overuse could accelerate the spondylosis.* Spine, 1992. **17**(3 Suppl): p. S1-6.

149. Wang, Y.J., et al., *Cervical intervertebral disc degeneration induced by unbalanced dynamic and static forces: a novel in vivo rat model.* Spine, 2006. **31**(14): p. 1532-8.

150. Barr, A.E. and M.F. Barbe, *Pathophysiological tissue changes associated with repetitive movement: a review of the evidence.* Phys Ther, 2002. **82**(2): p. 173-87.

151. Barbe, M.F., et al., *Chronic repetitive reaching and grasping results in decreased motor performance and widespread tissue responses in a rat model of MSD.* J Orthop Res, 2003. **21**(1): p. 167-76.

152. Chung, M.P., et al., *Role of repeated lung injury and genetic background in bleomycin-induced fibrosis.* Am J Respir Cell Mol Biol, 2003. **29**(3 Pt 1): p. 375-80.

153. Brown, R.F., R.B. Drawbaugh, and T.C. Marrs, *An investigation of possible models for the production of progressive pulmonary fibrosis in the rat. The effects of repeated intratracheal instillation of bleomycin.* Toxicology, 1988. **51**(1): p. 101-10.

154. Buckley, C.D., et al., *Fibroblasts regulate the switch from acute resolving to chronic persistent inflammation.* Trends Immunol, 2001. **22**(4): p. 199-204.

155. Kondo, T. and T. Ohshima, *The dynamics of inflammatory cytokines in the healing process of mouse skin wound: a preliminary study for possible wound age determination.* Int J Legal Med, 1996. **108**(5): p. 231-6.

156. Singh, V., et al., *Percutaneous Disc Decompression Using Coblation (Nucleoplasty TM) in the Treatment of Chronic Discogenic Pain.* Pain Physician, 2002. **5**(3): p. 250-9.

157. Ercelen, O., et al., *Radiofrequency lesioning using two different time modalities for the treatment of lumbar discogenic pain: a randomized trial.* Spine, 2003. **28**(17): p. 1922-7.

158. Barendse, G.A., et al., *Randomized controlled trial of percutaneous intradiscal radiofrequency thermocoagulation for chronic discogenic back pain: lack of effect from a 90-second 70 C lesion.* Spine, 2001. **26**(3): p. 287-92.

159. Nau, W.H. and C.J. Diederich, *Evaluation of temperature distributions in cadaveric lumbar spine during nucleoplasty.* Phys Med Biol, 2004. **49**(8): p. 1583-94.

160. Kregel, K.C., *Heat shock proteins: modifying factors in physiological stress responses and acquired thermotolerance.* J Appl Physiol, 2002. **92**(5): p. 2177-86.

161. Welch, W.J., *How cells respond to stress.* Sci Am, 1993. **268**(5): p. 56-64.

162. Ensor, J.E., et al., *Differential effects of hyperthermia on macrophage interleukin-6 and tumor necrosis factor-alpha expression.* Am J Physiol, 1994. **266**(4 Pt 1): p. C967-74.

163. Snyder, Y.M., et al., *Transcriptional inhibition of endotoxin-induced monokine synthesis following heat shock in murine peritoneal macrophages.* J Leukoc Biol, 1992. **51**(2): p. 181-7.

164. Meng, X. and A.H. Harken, *The interaction between Hsp70 and TNF-alpha expression: a novel mechanism for protection of the myocardium against post-injury depression.* Shock, 2002. **17**(5): p. 345-53.

165. Takao, T. and T. Iwaki, *A comparative study of localization of heat shock protein 27 and heat shock protein 72 in the developmental and degenerative intervertebral discs.* Spine, 2002. **27**(4): p. 361-8.

166. Walsh, A.L., O'Neill, C. W., Lotz, J. C., *Glucosamine HCL Alters Production of Inflammatory Mediators by Rat Intervertebral Disc Cells in Vitro.* in press.

167. Tonomura, H., et al., *Glutamine protects articular chondrocytes from heat stress and NO-induced apoptosis with HSP70 expression.* Osteoarthritis Cartilage, 2006. **14**(6): p. 545-53.

168. Cruz, T.F., R.A. Kandel, and I.R. Brown, *Interleukin 1 induces the expression of a heat-shock gene in chondrocytes.* Biochem J, 1991. **277 ( Pt 2)**: p. 327-30.

169. Wong, H.R., M. Ryan, and J.R. Wispe, *The heat shock response inhibits inducible nitric oxide synthase gene expression by blocking I kappa-B degradation and NF-kappa B nuclear translocation.* Biochem Biophys Res Commun, 1997. **231**(2): p. 257-63.

170. Shellman, Y.G., et al., *Fast response temperature measurement and highly reproducible heating methods for 96-well plates.* Biotechniques, 2004. **36**(6): p. 968-72, 974-6.

171. Imao, M., M. Nagaki, and H. Moriwaki, *Dual effects of heat stress on tumor necrosis factor-alpha-induced hepatocyte apoptosis in mice.* Lab Invest, 2006. **86**(9): p. 959-67.

172. Callahan, T.E., et al., *Heat shock attenuates oxidation and accelerates apoptosis in human neutrophils.* J Surg Res, 1999. **85**(2): p. 317-22.

173. Moseley, P.L., *Heat shock proteins and the inflammatory response.* Ann N Y Acad Sci, 1998. **856**: p. 206-13.

174. Yoo, C.G., et al., *Anti-inflammatory effect of heat shock protein induction is related to stabilization of I kappa B alpha through preventing I kappa B kinase activation in respiratory epithelial cells.* J Immunol, 2000. **164**(10): p. 5416-23.

175. Rylander, M.N., et al., *Thermally induced injury and heat-shock protein expression in cells and tissues.* Ann N Y Acad Sci, 2005. **1066**: p. 222-42.

176. Zhang, F., et al., *Green fluorescent protein selectively induces HSP70-mediated up-regulation of COX-2 expression in endothelial cells.* Blood, 2003. **102**(6): p. 2115-21.

177. Hasday, J.D., et al., *Exposure to febrile temperature modifies endothelial cell response to tumor necrosis factor-alpha.* J Appl Physiol, 2001. **90**(1): p. 90-8.

178. Park, C.H., et al., *Heat shock-induced matrix metalloproteinase (MMP)-1 and MMP-3 are mediated through ERK and JNK activation and via an autocrine interleukin-6 loop.* J Invest Dermatol, 2004. **123**(6): p. 1012-9.

179. Hosaka, Y., et al., *Effect of heat on synthesis of gelatinases and pro-inflammatory cytokines in equine tendinocytes.* Biomed Res, 2006. **27**(5): p. 233-41.

180. Ensor, J.E., E.K. Crawford, and J.D. Hasday, *Warming macrophages to febrile range destabilizes tumor necrosis factor-alpha mRNA without inducing heat shock.* Am J Physiol, 1995. **269**(5 Pt 1): p. C1140-6.

181. Schmidt, J.A. and E. Abdulla, *Down-regulation of IL-1 beta biosynthesis by inducers of the heat-shock response.* J Immunol, 1988. **141**(6): p. 2027-34.

182. Ding, X.Z., et al., *Over-expression of hsp-70 inhibits bacterial lipopolysaccharide-induced production of cytokines in human monocyte-derived macrophages.* Cytokine, 2001. **16**(6): p. 210-9.

183. Jaattela, M., et al., *Major heat shock protein hsp70 protects tumor cells from tumor necrosis factor cytotoxicity.* Embo J, 1992. **11**(10): p. 3507-12.

184. Guttman, S.D., et al., *Heat shock, deciliation and release from anoxia induce the synthesis of the same set of polypeptides in starved T. pyriformis.* Cell, 1980. **22**(1 Pt 1): p. 299-307.

185. Marber, M.S., et al., *Overexpression of the rat inducible 70-kD heat stress protein in a transgenic mouse increases the resistance of the heart to ischemic injury.* J Clin Invest, 1995. **95**(4): p. 1446-56.

186. Weitzel, G., U. Pilatus, and L. Rensing, *Similar dose response of heat shock protein synthesis and intracellular pH change in yeast.* Exp Cell Res, 1985. **159**(1): p. 252-6.

187. Sciandra, J.J. and J.R. Subjeck, *The effects of glucose on protein synthesis and thermosensitivity in Chinese hamster ovary cells.* J Biol Chem, 1983. **258**(20): p. 12091-3.

188. Owens, B.D., B.J. Stickles, and B.D. Busconi, *Radiofrequency energy: applications and basic science.* Am J Orthop, 2003. **32**(3): p. 117-20; discussion 120-1.

189. Wetzel, F.T., T.A. McNally, and F.M. Phillips, *Intradiscal electrothermal therapy used to manage chronic discogenic low back pain: new directions and interventions.* Spine, 2002. **27**(22): p. 2621-6.

190. Biyani, A., et al., *Intradiscal electrothermal therapy: a treatment option in patients with internal disc disruption.* Spine, 2003. **28**(15 Suppl): p. S8-14.

191. Heary, R.F., *Intradiscal electrothermal annuloplasty: the IDET procedure.* J Spinal Disord, 2001. **14**(4): p. 353-60.

192. Field, S., Hand, JW, *An Introduction to the practical aspects of clinical hyperthermia*. 1990, New York: Taylor & Francis.

193. Dewey, W.C., *Arrhenius relationships from the molecule and cell to the clinic.* Int J Hyperthermia, 1994. **10**(4): p. 457-83.

194. Rauch, B., et al., *Comparison of techniques for determination of chondrocyte viability after thermal injury.* Am J Vet Res, 2006. **67**(8): p. 1280-5.

195. Flory, P., Garrett RR, *Phase transitions in collagen and gelatin systems.* J Am Chem Soc, 1958. **80**: p. 4836-4845.

196. Le Lous, M., et al., *Age related evolution of stable collagen reticulation in human skin.* Connect Tissue Res, 1985. **13**(2): p. 145-55.

197. Hayashi, K. and M.D. Markel, *Thermal capsulorrhaphy treatment of shoulder instability: basic science.* Clin Orthop Relat Res, 2001(390): p. 59-72.

198. Wells, P.B., et al., *Histological evidence for the role of mechanical stress in modulating thermal denaturation of collagen.* Biomech Model Mechanobiol, 2005. **4**(4): p. 201-10.

199. Bischof, J., He X, *Thermal Stability of Proteins.* Ann. N.Y. Scad. Sci., 2005. **1066**: p. 12-33.

200. Allain, J.C., Le Lous, M., Cohen-Solal, L., Basin, S., Maroteaux, P., *Isometric tensions develooped during the hydrothermal swelling of rat skin.* Connect Tissue Res, 1980. **7**: p. 127-133.

201. Houpt, J.C., E.S. Conner, and E.W. McFarland, *Experimental study of temperature distributions and thermal transport during radiofrequency current therapy of the intervertebral disc.* Spine, 1996. **21**(15): p. 1808-12; discussion 1812-3.

202. Goldberg, S.N., et al., *Tissue ablation with radiofrequency: effect of probe size, gauge, duration, and temperature on lesion volume.* Acad Radiol, 1995. **2**(5): p. 399-404.

203. Flandin, F., C. Buffevant, and D. Herbage, *A differential scanning calorimetry analysis of the age-related changes in the thermal stability of rat skin collagen.* Biochim Biophys Acta, 1984. **791**(2): p. 205-11.

204. Maitland, D.J. and J.T. Walsh, Jr., *Quantitative measurements of linear birefringence during heating of native collagen.* Lasers Surg Med, 1997. **20**(3): p. 310-8.

205. Pauza, K.J., et al., *A randomized, placebo-controlled trial of intradiscal electrothermal therapy for the treatment of discogenic low back pain.* Spine J, 2004. **4**(1): p. 27-35.

206. Bogduk, N. and M. Karasek, *Two-year follow-up of a controlled trial of intradiscal electrothermal anuloplasty for chronic low back pain resulting from internal disc disruption.* Spine J, 2002. **2**(5): p. 343-50.

207. Lee, M.S., et al., *Intradiscal Electrothermal Therapy (IDET) for Treatment of Chronic Lumbar Discogenic Pain: A Minimum 2-Year Clinical Outcome Study.* Pain Physician, 2003. **6**(4): p. 443-8.

208. Freeman, B.J., et al., *Does intradiscal electrothermal therapy denervate and repair experimentally induced posterolateral annular tears in an animal model?* Spine, 2003. **28**(23): p. 2602-8.

209. Pollintine, P., G. Findlay, and M.A. Adams, *Intradiscal electrothermal therapy can alter compressive stress distributions inside degenerated intervertebral discs.* Spine, 2005. **30**(6): p. E134-9.

210. Shah, R.V., et al., *Intradiskal electrothermal therapy: a preliminary histologic study.* Arch Phys Med Rehabil, 2001. **82**(9): p. 1230-7.

211. Bono, C.M., et al., *Temperatures within the lumbar disc and endplates during intradiscal electrothermal therapy: formulation of a predictive temperature map in relation to distance from the catheter.* Spine, 2004. **29**(10): p. 1124-9; discussion 1130-1.

212. Hayashi, K., et al., *The effect of nonablative laser energy on joint capsular properties. An in vitro histologic and biochemical study using a rabbit model.* Am J Sports Med, 1996. **24**(5): p. 640-6.

213. Bass, E.C., et al., *Intradiscal thermal therapy does not stimulate biologic remodeling in an in vivo sheep model.* Spine, 2006. **31**(2): p. 139-45.

214. Smith, H.P., J.M. McWhorter, and V.R. Challa, *Radiofrequency neurolysis in a clinical model. Neuropathological correlation.* J Neurosurg, 1981. **55**(2): p. 246-53.

215. Rosen, S. and F. Falco, *Radiofrequency stimulation of intervertebral discs.* Pain Physician, 2003. **6**(4): p. 435-8.

216. Weinstein, J.N., Gordon, S.L., *Low Back Pain: A Scientific and Cliinical Overview*. 1996, Rosemint, IL: American Academy of Orthopaedic Surgeons. 472-628.

217. Grunenfelder, J., et al., *Heat shock protein upregulation lowers cytokine levels after ischemia and reperfusion.* Eur Surg Res, 2001. **33**(5-6): p. 383-7.

218. Ulrich, J.A., Liebenberb, E.C., Thuillier, D.U., Lotz, J.C., *Repeated Disc Injury Causes Persistent Inflammation.* in press.

219. Hojo, T., et al., *Effect of heat stimulation on viability and proteoglycan metabolism of cultured chondrocytes: preliminary report.* J Orthop Sci, 2003. **8**(3): p. 396-9.

220. Iocono, J.A., et al., *Interleukin-8 levels and activity in delayed-healing human thermal wounds.* Wound Repair Regen, 2000. **8**(3): p. 216-25.

221. Modic, M.T., et al., *Imaging of degenerative disk disease.* Radiology, 1988. **168**(1): p. 177-86.

222. Kjaer, P., et al., *Modic changes and their associations with clinical findings.* Eur Spine J, 2006. **15**(9): p. 1312-9.

**Publishing Agreement**

It is the policy of the University to encourage the distribution of all theses and dissertations. Copies of all UCSF theses and dissertations will be routed to the library via the Graduate Division. The library will make all theses and dissertations accessible to the public and will preserve these to the best of their abilities, in perpetuity.

I hereby grant permission to the Graduate Division of the University of California, San Francisco to release copies of my thesis or dissertation to the Campus Library to provide access and preservation, in whole or in part, in perpetuity.

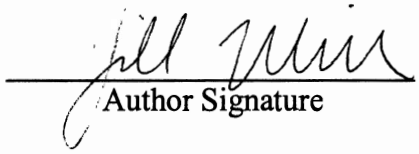

Author Signature

2/24/07

Date